Final Spatially-Constrained Inversions Report and Data Delivery for the Airborne Electromagnetic Survey of Area 1 and Area 2, North Dakota for the North Dakota Department of Water Resources

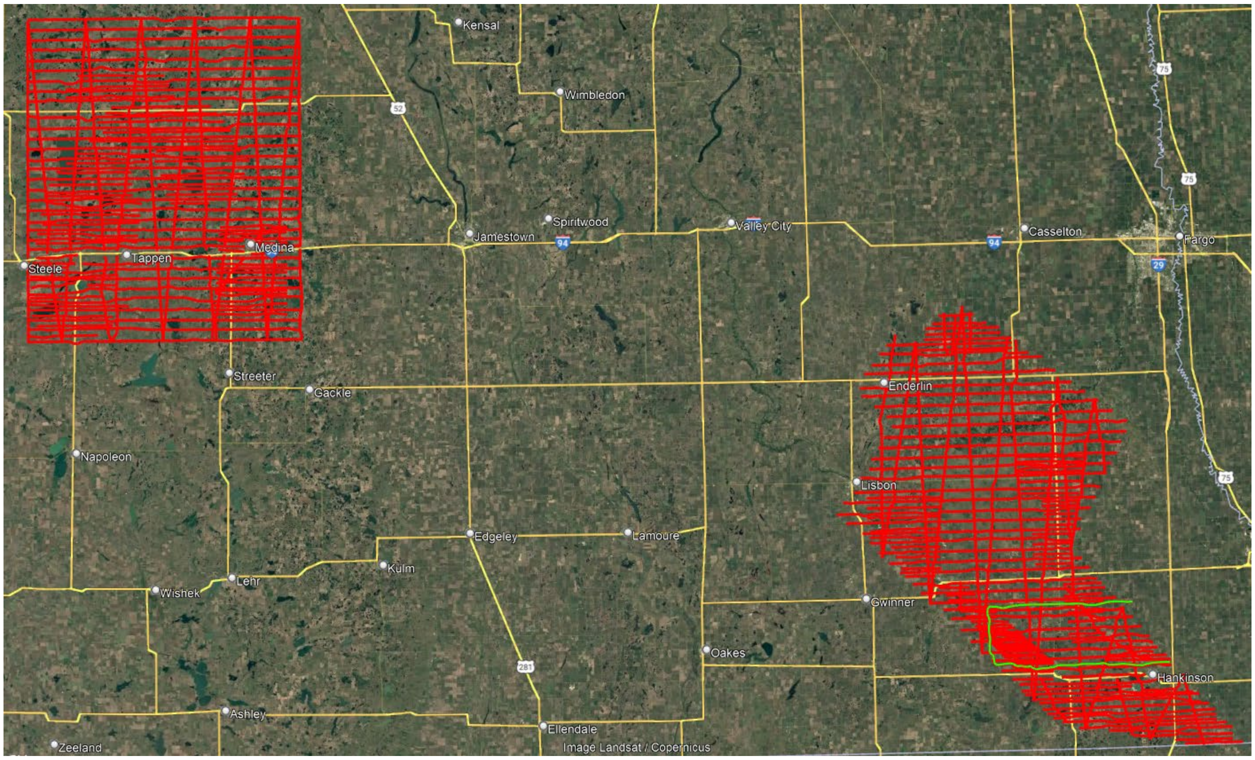

Jared Dale Abraham
Principal Geophysicist/Geologist
(303) 905-6240

Theodore H. Asch
Research Geophysicist
(720) 415-7312

Aqua Geo Frameworks, LLC
10848 Ridge Road
Fort Laramie, WY 82212-7614

Disclaimer:

AGF conducted this project using the current standards of the geophysical industry and used in-house quality control standards to produce this geophysical survey and products. The geophysical methods and procedures described in this report are applicable to the particular project objectives, and these methods have been successfully applied by AGF to investigations and projects of similar size and nature. However, field or subsurface conditions may differ from those anticipated, and the resultant data may not achieve the project objectives. AGF's services were performed consistent with the professional skill and care ordinarily provided by professional geophysicists under the same or similar circumstances. No other warranty or representation, either expressed or implied, is made by AGF in connection with its services unless in writing and signed by an authorized representative of AGF

February 4, 2025

Table of Contents

List of Figures

List of Tables

.

1. Introduction

The North Dakota Department of Water Resources (NDDWR) required airborne electromagnetic (AEM) data from two areas in central and southeastern North Dakota (Figure 1-1) in order to implement ground water management plans. NDDWR contracted Aqua Geo Frameworks, LLC (AGF) and SkyTEM to implement an AEM survey of selected areas within North Dakota. AGF performed the AEM acquisition QA/QC and advanced processing and inversion of SkyTEM's 304M system data. Specifically, AGF checked on a daily basis the SkyTEM 304M acquisition parameters (flight height, tilt-pitch, tilt-roll, ground speed) and conducted Laterally-Constrained Inversions (LCI) and Spatially-Constrained Inversions (SCI) of the 304M data that was compared to existing borehole data. The survey was implemented in two phases, one in an area in central North Dakota (Area 1) and the other in the southeast corner of the State (Area 2). The "as-flown" flight lines for Area 1 and Area 2 are presented in Figure 1-2 and Figure 1-3, respectively.

2. Schedule/Timeline

SkyTEM mobilized the 304M to the Wahpeton area on July 6, 2024. The system was checked, and ground tests and airborne tests were conducted on July 7, 2024, and production began and continued through July 25, 2024. Preliminary processing and LCI's were performed on the data from July 8, 2024 until July 26, 2024, as data was made available from SkyTEM.

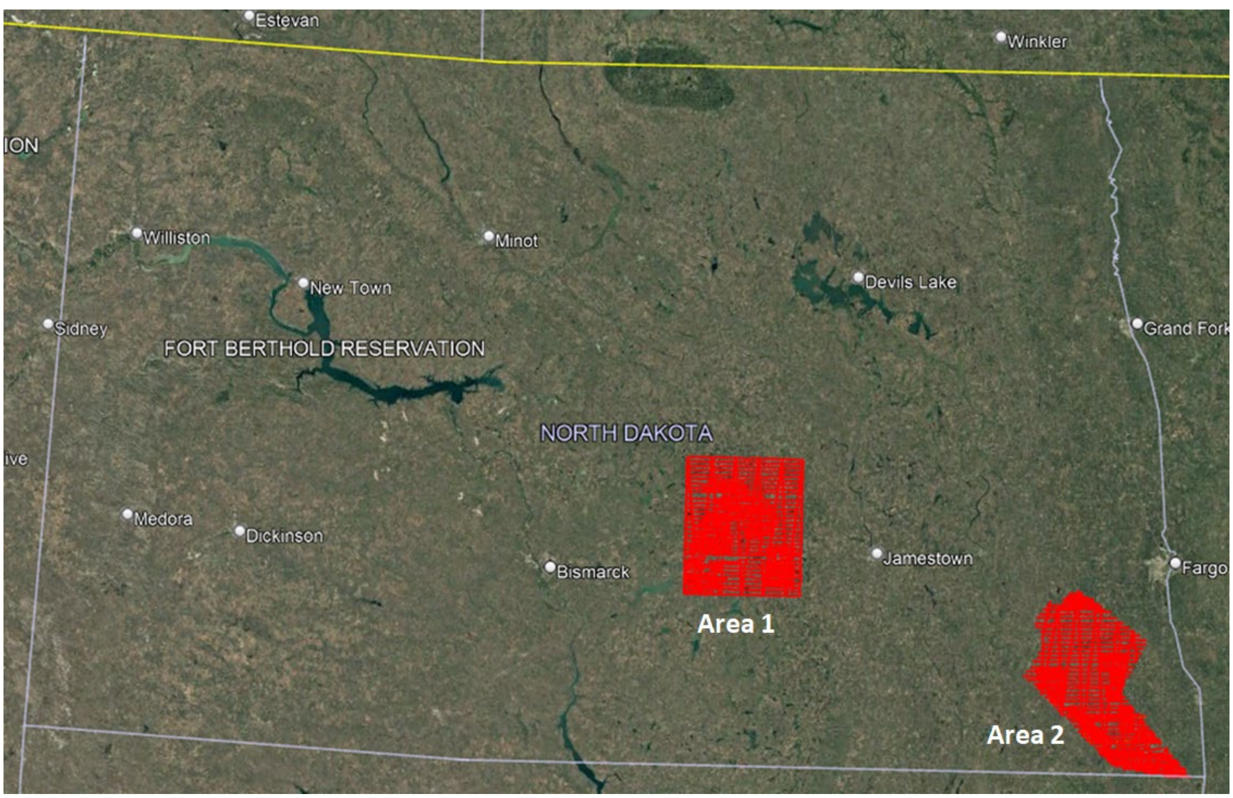

Figure 1-1. General location image in Google Earth of the Area 1 and Area 2 AEM survey areas in central and southeastern North Dakota, respectively.

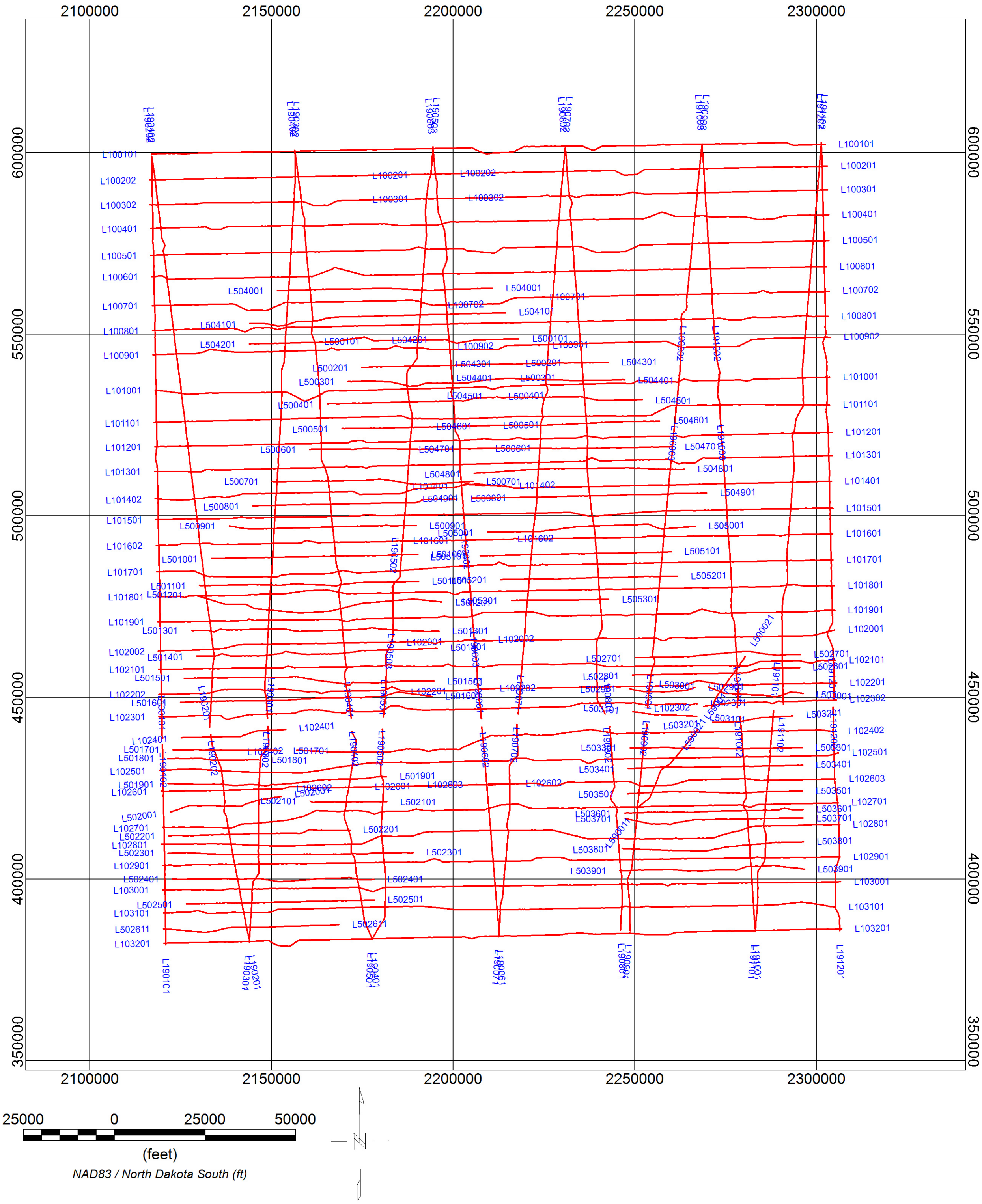

Figure 1-2. Area 1 as-flown SkyTEM 304M AEM data acquisition within central North Dakota.

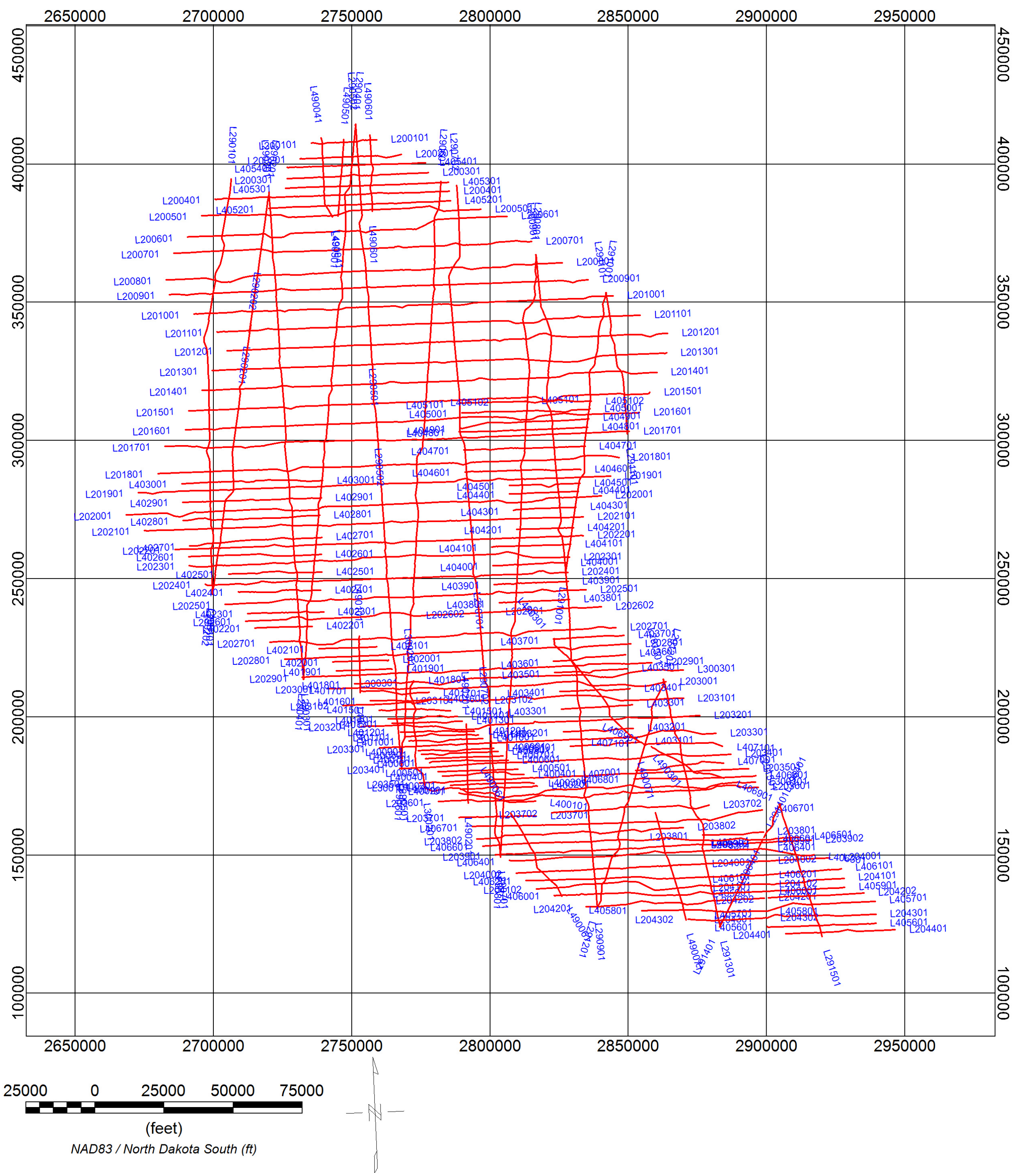

Figure 1-3. Area 2 as-flown SkyTEM 304M AEM data acquisition in southeastern North Dakota.

3. System Calibration/Ground Tests

3.1 Test Line Calibration

The SkyTEM 304M system was flown along a designated ‘test’ line in Area 2 at the start of the survey (Figure 3-1). The calibration process involved acquiring data with the system over the test hole locations. Then, acquired data were processed and a scale factor (time and amplitude) was applied so that the inversion process produces the model that approximates the known geology at the test hole locations. Final calibrations received from SkyTEM were applied to the data before the final SCI inversions.

3.2 System Ground Tests

Ground tests involved checking for system operation including the following sub-systems: 1) transmitter (Tx) current amplitude and stability including waveform; 2) receiver (Rx) functionality 3) altimeter operation; 4) GPS operation; 5) altitude sensor operation and calibration; 6) navigation and communication; 7) airborne magnetometer operation; 8) base station magnetometer stability and field strength stability; and 9) Differential Global Positioning Systems (DGPS) base station operation.

3.3 System Airborne Tests

Airborne tests were conducted by SkyTEM to verify the operation of the 304M system and are described in the SkyTEM report on the data acquisition.

3.4 Boreholes

Many borehole lithology logs were downloaded from the NDDWR Map Services (NDDWR, 2024), including both “Test Holes” and “Observation Wells”, for the general area of the survey. The boreholes were then down-sampled to only show the holes with NDDWR ownership within the database. In addition to the downloaded lithology logs, NDDWR provided geophysical logs for the test holes.

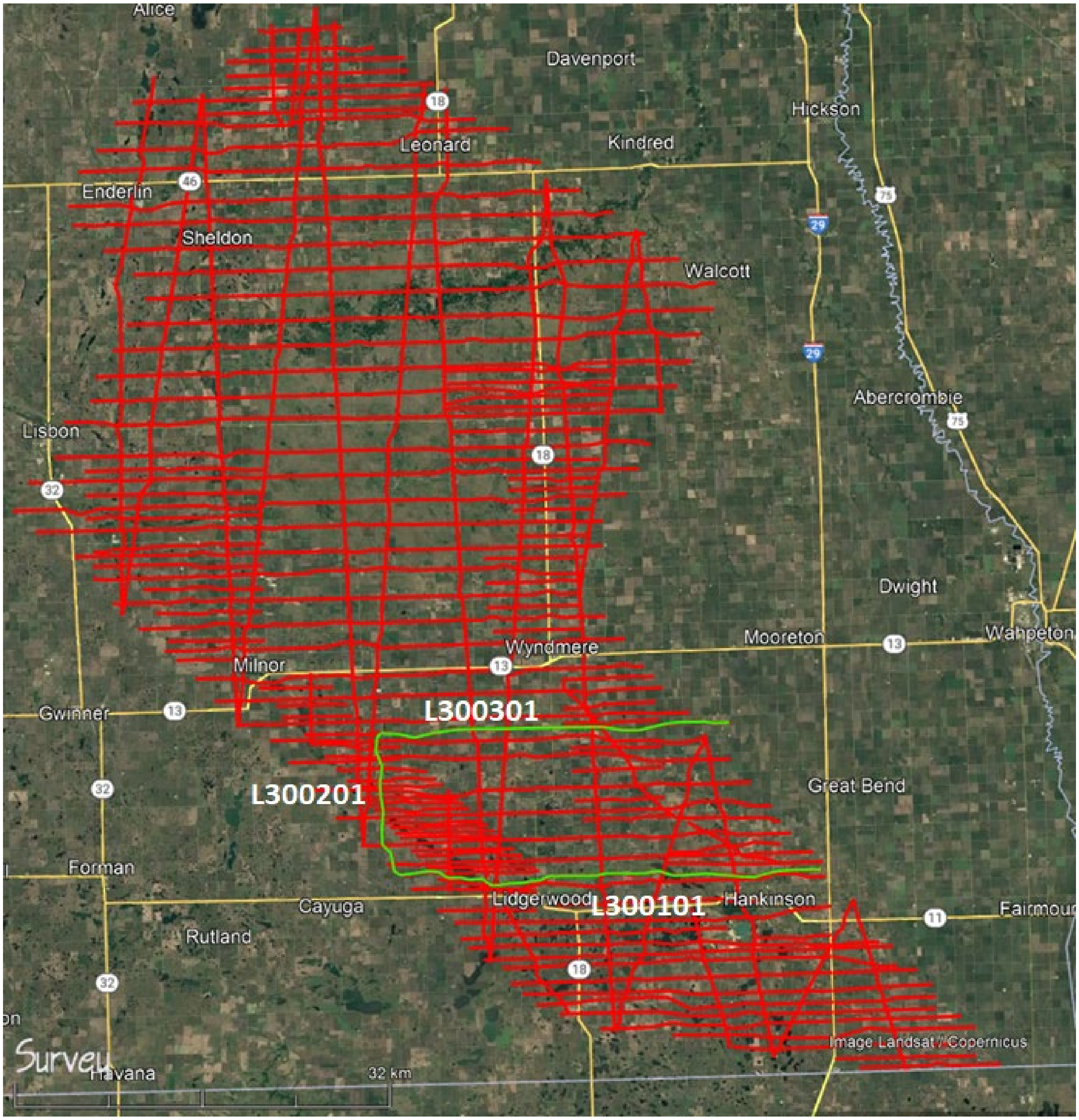

Figure 3-1. Google Earth image showing the Area 2 "test" line (green line) made up of what would become flight lines L300101, L300201, and L300301.

4. Data Acquisition

4.1 Acquisition Timing and As-Flown lines

The NDDWR 2024 AEM data acquisition was flown out of the Harry Stern Airport Wahpeton, Sky Haven Airport Enderlin, Thompson private airfield, Jamestown Regional Airport, and the Whitman private airfield. The production flights took place from July 7-25, 2024 and a total of forty-three (43) were required to acquire the 2024 Area 1 and Area 2 AEM data. As the 304M system was ferried from Nebraska, Area 2 was flown first. The Area 1 and Area 2 infill flight lines were flown based on the results of the preliminary LCI's of the 304M data. Line-km totals from each flight are provided in Table 4-1. Note that the 304M data in the databases are indexed by line and flight number. Figure 4-1 and Figure 4-2 present an "As-Flown" map view as well as timing of the data collection within Area 1 and Area 2, respectively. In some locations, the as-flown lines deviate from the planned lines due to infrastructure and safety as determined by the pilot. The line totals were calculated from the preliminary databases using Geosoft Oasis montaj Total Distance GX (Geosoft, 2024)

Table 4-1. Flight line production by flight.

Date	# Flights	Line-km Total	Line-mile Total	
7/7/2024	1	152.0	94.5	AREA 2 3302.4 line-km
7/8/2024	2	281.6	175.0	
7/9/2024	3	539.5	335.3	
7/10/2024	3	458.4	284.9	
7/11/2024	2	322.7	200.6	
7/12/2024	1	137.2	85.3	
7/13/2024	3	546.7	339.8	
7/14/2024	3	499.8	310.6	
7/15/2024	1	82.4	51.2	
7/16/2024	3	282.1	175.3	
7/17/2024	1	169.9	105.6	AREA 1 3441.7 line-km
7/18/2024	3	505.0	313.9	
7/19/2024	3	524.2	325.8	
7/20/2024	3	488.6	303.7	
7/21/2024	3	510.5	317.3	
7/22/2024	3	460.3	286.1	
7/23/2024	1	186.2	115.7	
7/24/2024	2	328.2	204.0	
7/25/2024	2	268.8	167.1	
	43			
Total		6744.1	4191.5	

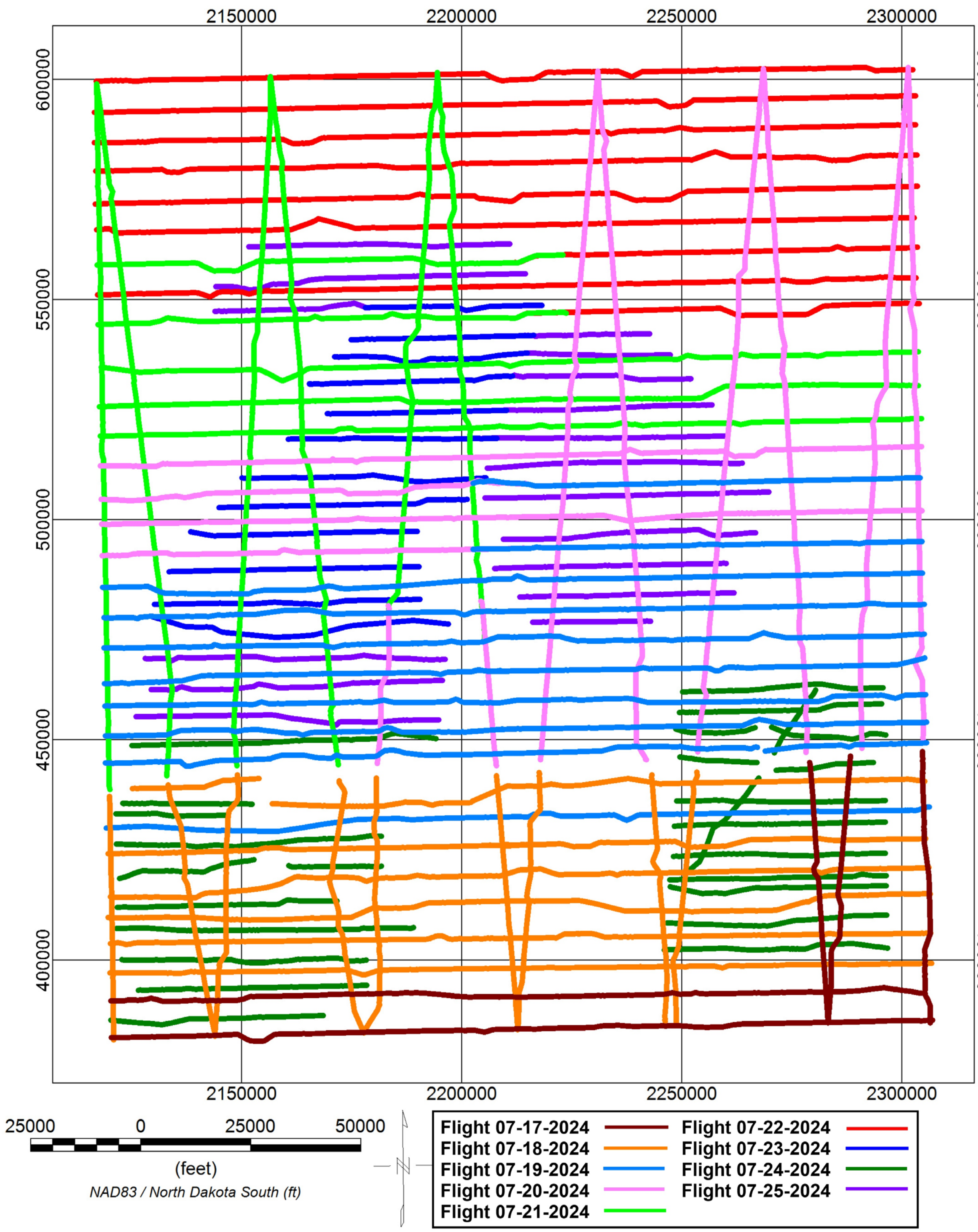

Figure 4-1. As-Flown map showing timing of the Area 1 AEM survey data acquisition. The map projection is NAD83 North Dakota State Plane South in feet.

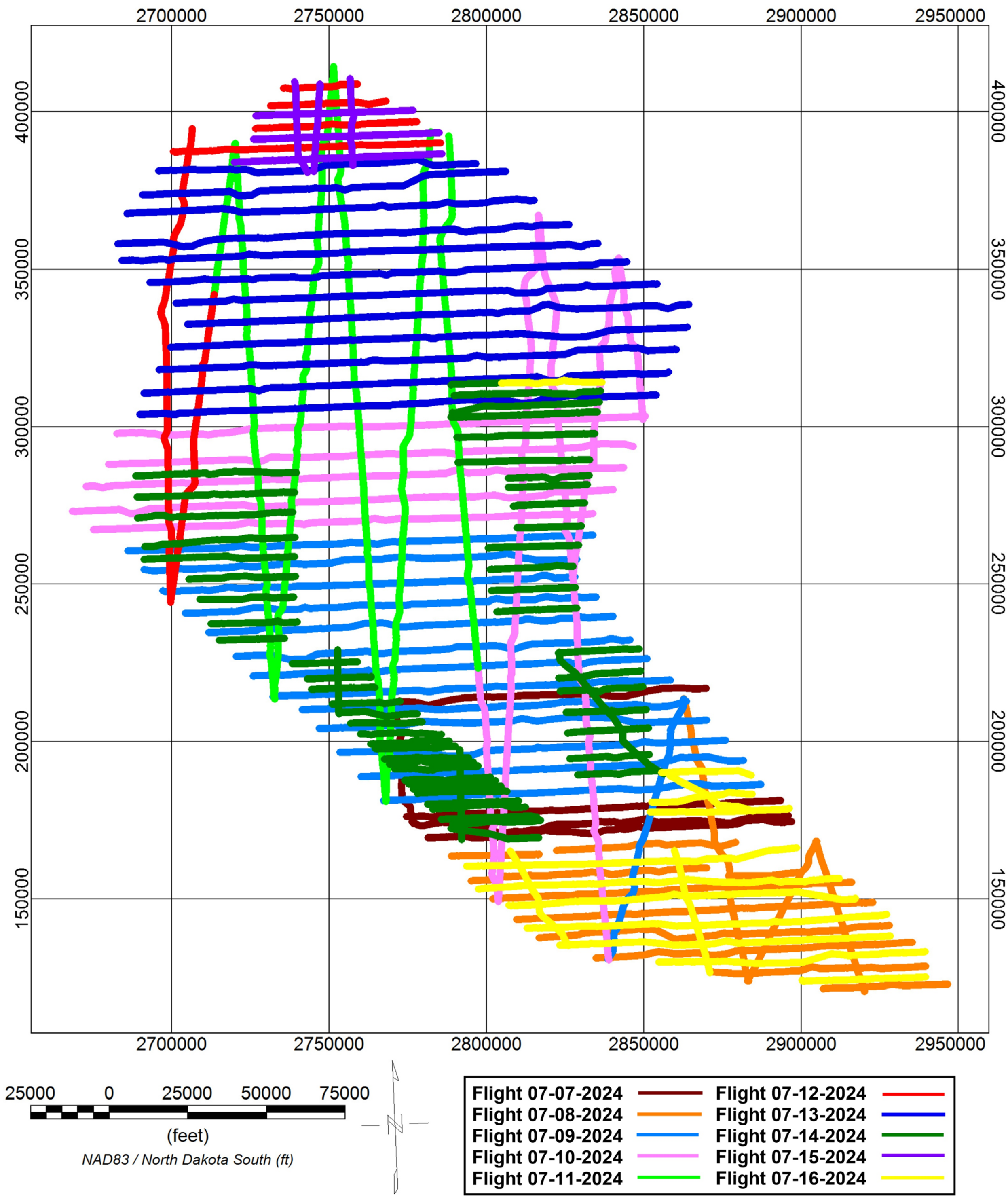

Figure 4-2. As-Flown map showing timing of the Area 2 AEM survey data acquisition. The map projection is NAD83 North Dakota State Plane South in feet.

4.2 System Flight Height, Ground Speed, and Tilt (Pitch, Roll) Parameters

The system height was specified at ~30 meters (98.4 ft); however, due to safety and other judgments by the pilot the flight heights deviated. The goal was to maintain a height as low as possible in the window from 82 to 164 ft (25 to 50 m) above ground level (AGL). The mean height for Area 1 was 113 ft (34.4 m) with a minimum of 57 ft (17.5 m) and a maximum of 418 ft (127.3 m); and for Area 2 the mean height was 119 ft (36.2 m) with a minimum of 70 ft (21.1 m) and the maximum of 306 ft (93.2 m). The maximum flight heights were encountered over large powerlines or other obstacles. Those data were removed from the dataset before inversion due to EM coupling so as to not impact the final product. Maps of the flight heights throughout the survey area are presented in Figure 4-3 for Area 1 and in Figure 4-4 for Area 2.

Maps of the equivalent ground speeds recorded for the Area 1 and Area 2 304M AEM surveys are presented in Figure 4-5 and Figure 4-6. respectively. Ground speed mean for Area 1 was 53 miles/hr (85.3 km/hr), the minimum was 23 miles/hr (36.6 km/hr) and the maximum was 81 miles/hr (130 km/hr). For Area 2 the ground speed mean was 53 miles/hr (86 km/hr), the minimum was 19 miles/hr (31 km/hr), and maximum was 79 miles/hr (127 km/hr).

Maps of the tilt-pitch angle (X-direction) recorded for the Area 1 and Area 2 304M AEM surveys are presented in Figure 4-7 and Figure 4-8. respectively. The tilt-pitch angle mean for Area 1 was -1.2 degrees, the minimum was -15.7 degrees, and the maximum was 11.0 degrees. For Area 2 the tilt-pitch mean was -1.1 degrees, the minimum -14.7 degrees, and maximum was 13.2 degrees.

Maps of the tilt-roll angle (Y-direction) recorded for the Area 1 and Area 2 304M AEM surveys are presented in Figure 4-9 and Figure 4-10. respectively. The tilt-roll angle mean for Area 1 was 1.2 degrees, the minimum was -6.3 degrees, and the maximum was 10.7 degrees. For Area 2 the tilt-roll mean was 1.1 degrees, the minimum -9.5 degrees, and maximum was 17.9 degrees.

4.3 Power Line Noise Intensity and Magnetics

The SkyTEM 304M system is configured to record an estimate of the amplitude of the 60 Hz signals in the "_60Hz_Intensity" channel (or the power line noise intensity (PLNI)). These PLNI maps are useful when investigating the impacts of powerlines on the data quality. The 60 Hz powerline signals have little impact on the Rx signal due to time-gating and proper filtering. However, the conductive wires that are used to transmit the power do cause EM coupling impacts on the data and those data need to be removed prior to inversion. The PLNI for the Area 1 and Area 2 AEM surveys are presented in Figure 4-11 and Figure 4-12, respectively.

As part of the SkyTEM 304M system, a Total Field magnetometer is included in the data acquisition package. The magnetic field signal is useful for determining deep seated geological contacts and is also extremely valuable for locating intrusive bodies. Neither of those was the target of the surveys within Area 1 or Area 2. However, the magnetic field is also sensitive to anthropogenic features that contain ferrous metal and is also used in the electromagnetic decoupling process. A plot of the magnetic Total Field intensity in the Area 1 AEM survey area is presented in Figure 4-13 and for Area 2 in Figure 4-14.

Both geological structure and cultural features can be identified within the survey area, but the signal is dominated by the complex basement features.

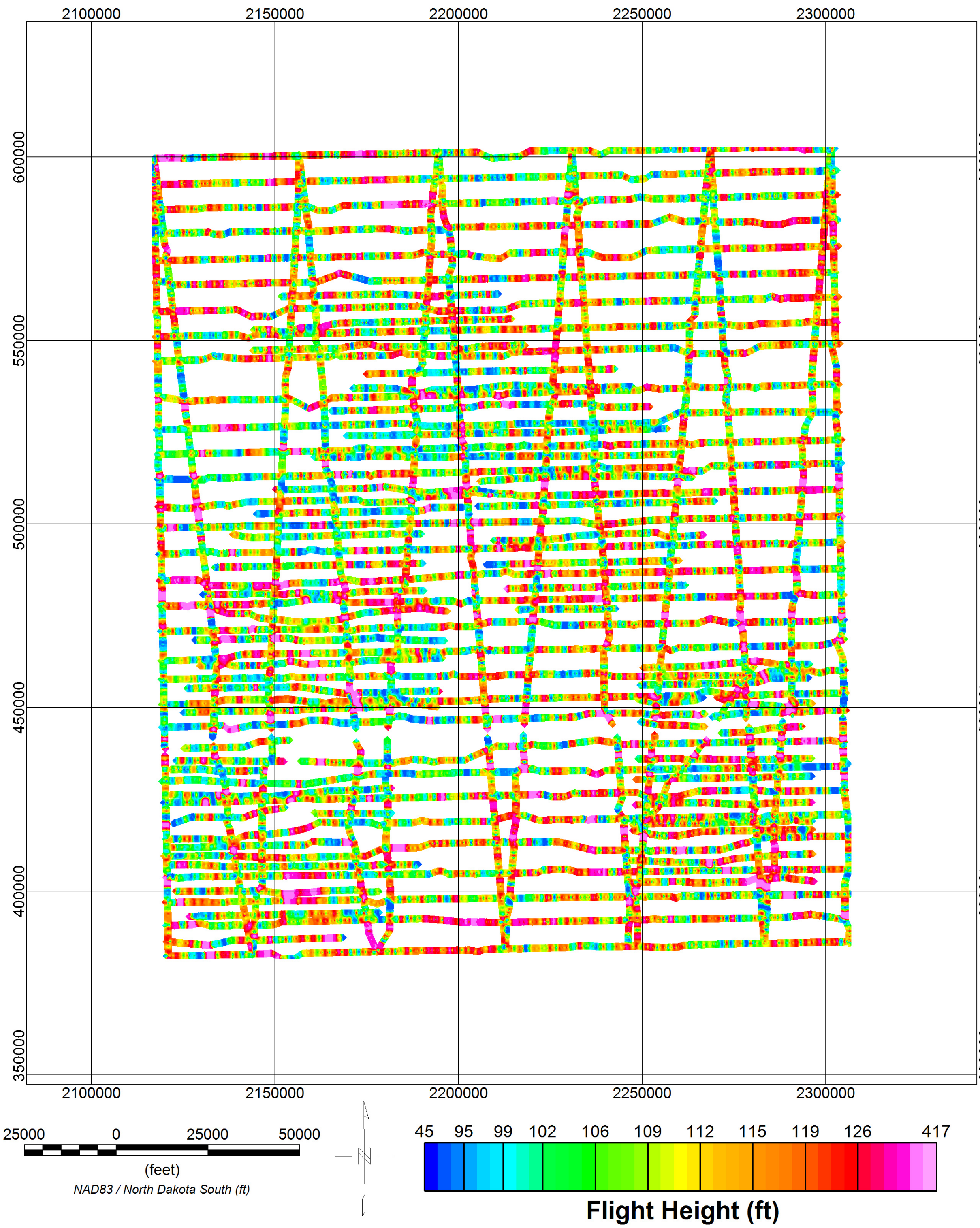

Figure 4-3. Map of the system height recorded during the Area 1 AEM survey. The map projection is NAD83 North Dakota State Plane South in feet.

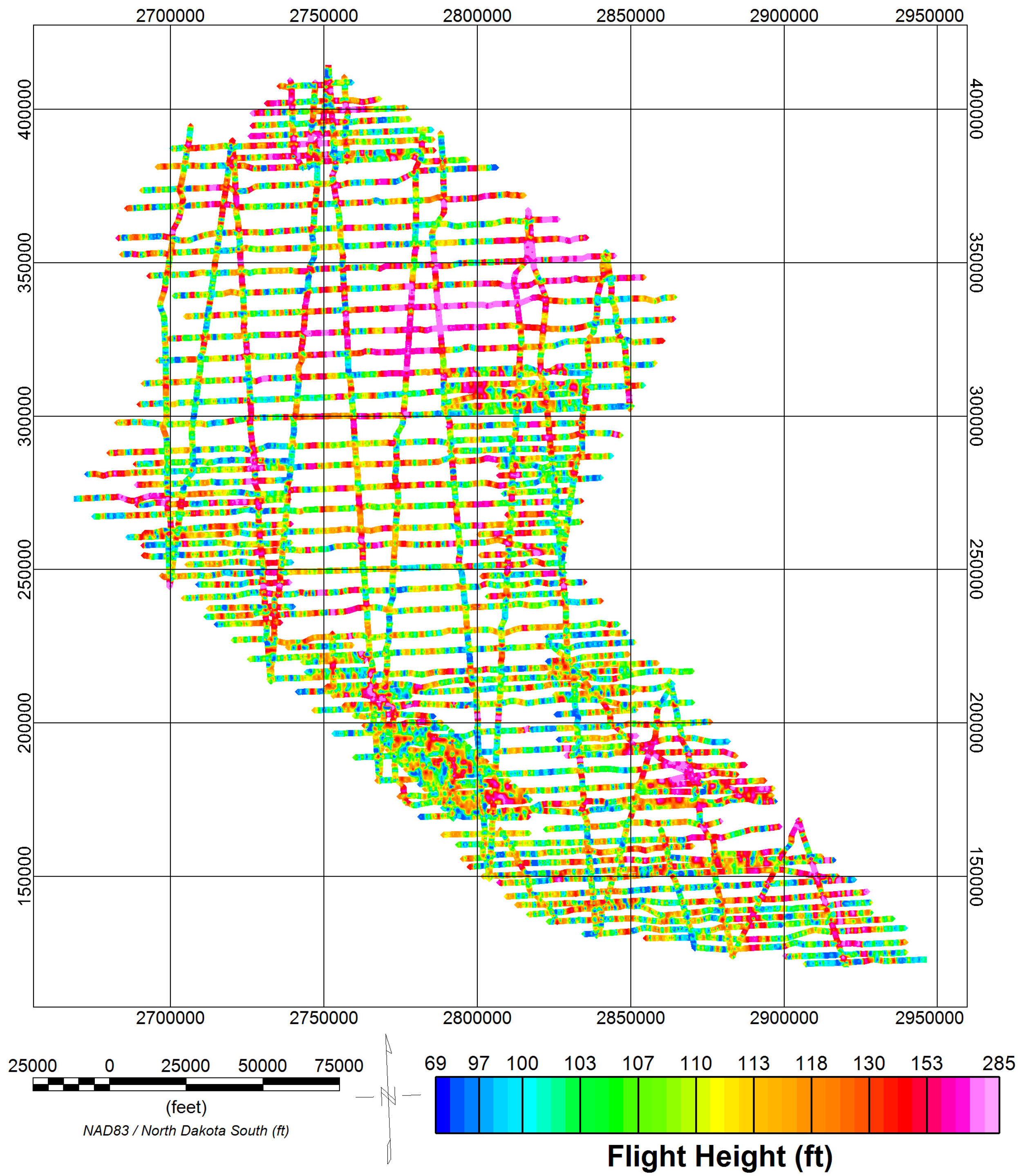

Figure 4-4. Map of the system height recorded during the Area 2 AEM survey. The map projection is NAD83 North Dakota State Plane South in feet.

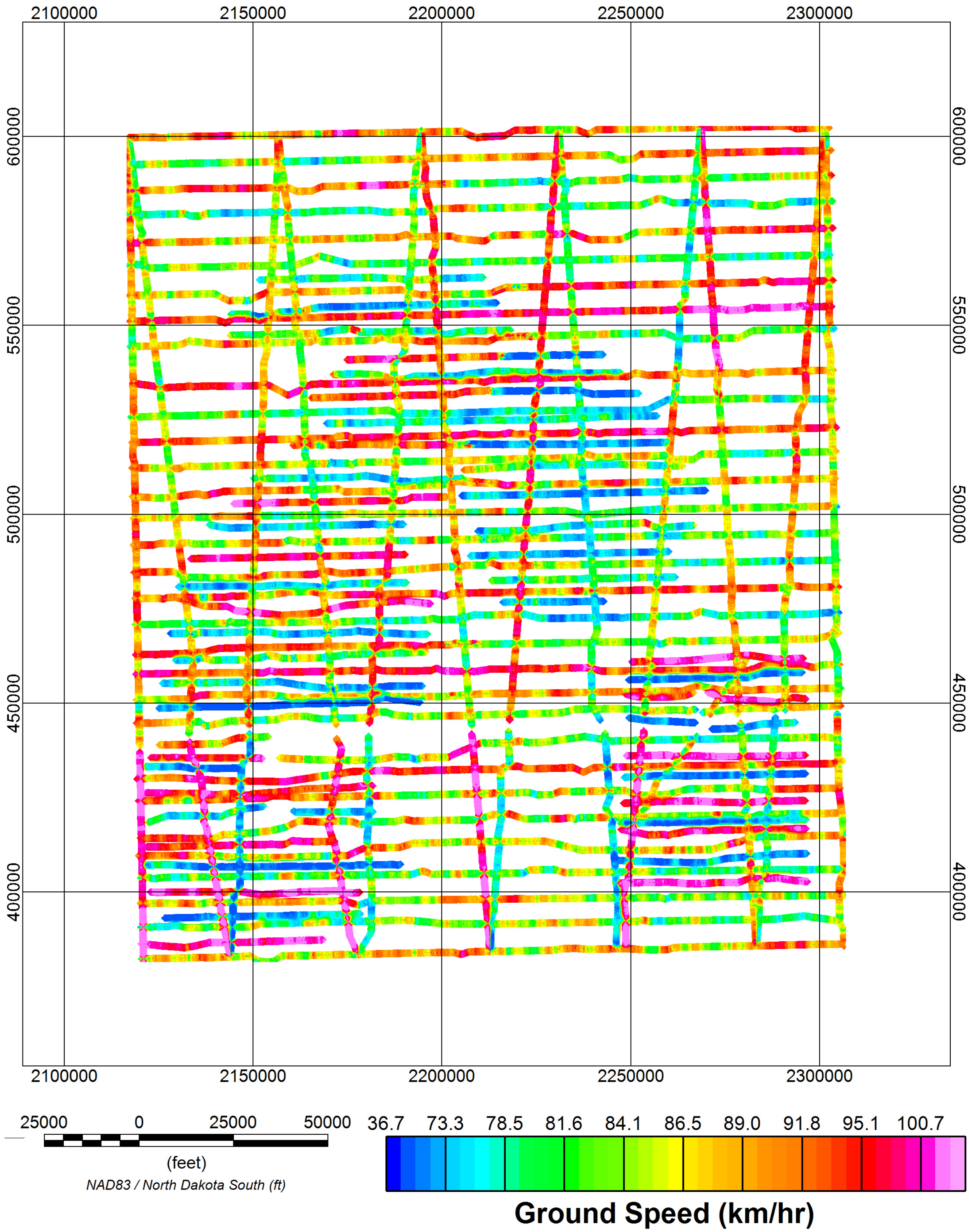

Figure 4-5. Map of the system equivalent ground speed recorded during the Area 1 AEM survey. The map projection is NAD83 North Dakota State Plane South in feet.

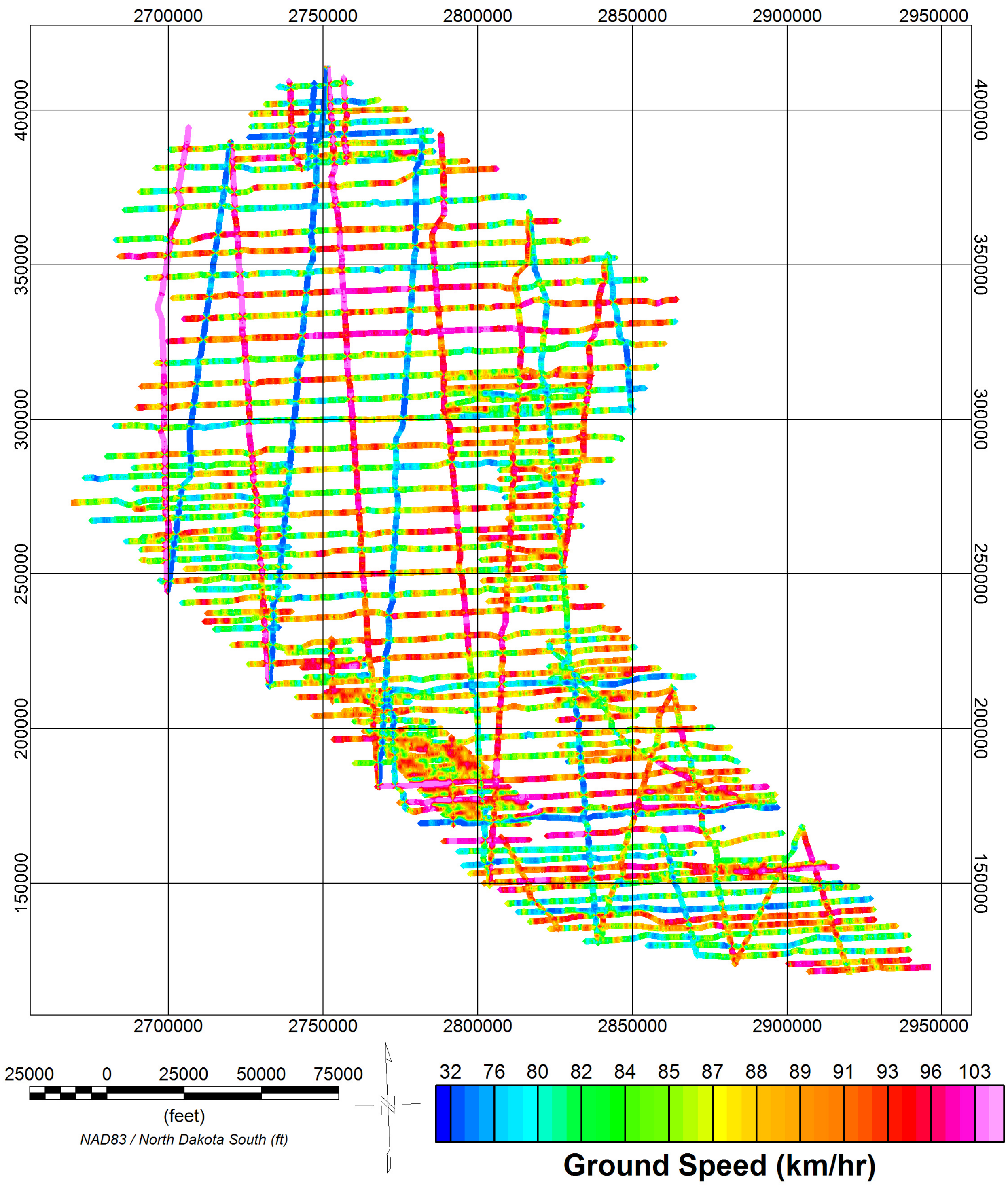

Figure 4-6. Map of the system equivalent ground speed recorded during the Area 2 AEM survey. The map projection is NAD83 North Dakota State Plane South in feet.

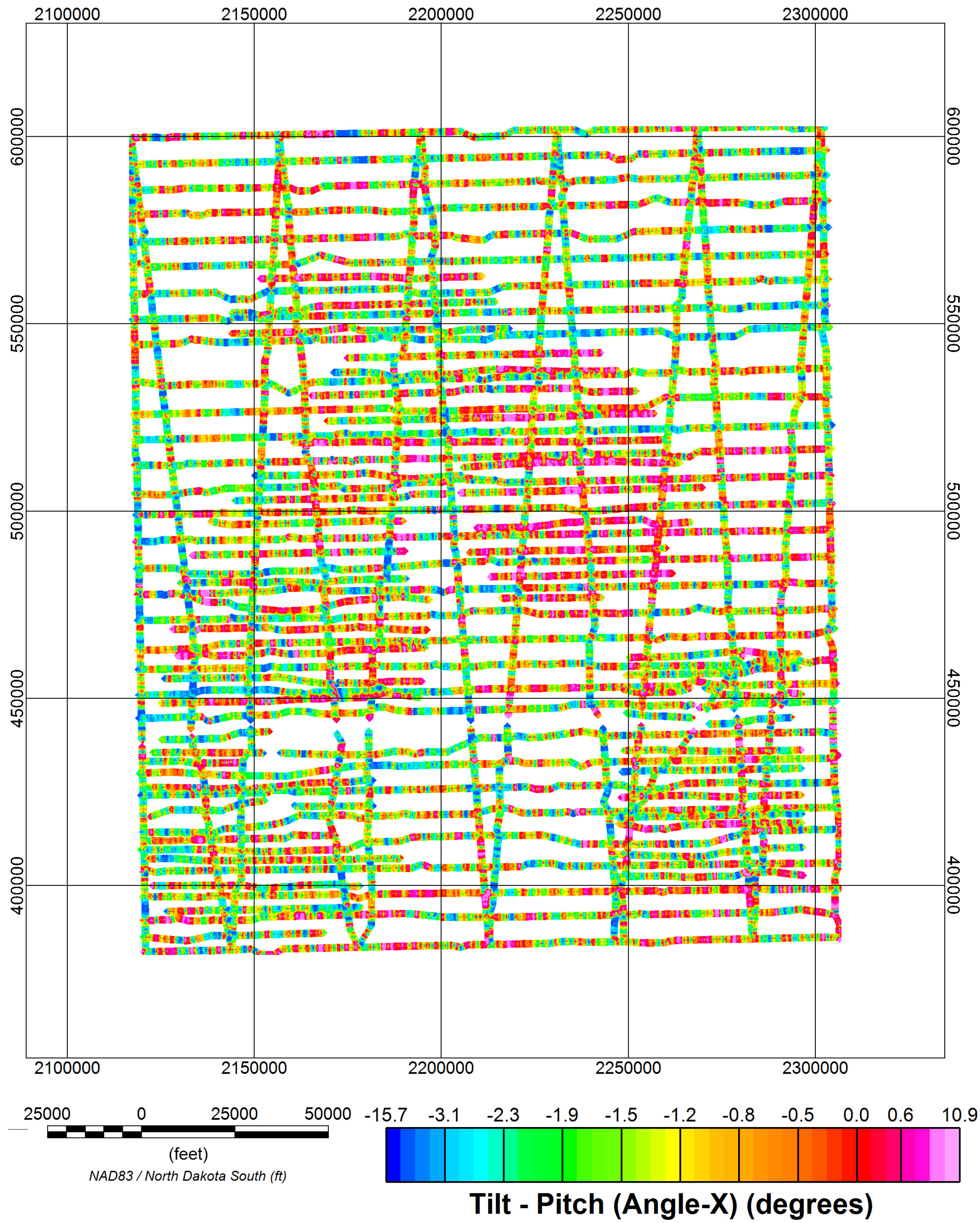

Figure 4-7. Map of the system tilt in the X-direction, the Pitch, recorded during the Area 1 AEM survey. The map projection is NAD83 North Dakota State Plane South in feet.

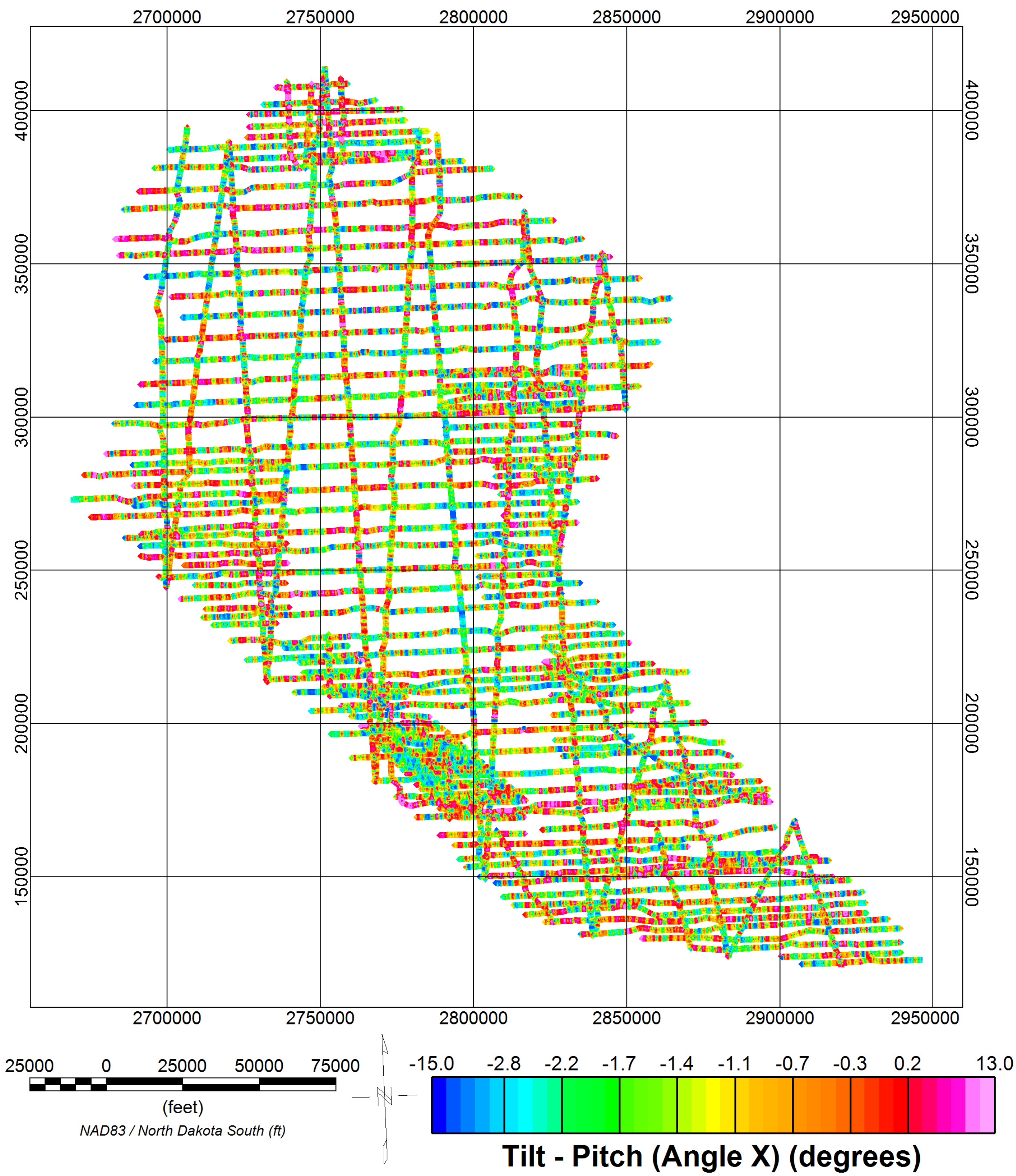

Figure 4-8. Map of the system tilt in the X-direction, the Pitch, recorded during the Area 2 AEM survey. The map projection is NAD83 North Dakota State Plane South in feet.

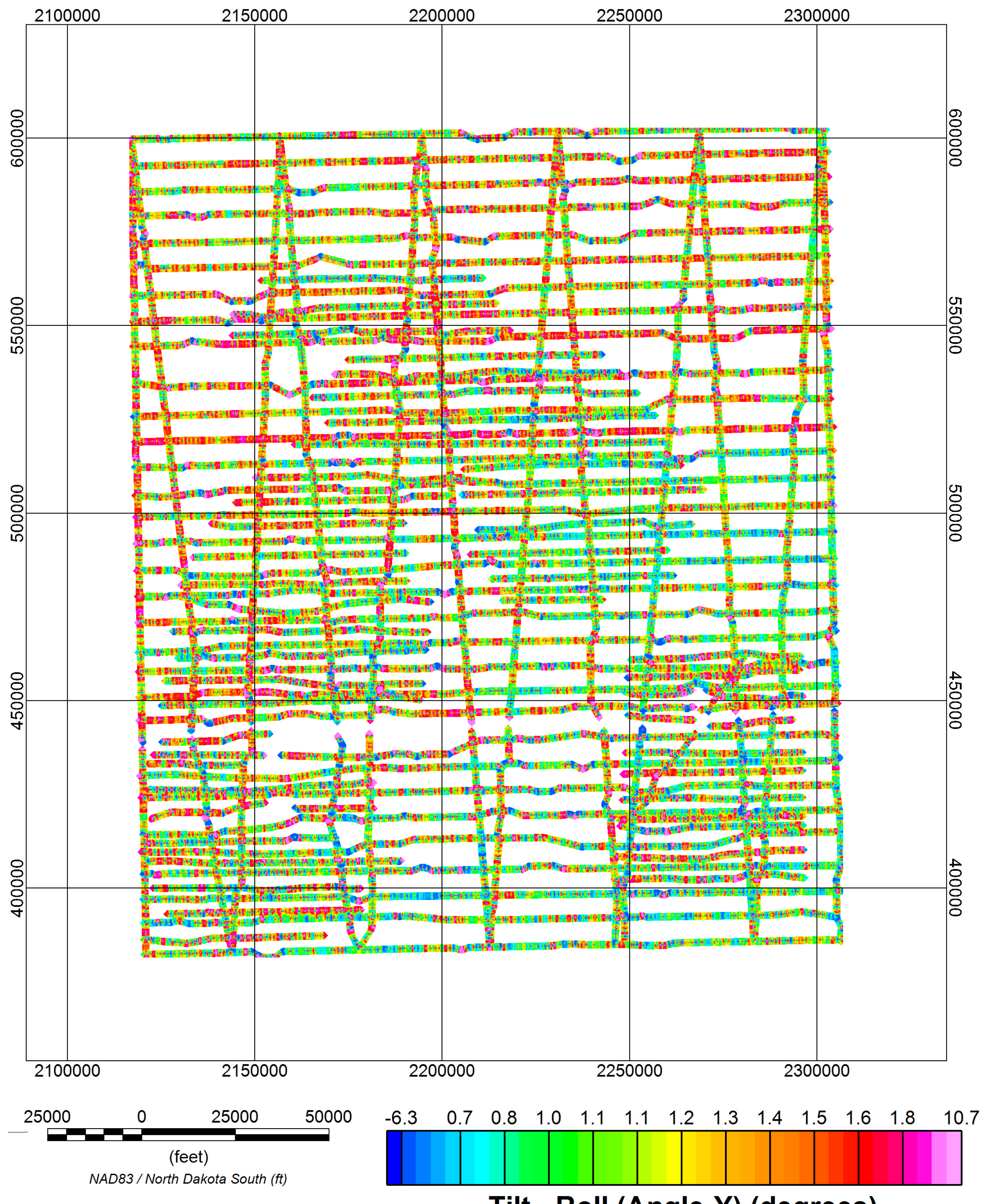

Figure 4-9. Map of the system tilt in the Y-direction, the Roll, recorded during the Area 1 AEM survey. The map projection is NAD83 North Dakota State Plane South in feet.

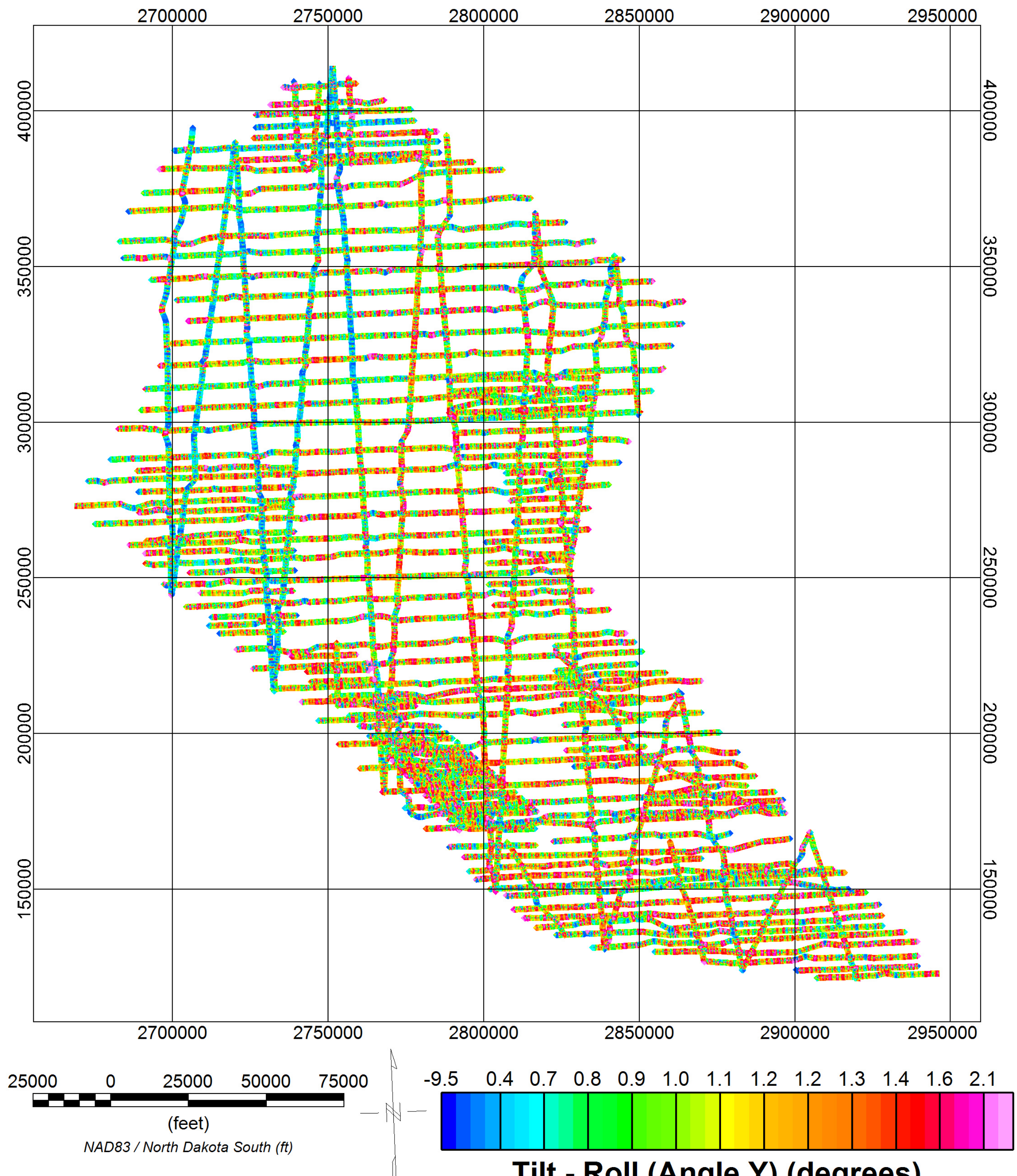

Figure 4-10. Map of the system tilt in the Y-direction, the Roll, recorded during the Area 2 AEM survey. The map projection is NAD83 North Dakota State Plane South in feet.

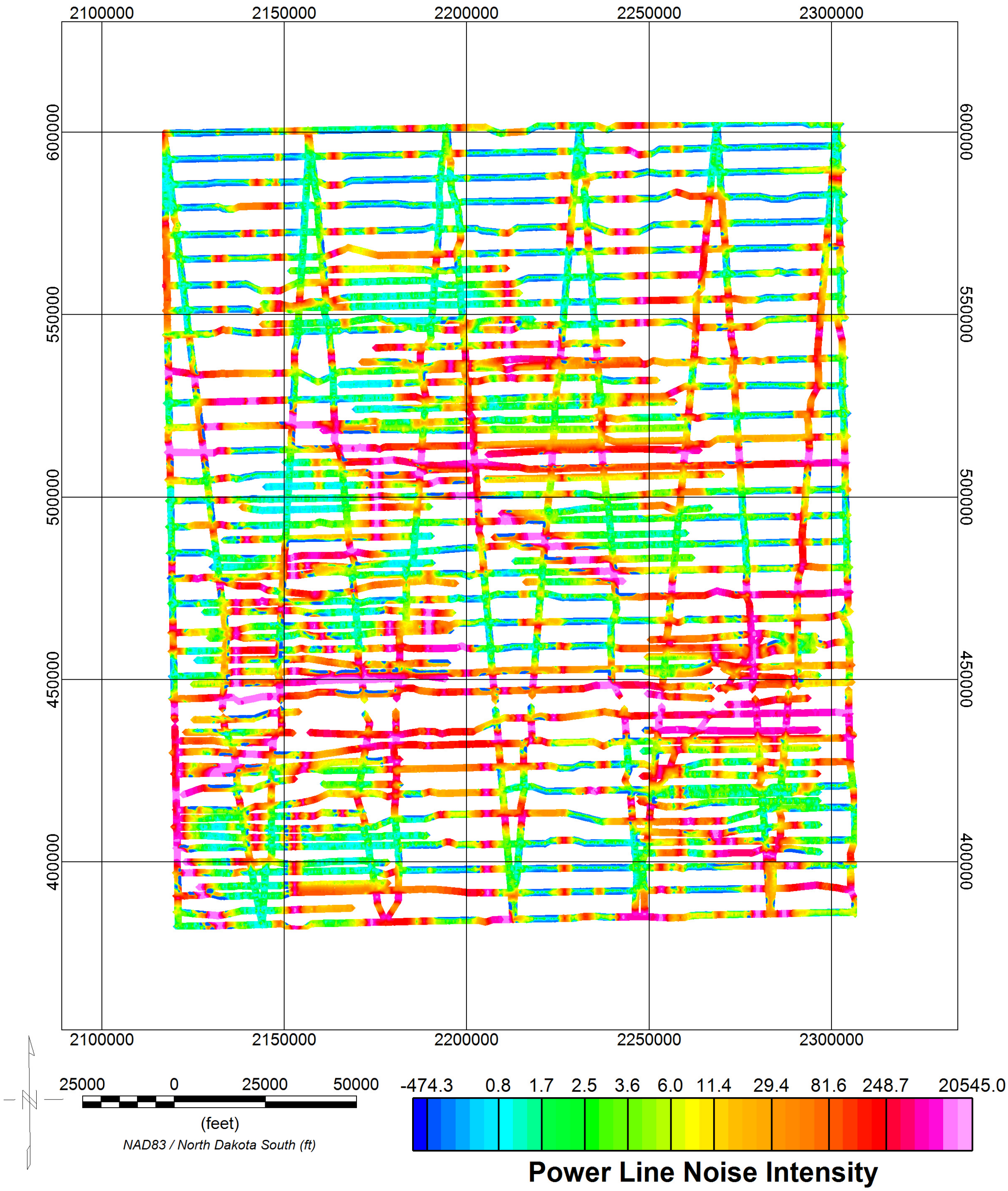

Figure 4-11. Map of the 60 Hz Power Line Noise Intensity (PLNI) recorded during the Area 1 AEM survey. The map projection is NAD83 North Dakota State Plane South in feet.

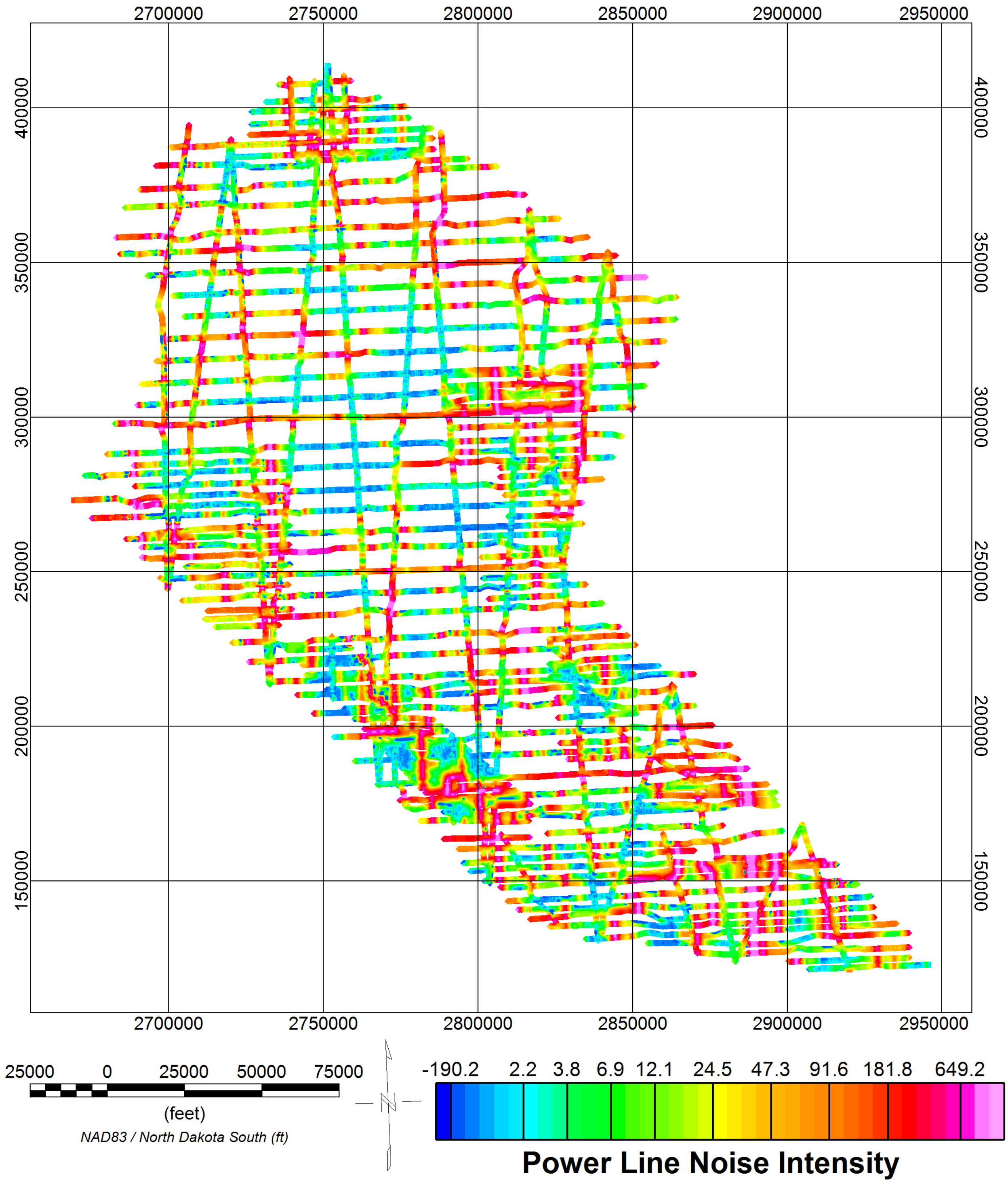

Figure 4-12. Map of the 60 Hz Power Line Noise Intensity (PLNI) recorded during the Area 2 AEM survey. The map projection is NAD83 North Dakota State Plane South in feet.

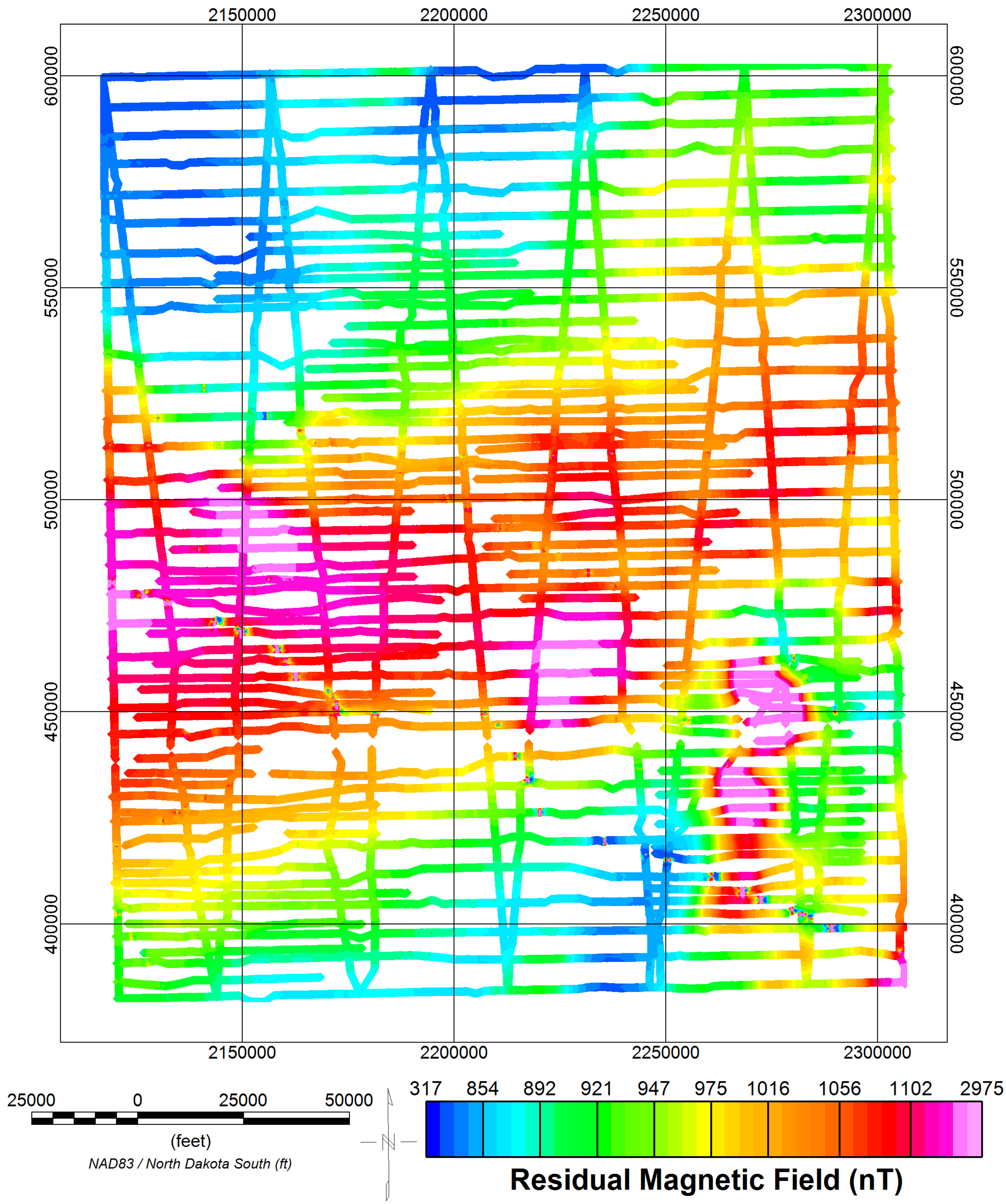

Figure 4-13. Residual magnetic total field (RMF) Intensity for the Area 1 AEM survey area. The map projection is NAD83 North Dakota State Plane South in feet.

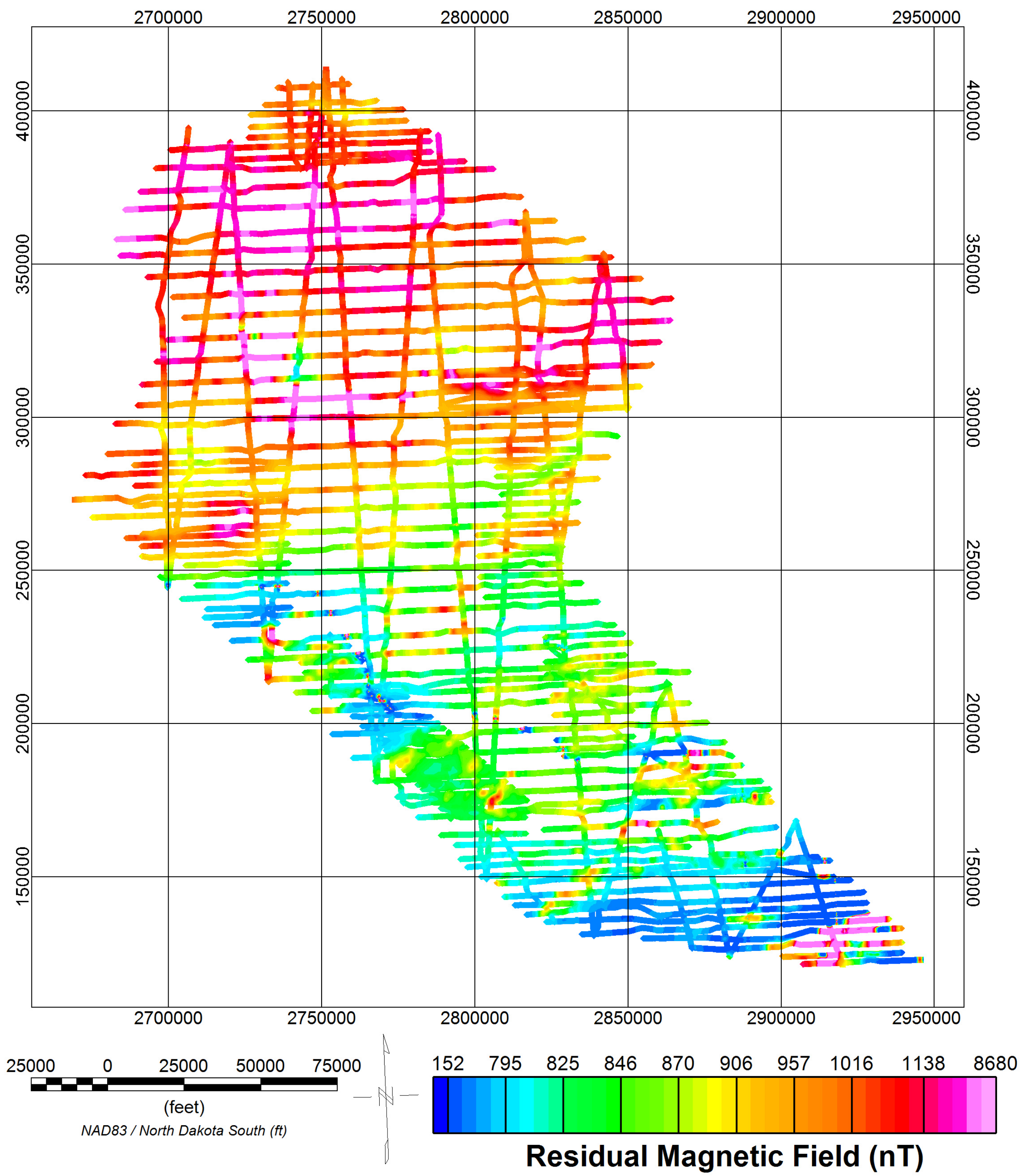

Figure 4-14. Residual magnetic total field (RMF) Intensity for the Area 2 AEM survey area. The map projection is NAD83 North Dakota State Plane South in feet.

5. Processing and Laterally Constrained Inversions

5.1 Primary Field Processing

A standard SkyTEM data acquisition procedure involves review of acquired raw data by SkyTEM for Primary Field Compensation (PFC) prior to continued data processing by AGF (Schamper et al., 2014). The primary field of the transmitter affects the recorded early time gates which, in the case of the Low Moment (LM), are helpful in resolving the near surface resistivity structure of the ground. The LM waveform is calculated and then used in the PFC correction to correct the early time gates.

5.2 Automatic Processing

The AEM data collected by the SkyTEM304M were processed using Aarhus Workbench version 2024.1.1 (at Aarhus Geosoftware (https://www.aarhusgeosoftware.dk/aarhus-workbench) described in HydroGeophysics Group, Aarhus University (2011).

Automatic processing algorithms provided within the Workbench program are initially applied to the AEM data. DGPS locations were filtered using a stepwise, second-order polynomial filter of 10 seconds with a beat time of 0.5 second, based on flight acquisition parameters. The altitude data were corrected using a series of two polynomial filters. The lengths of the eighth-order polynomial filters were set to 15 seconds and 12 seconds with shift lengths of six (6) seconds. The lower and upper thresholds were 1 and 100 meters, respectively.

Trapezoidal spatial averaging filters were next applied to the AEM data. The times used to define the trapezoidal filters for the SkyTEM 304M data were 1.0×10^{-5} sec, 1.0×10^{-4} sec, and 1.0×10^{-3} sec with widths of 3, 6, and 18 seconds. The trapezoid sounding distance was set to 1.0 seconds and the left/right setting, which requires the trapezoid to be complete on both sides, was turned on. The spike factor and minimum number of gates (as a percent (%)) were both set to 20 percent.

5.3 Manual Processing and Laterally-Constrained Inversions

After the implementation of the automatic filtering, the AEM data were manually examined using a sliding two-minute time window. The data were examined for possible electromagnetic coupling with surface and buried utilities and metal, as well as for late time-gate noise. Data affected by these were removed. Areas were also cut out where the system height was flown greater than approximately 65 m (213 ft) above the ground surface which caused a severe decrease in the signal level.

The AEM data were then inverted using a Laterally-Constrained Inversion (LCI) algorithm (Aarhus Geosoftware, 2024). The LCI uses nearby soundings along the flight lines as constraints. The profile and depth slices were examined, and any remaining electromagnetic couplings were masked out of the data set. Vertical constraints on the resistivity were set at 2.7 and at 1.6 for the horizontal resistivity constraints with a reference distance of 100 m (328 ft) and a fall-off power of 0.75. The data were processed, edited, and inverted as they became available with the goal of having the analysis of each day's acquired data completed before the next data became available. The smooth model 40-layer structure used in the LCI inversions is presented in Table 5-1.

Table 5-1. Thickness and depth to bottom for each layer in the AEM earth models for the Laterally- (LCI) and Spatially-Constrained (SCI) inversions. The thickness of the model layers increase with depth as the resolution of the AEM technique decreases.

Layer	Depth to Bottom (ft)	Thickness (ft)	Depth to Bottom (m)	Thickness (m)	Layer	Depth to Bottom (ft)	Thickness (ft)	Depth to Bottom (m)	Thickness (m)
1	6.6	6.6	2.0	2.0	21	276.8	23.0	84.3	7.0
2	13.6	7.0	4.1	2.1	22	301.2	24.4	91.8	7.5
3	21.0	7.4	6.4	2.3	23	327.3	26.0	99.7	7.9
4	28.9	7.9	8.8	2.4	24	355.0	27.7	108.2	8.4
5	37.4	8.4	11.4	2.6	25	384.5	29.5	117.2	9.0
6	46.3	9.0	14.1	2.7	26	415.9	31.4	126.7	9.6
7	55.9	9.6	17.0	2.9	27	449.3	33.4	136.9	10.2
8	66.1	10.2	20.1	3.1	28	484.9	35.6	147.8	10.9
9	76.9	10.8	23.4	3.3	29	522.8	37.9	159.3	11.6
10	88.4	11.5	26.9	3.5	30	563.2	40.4	171.6	12.3
11	100.7	12.3	30.7	3.7	31	606.1	42.9	184.7	13.1
12	113.8	13.1	34.7	4.0	32	651.9	45.7	198.7	13.9
13	127.7	13.9	38.9	4.2	33	700.6	48.7	213.5	14.8
14	142.5	14.8	43.4	4.5	34	752.4	51.8	229.3	15.8
15	158.3	15.8	48.2	4.8	35	807.6	55.2	246.1	16.8
16	175.1	16.8	53.3	5.1	36	866.3	58.8	264.0	17.9
17	192.9	17.9	58.8	5.4	37	928.9	62.5	283.1	19.1
18	212.0	19.0	64.6	5.8	38	995.5	66.6	303.4	20.3
19	232.2	20.3	70.8	6.2	39	1066.4	70.9	325.0	21.6
20	253.8	21.6	77.3	6.6					

6. Spatially-Constrained Inversions

Following the initial decoupling and LCI analysis, Spatially-Constrained Inversions (SCI) were performed. SCIs use EM data along, and across, flight lines within user-specified distance criteria (Viezzoli et al., 2008).

Area 1 and Area 2 data were inverted using SCI smooth models with 40 layers, each with a starting resistivity of 5 ohm-m (equivalent to a 5 ohm-m halfspace). The thicknesses of the first layers of the models were about 2 m (6 ft) with the thicknesses of the consecutive layers increasing by a factor of about 1.08. The depths to the bottoms of the 39th layers were set to 325 m (1,066 ft), with thicknesses up to about 21 m (71 ft). The thicknesses of the layers increase with depth (Table 4-1) as the resolution of the technique decreases. The spatial reference distance, ***s***, for the constraints was set to 328 ft (100 m) with power law fall-off of 0.75. The vertical and lateral constraints, ***ResVerSTD*** and ***ResLatStD***, were set to 2.4 and 1.4, respectively, for all layers.

After final processing, 2,998.1 line-km (1,863.3 line-miles) of data were retained in Area 1 and 2,682.6 line-km (1,667.3 line-miles) of data were retained in Area 2 for the final inversions. This amounts to a data retention of about 87.1% for Area 1 and about 81.2% for Area 2. This high retention percentage is due to the careful optimization of flight line design for the Area 1 and Area 2 AEM surveys. An image of the comparison between the As-Flown flight lines and the data retained for inversion for Area 1 is presented in Figure 6-1 and for Area 2 in Figure 6-2.

In addition to the recovered resistivity models, the SCIs also produce data residual error values (single sounding error residuals) and Depth of Investigation (DOI) estimates. The data residuals compare the measured data with the response of the individual inverted models (Christensen et al., 2009). The DOI provides a general estimate of the depth to which the AEM data are sensitive to changes in the resistivity distribution at depth (Christiansen and Auken, 2012). Two DOI's are calculated: a "Conservative/Upper" DOI at a cumulative sensitivity of 1.2 and a "Standard/Lower" DOI set at a cumulative sensitivity of 0.6. A more detailed discussion on the DOI can be found in Asch et al. (2015). The Upper and Lower DOI's for Area 1 are presented in Figure 6-3 and Figure 6-4, respectively, and for Area 2 in Figure 6-5 and Figure 6-6, respectively.

These DOI plots are influenced by the electrical conductivity of the earth materials, EM noise, and system elevation. In the area of the survey, they are predominately reflections of the depth of the Cretaceous Pierre Shale. The spatial patterns are a good image of the bedrock configuration but should not be used as a depth of the bedrock as the system penetrates, and is able to image, into the Cretaceous Pierre Shale.

Figure 6-7 presents a histogram of the Area 1 AEM SCI inversion data/model residuals and Figure 6-8 presents a histogram of the Area 2 AEM SCI inversion data/model residuals. A Google Earth map of the SCI data residuals for the Area 1 AEM study area is presented in Figure 6-9 and a similar image of the data/model residuals for the Area 2 AEM study area is presented in Figure 6-10.The residual error equals, per sounding, the square root of the sum of the square of the true data minus the model value divided by the true data (Auken et al., 2015; Christiansen et al., 2016). What is important to note on these residual plots is that while there is a distribution of residual error between 0.19 and 0.68 for Area 1 and 0.17 and 0.70 for Area 2, the maximum amplitudes of the SCI residual error for both these areas are quite low. Typical residual errors are usually in the range of 0.50 -0.80. The errors for Area 1 and Area 2 are within these common error ranges. Typically, higher errors occur over power lines, which are usually located along roads and river channels. That is likely what can be observed over Area 1 and Area 2 in Figure 6-9 and Figure 6-10, respectively.

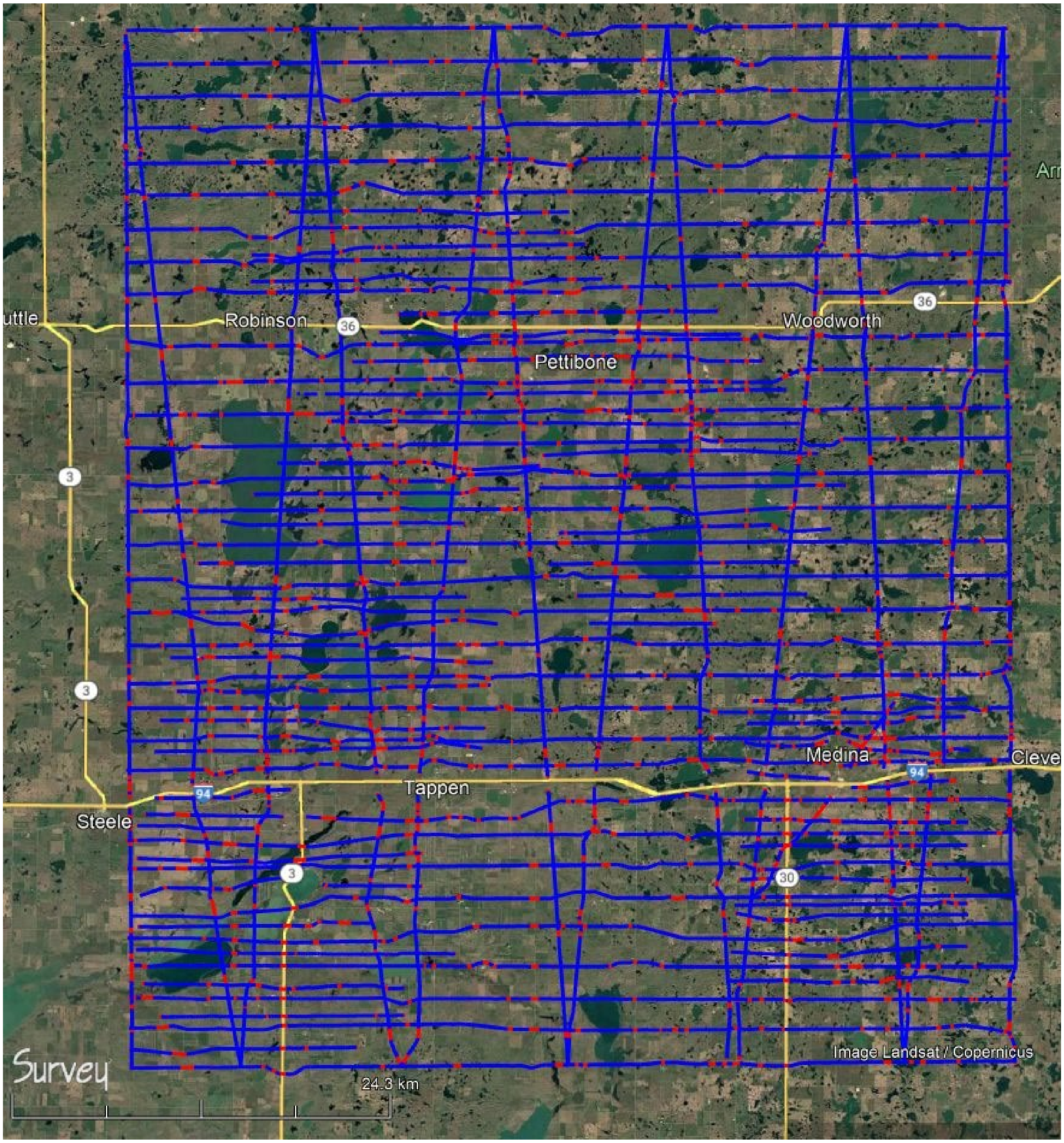

Figure 6-1. Comparison of the acquired data (red) versus the final retained data (blue) for the NDDWR Area 1 AEM survey area Final SCI inversion. This kmz is included in Appendix 3 Deliverables\KMZ.

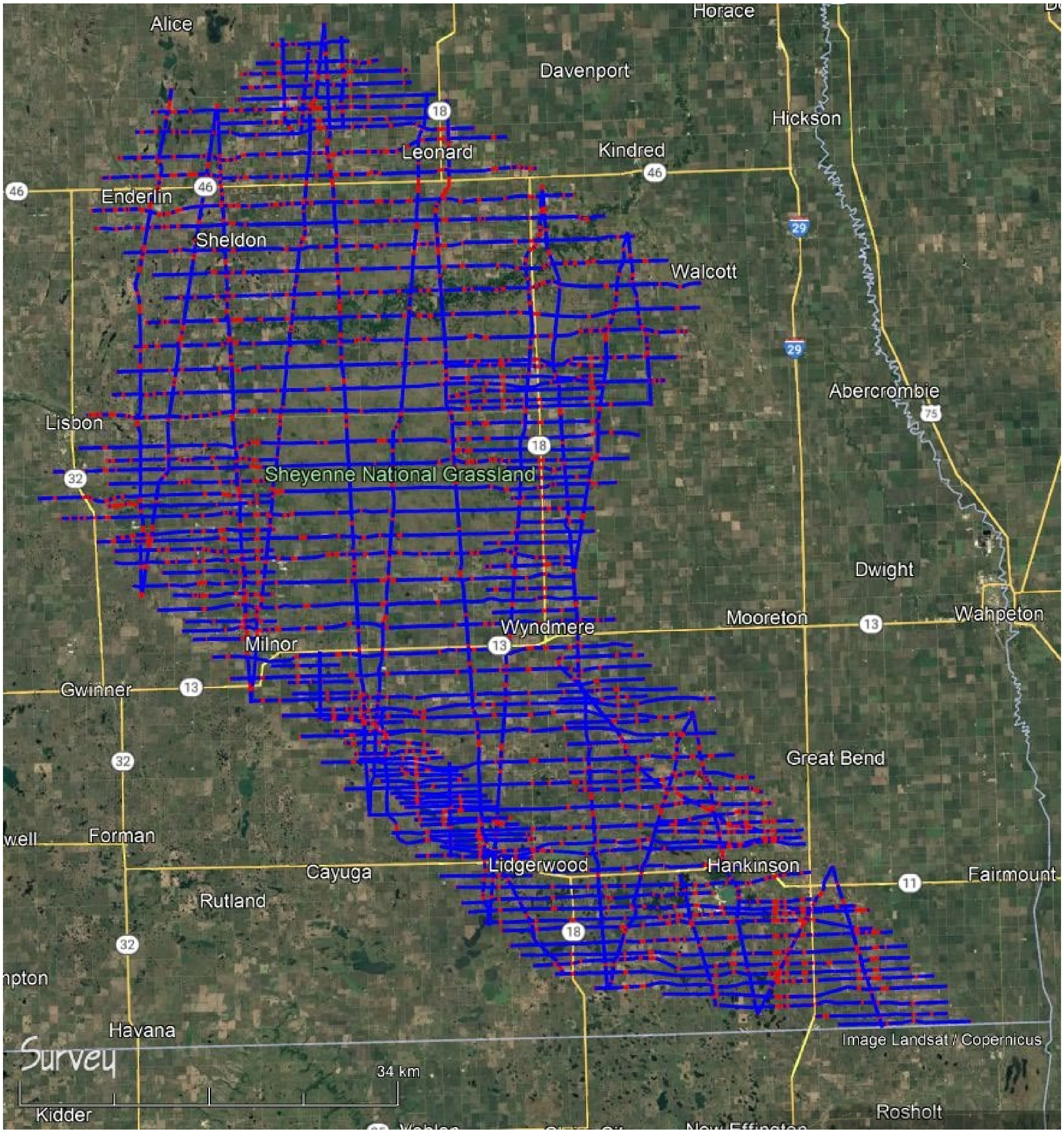

Figure 6-2. Comparison of the acquired data (red) versus the final retained data (blue) for the NDDWR Area 2 AEM survey area Final SCI inversion. This kmz is included in Appendix 3 Deliverables\KMZ.

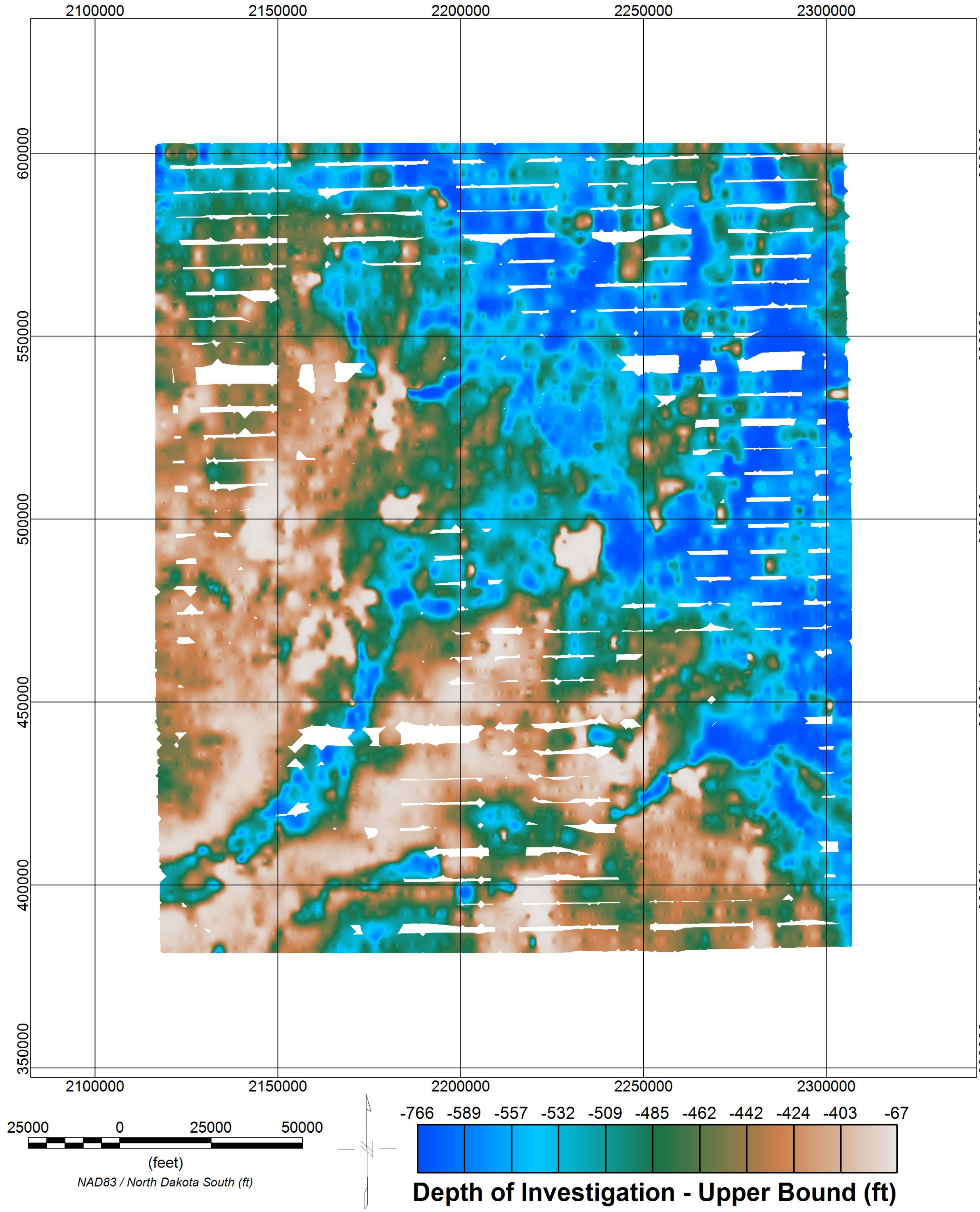

Figure 6-3. Map of the Upper Depth of Investigation for the Area 1 AEM SCI inversion. These data are included as a Google Earth KMZ file in Appendix 3. The map projection is NAD83 North Dakota State Plane South in feet.

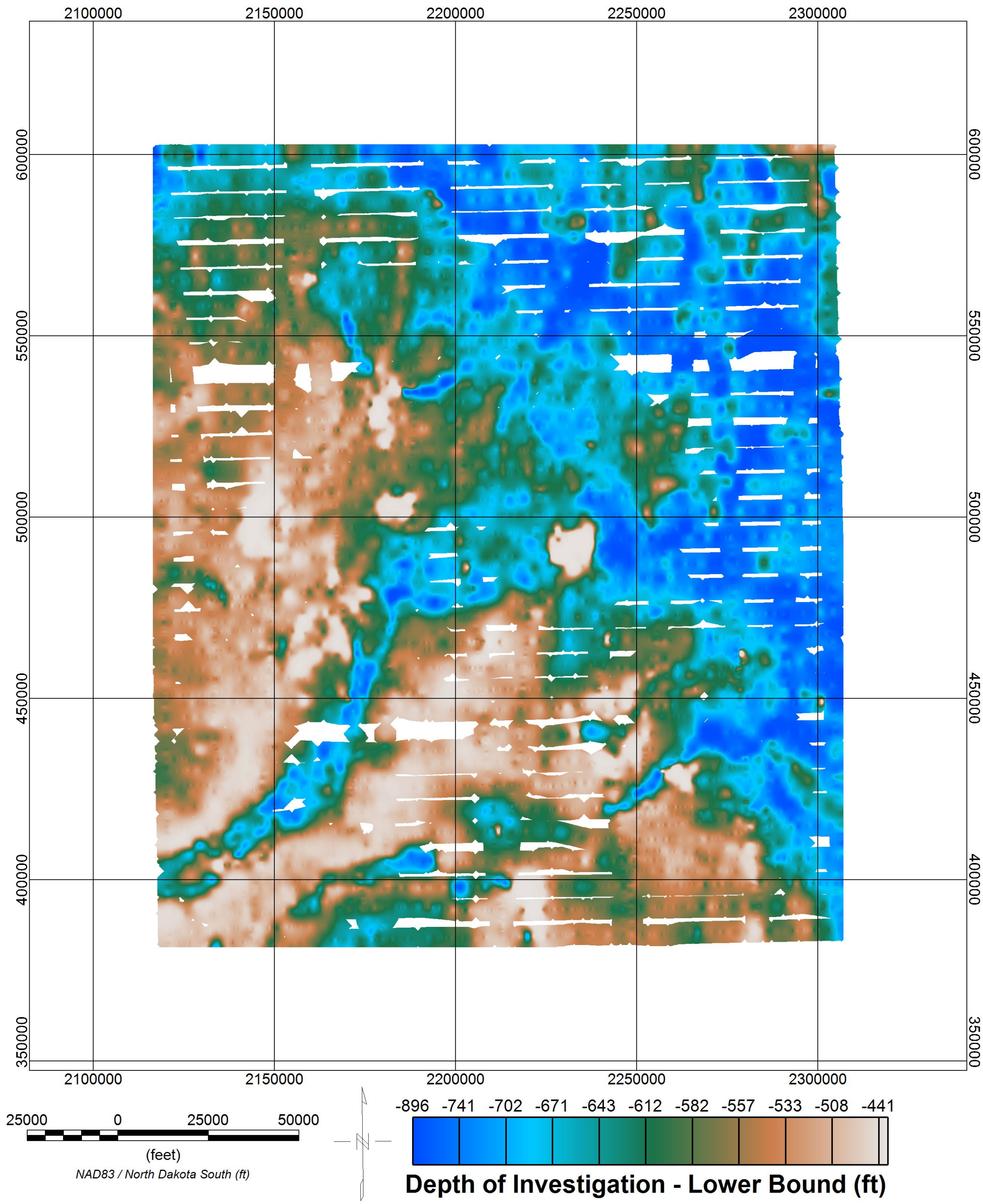

Figure 6-4. Map of the Lower Depth of Investigation for the Area 1 AEM SCI inversion. These data are included as a Google Earth KMZ file in Appendix 3. The map projection is NAD83 North Dakota State Plane South in feet.

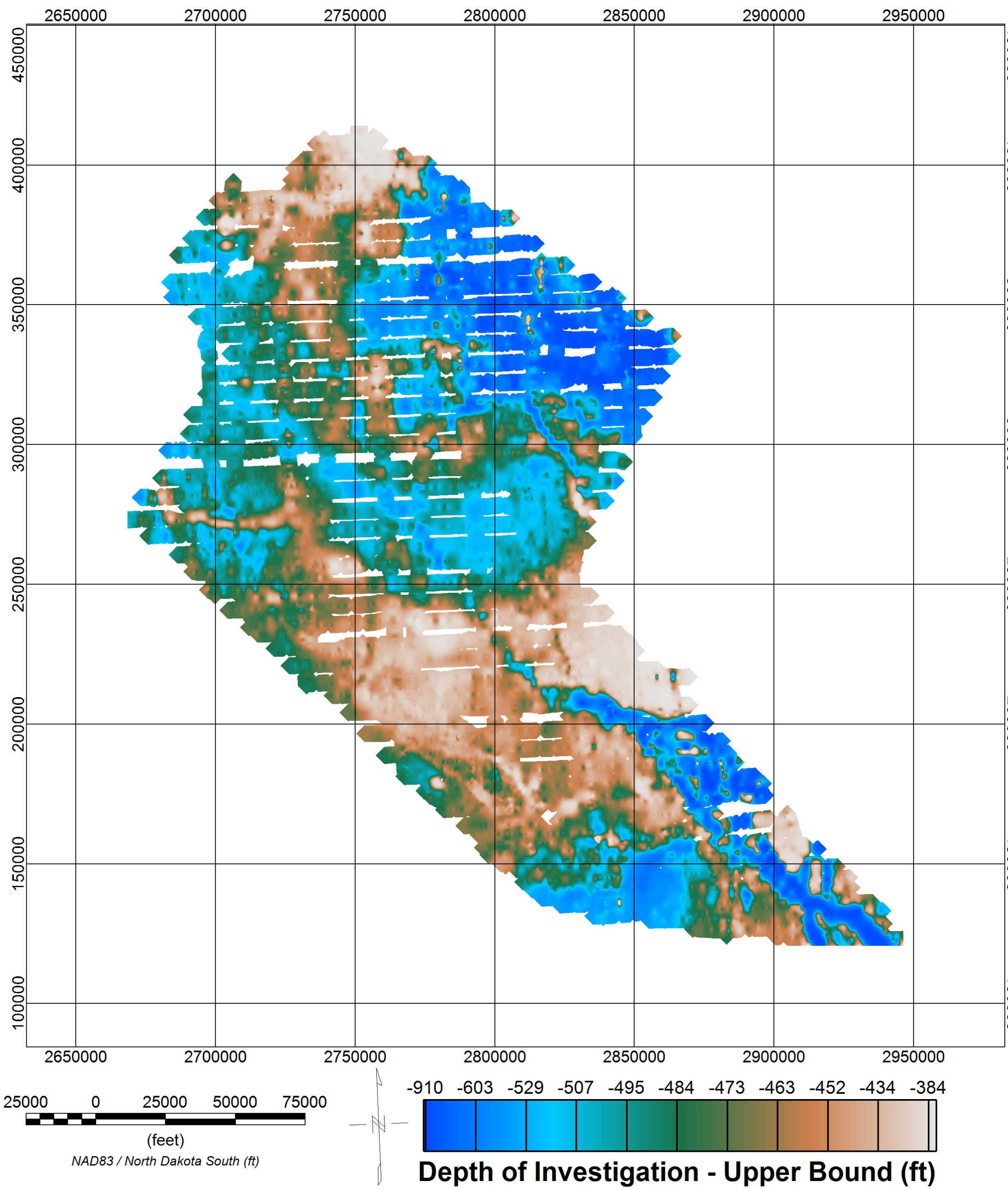

Figure 6-5. Map of the Upper Depth of Investigation for the Area 2 AEM SCI inversion results. These data are included as a Google Earth KMZ file in Appendix 3. The map projection is NAD83 North Dakota State Plane South in feet.

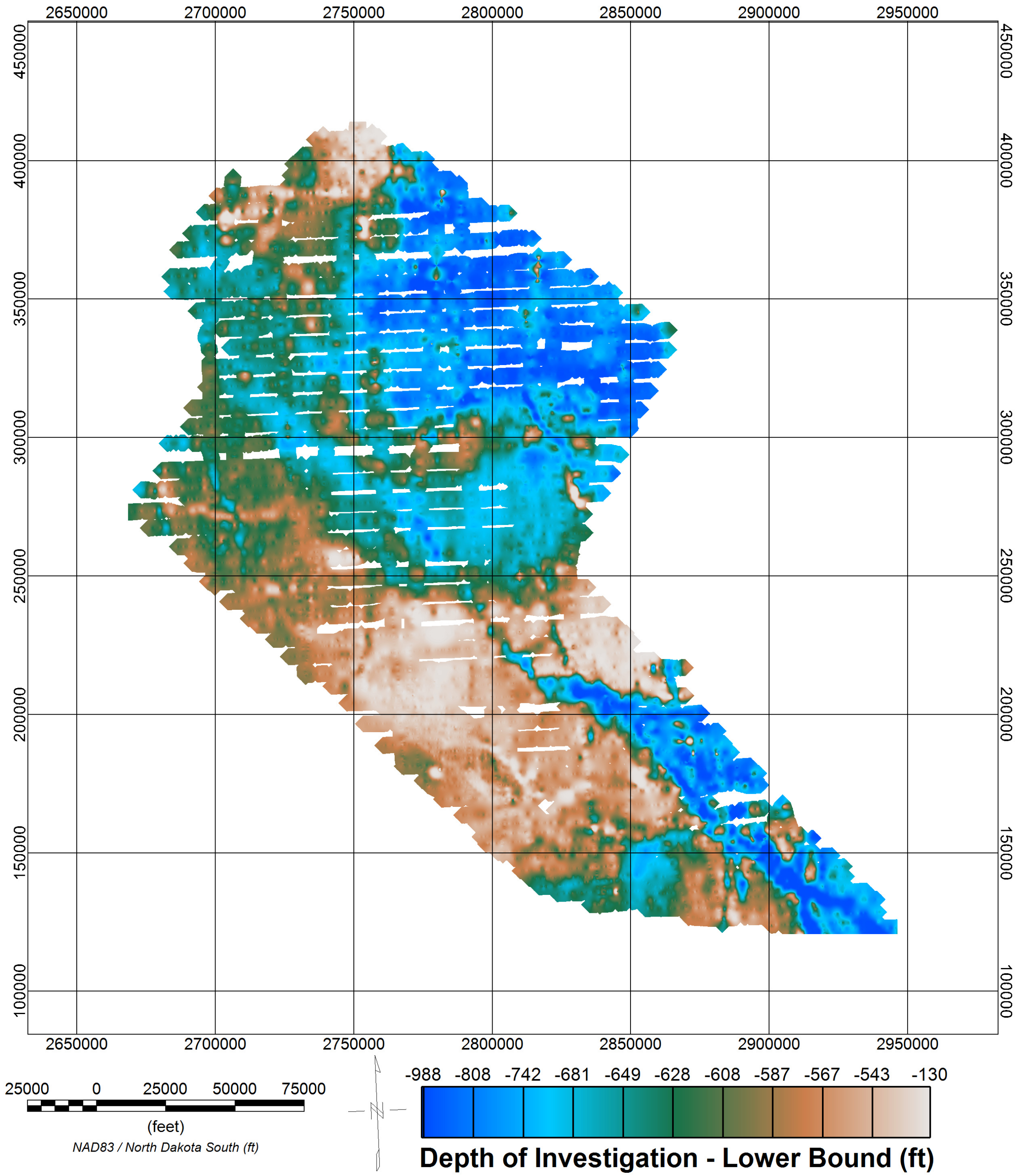

Figure 6-6. Map of the Lower Depth of Investigation for the Area 2 AEM SCI inversion results. These data are included as a Google Earth KMZ file in Appendix 3. The map projection is NAD83 North Dakota State Plane South in feet.

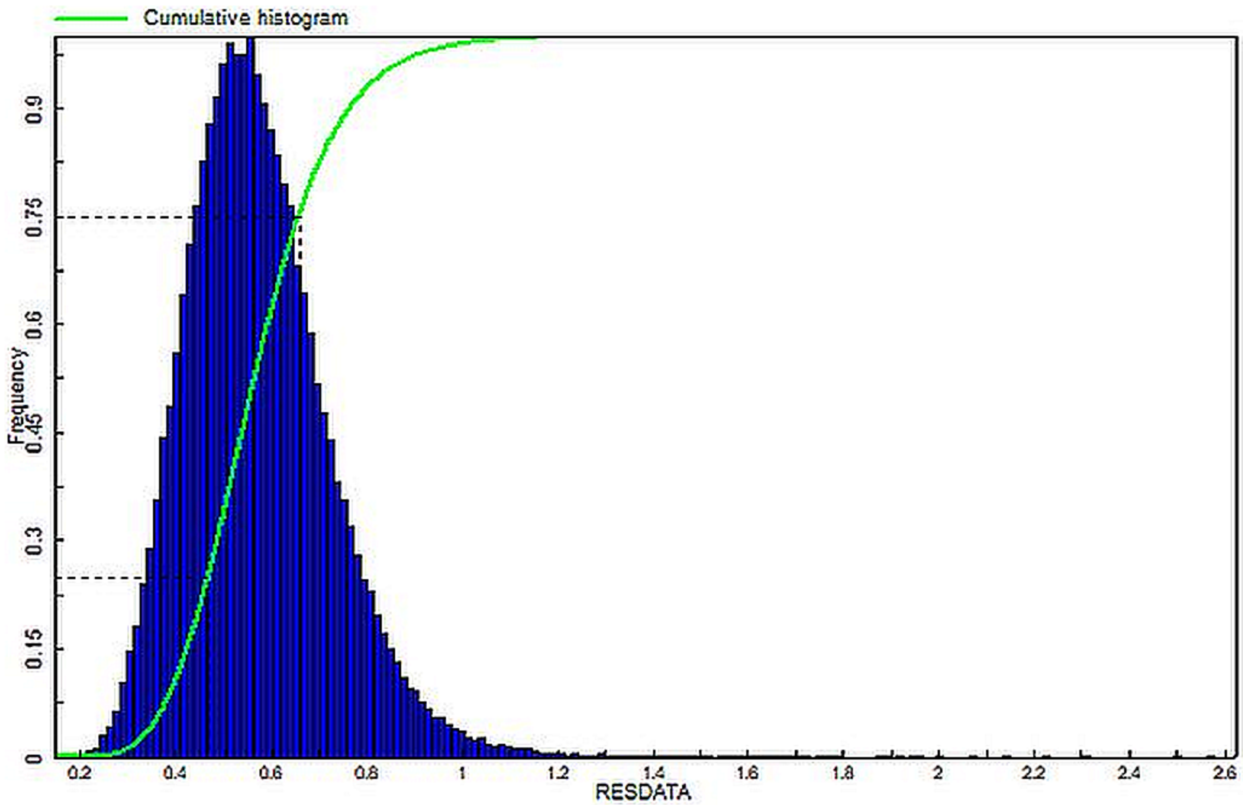

Figure 6-7. Data/model residual histogram for the NDDWR Area 1 SCI inversion results.

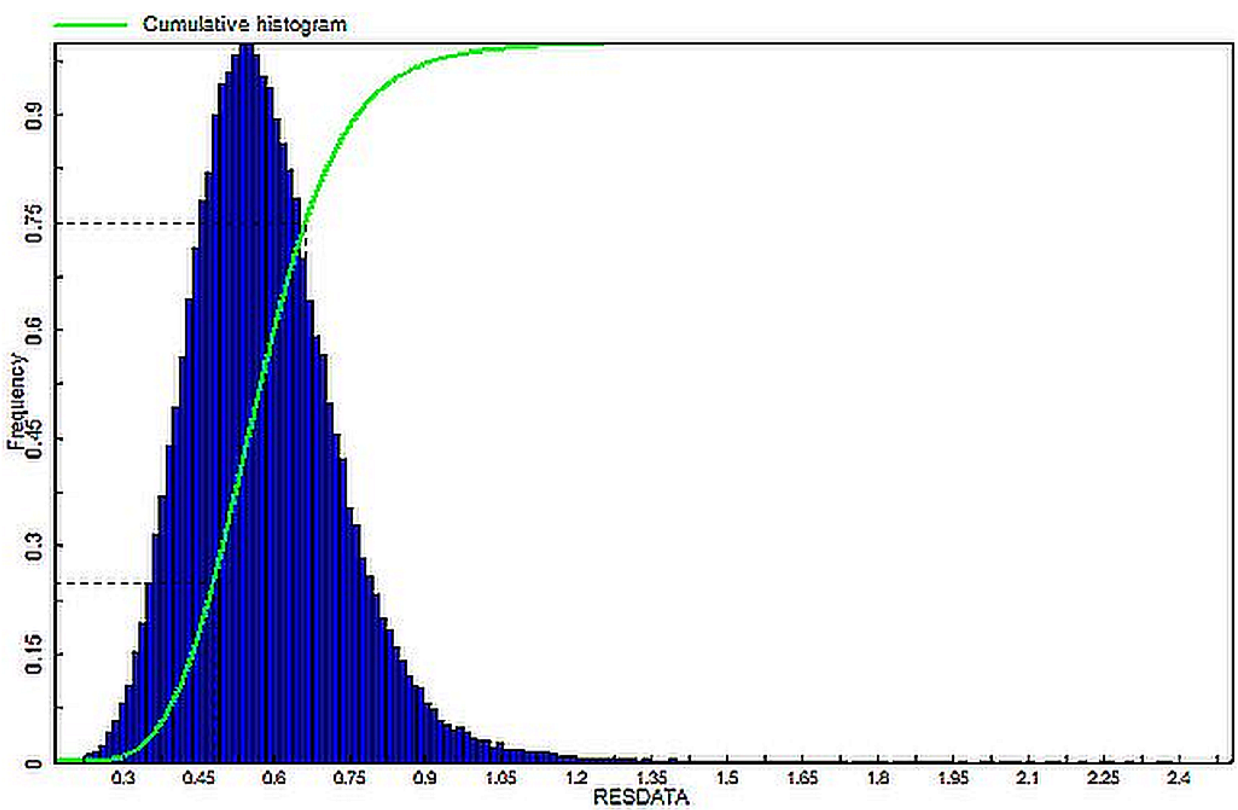

Figure 6-8. Data/model residual histogram for the NDDWR Area 2 SCI inversion results.

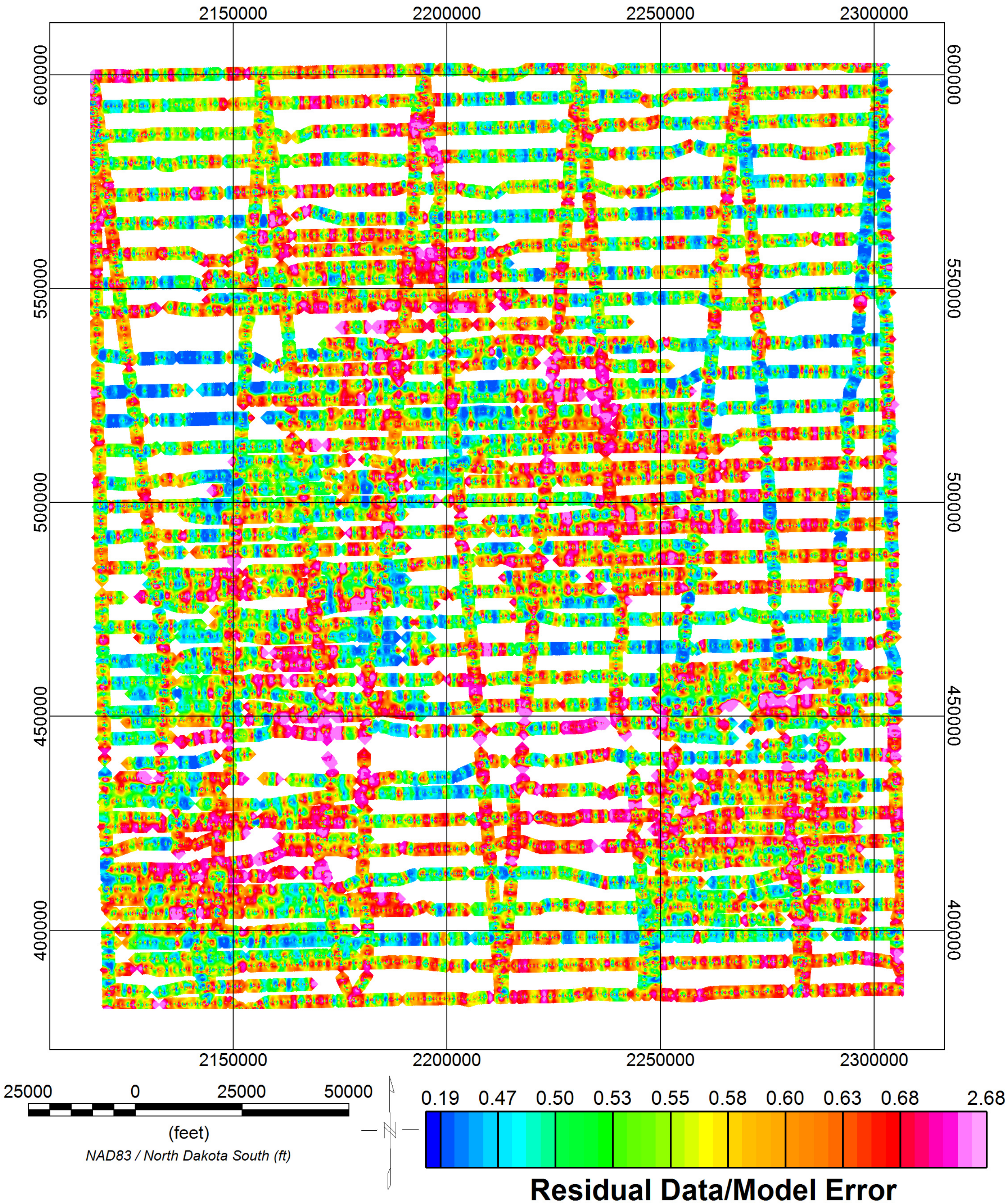

Figure 6-9. Map of data residuals for the Area 1 AEM SCI inversion results. These data are included as a Google Earth KMZ file in Appendix 3. The map projection is NAD83 North Dakota State Plane South in feet.

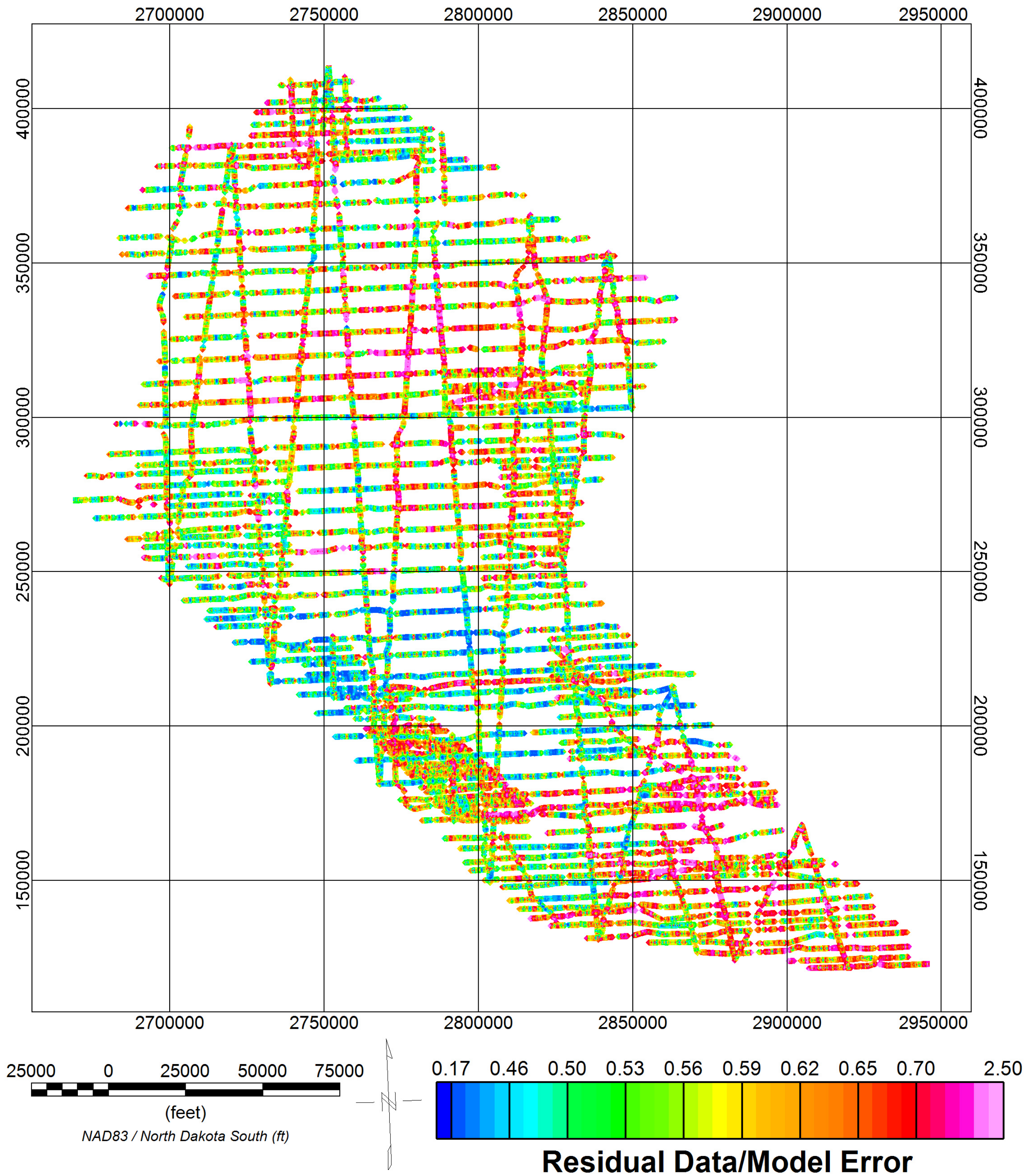

Figure 6-10. Map of data residuals for the Area 2 AEM SCI inversion results. These data are included as a Google Earth KMZ file in Appendix 3. The map projection is NAD83 North Dakota State Plane South in feet.

7. Comparison of AEM Inversion Results to Boreholes

7.1 Construct the Project Digital Elevation Model

To ensure that the elevation used in the project is constant for all the data sources (i.e. boreholes and AEM) a Digital Elevation Model (DEM) was constructed for Area 1 and Area 2. The data were downloaded from the National Elevation Dataset (NED) located at the National Map Website (U.S. Geological Survey, 2024) at a resolution of 1 arc-second or approximately 100 ft. The geographic coordinates for the Area 1 and Area 2 are North American Datum of 1983 (NAD83), State Plane North Dakota South (International foot), and the elevation values are referenced to the North American Vertical Datum of 1988 (NAVD 88) (in feet). The 100 ft grid cell size was used throughout the project and resulting products. Figure 7-1 and Figure 7-2 are maps of the DEM of Area 1 and Area 2, respectively. The vertical relief of the topography under the flight lines for Area 1 was 789 ft with a minimum elevation of 1,531 ft and a maximum elevation of 2,320 ft. The vertical relief of the topography under Area 2 flight lines was 1,199 ft with a minimum elevation of 879 ft and a maximum elevation of 2,078 ft. These respective DEM's were used to reference all elevations within the survey areas. The Binary Floating-Point Raster files (*.flt) can be found in *Appendix 3 Deliverables\Grids\DEM* as well as the QGIS package (as .tif files).

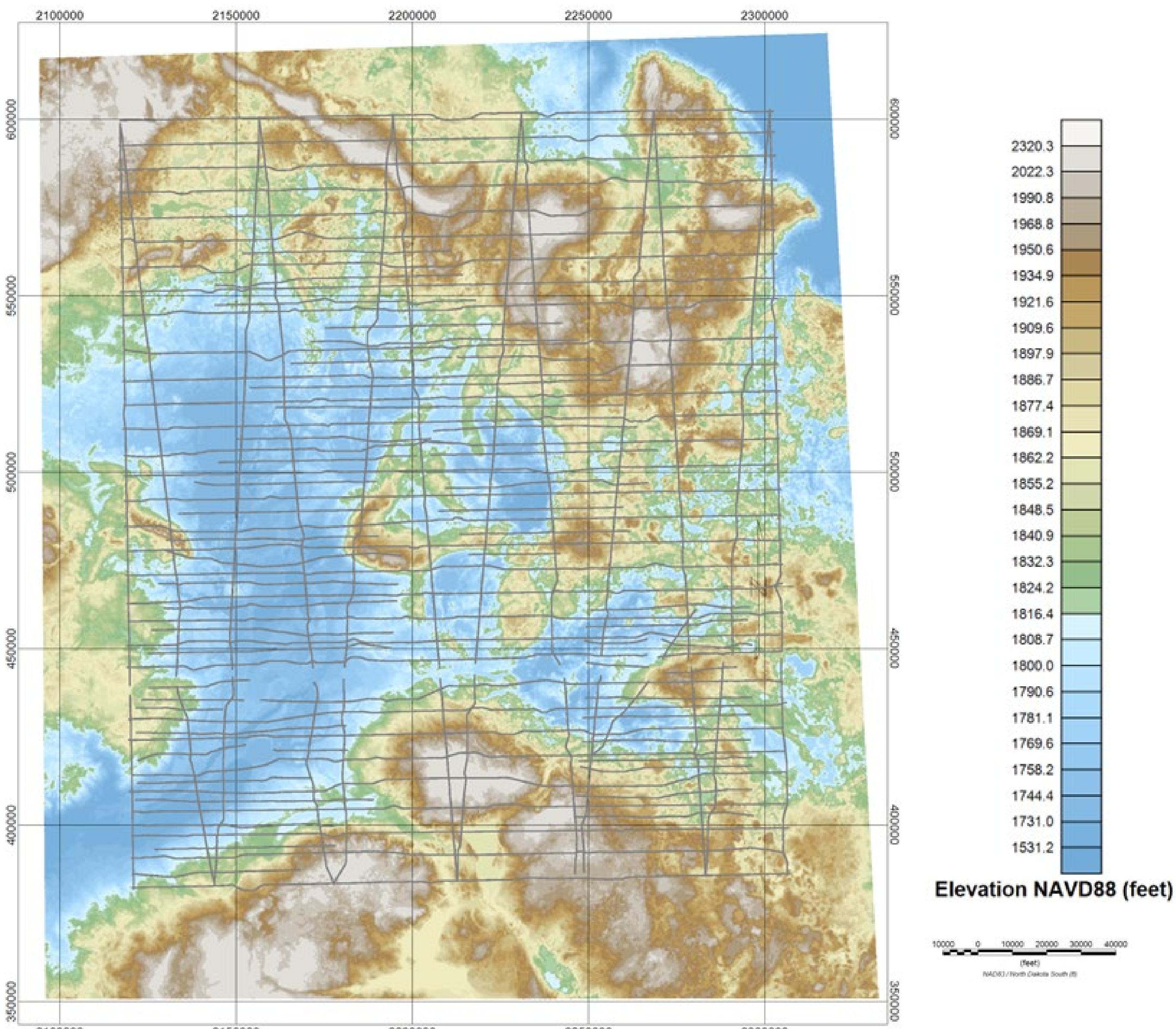

Figure 7-1. Digital elevation model (DEM) of the Area 1 AEM survey area. Flight Lines are indicated by gray lines.

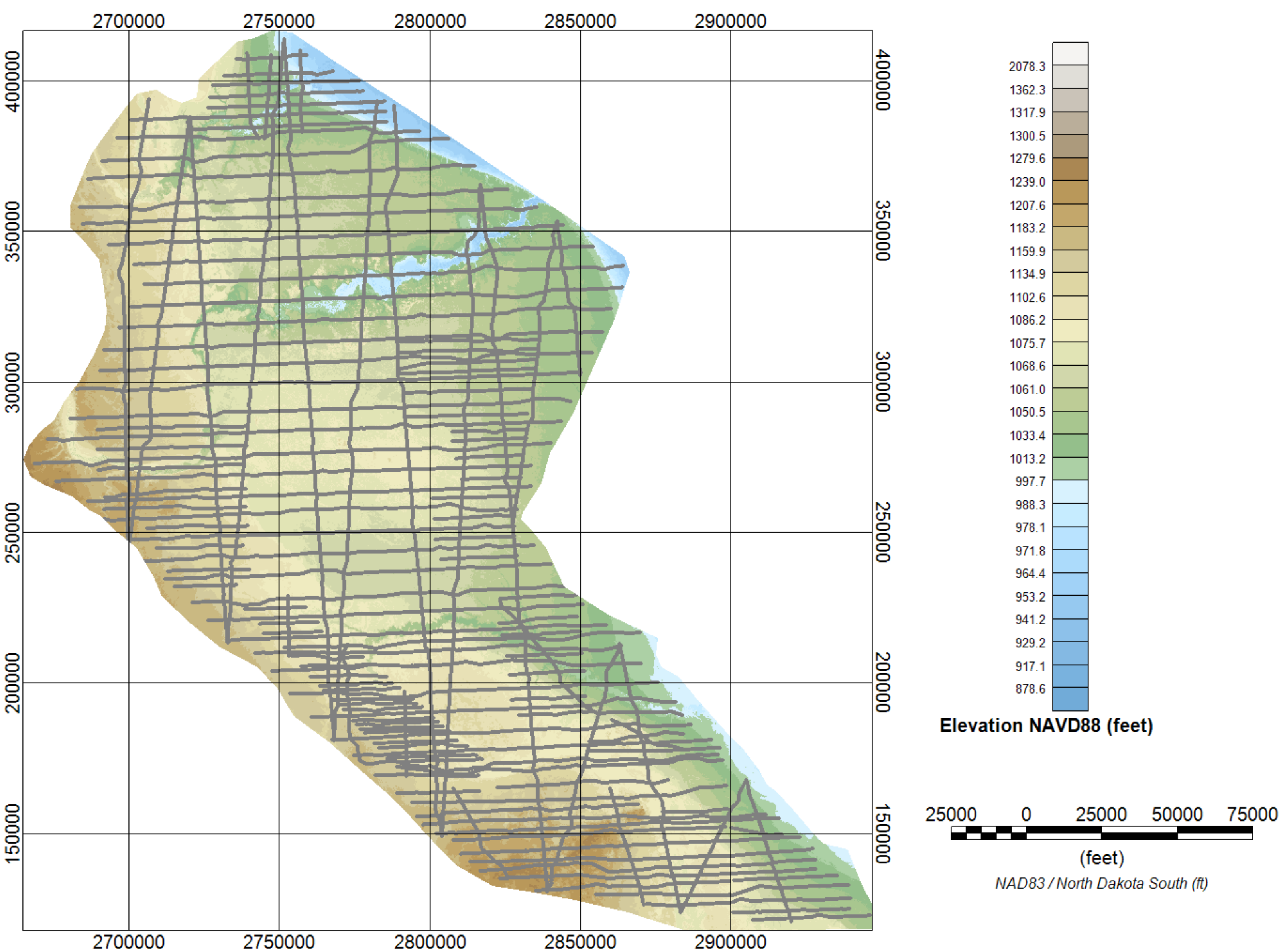

Figure 7-2. Digital elevation model (DEM) of the Area 2 AEM survey area. Flight Lines are indicated by gray lines.

7.2 Display of the AEM Inversions in 2D and 3D

Two-dimensional (2D) and three-dimensional (3D) images of the SCI inversion results have been developed using Datamine Discover PA (Datamine Discover, 2024). An example 2D-profile from Area 1 for line L101602is presented in Figure 7-3. Each profile has a unique length, and the profiles are fitted to the size of the profile page. Each profile has a small index map on the upper right showing the location of the survey flight lines with the red line indicating the current profile being displayed. On the upper left is a flight location 2D map of the displayed profile on an aerial photo background map. The horizontal scale of the flight path map is exactly the same as the profile. The lower profile is the AEM SCI inverted resistivity (ohm-m) profile along with the lithology of any borehole that is located within 500 feet of the flight line. The color scale is in log-space and stretches from 7 to 100 ohm-m (blue to pink). The vertical exaggeration is set high to allow inspection of the details of the inversions. It is important to note that the vertical exaggeration will change with the changing profile length. *Appendix 1-2D Profiles* contains all the flight line 2D profiles in this full format as well as profiles showing no boreholes; profiles showing boreholes located within 1,000 feet of the flight line; and profiles showing boreholes located within 1,500 feet of the flight line. There is also a simplified format that is only the profile of the SCI inversion with no location maps, legends, or descriptive text.

The gray dashed lines, when visible, are the bounds of the upper and lower depth of investigation (DOI). The DOI provides a general estimate of the depth to which the AEM data are sensitive to changes in the resistivity distribution at depth (Christiansen and Auken, 2012). Two DOI's are calculated: an "Upper" DOI at a cumulative sensitivity of 1.2 and a "Lower" DOI set at a cumulative sensitivity of 0.6. A more detailed discussion on the DOI can be found in Asch et al. (2015).

3D Fence Diagrams were constructed using a vertical exaggeration of 1:10 of the geolocated profiles using the same 7-100 ohm-m log color scale used in the 2D Profiles. Figure 7-4 is a 3D fence diagram example of Area 1 looking toward the north. Figure 7-5 is an 3D fence diagram example of the Area 2 looking north. It is important to note that the resistivity correlates between lines and that there are no sharp breaks in the resistivities over the area of the survey. This indicates good calibration and consistent system performance. A series of images of the 3D fence diagrams for both Area 1 and Area 2 are contained within *Appendix 2 – 3D Images*.

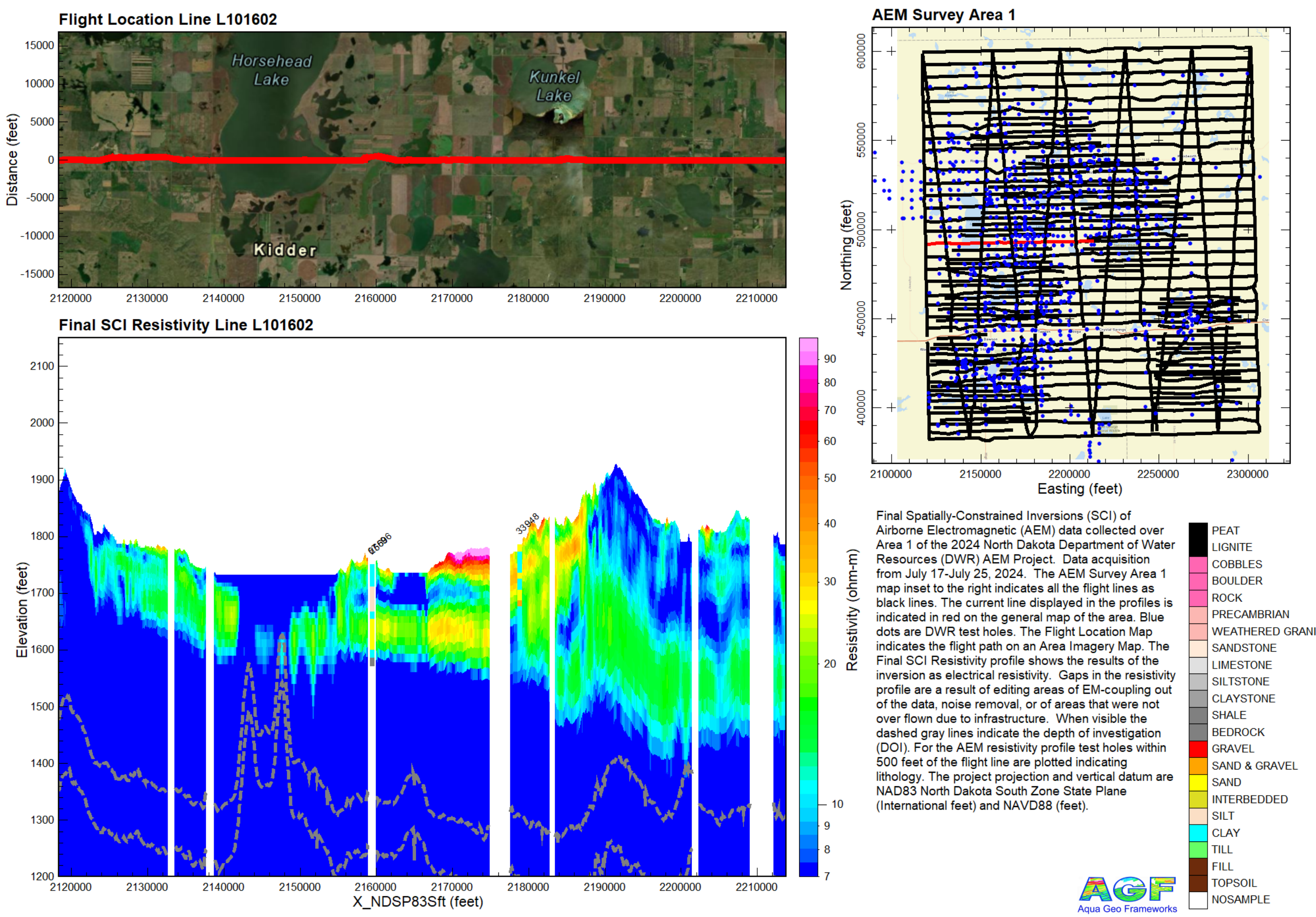

Figure 7-3. Example 2D profile displaying the results of the SCI inversion of Area 1 survey flight line L101602 including borehole lithologies within 500 of the flight line. The resistivity color scale and lithology legend are on the right side of the profile.

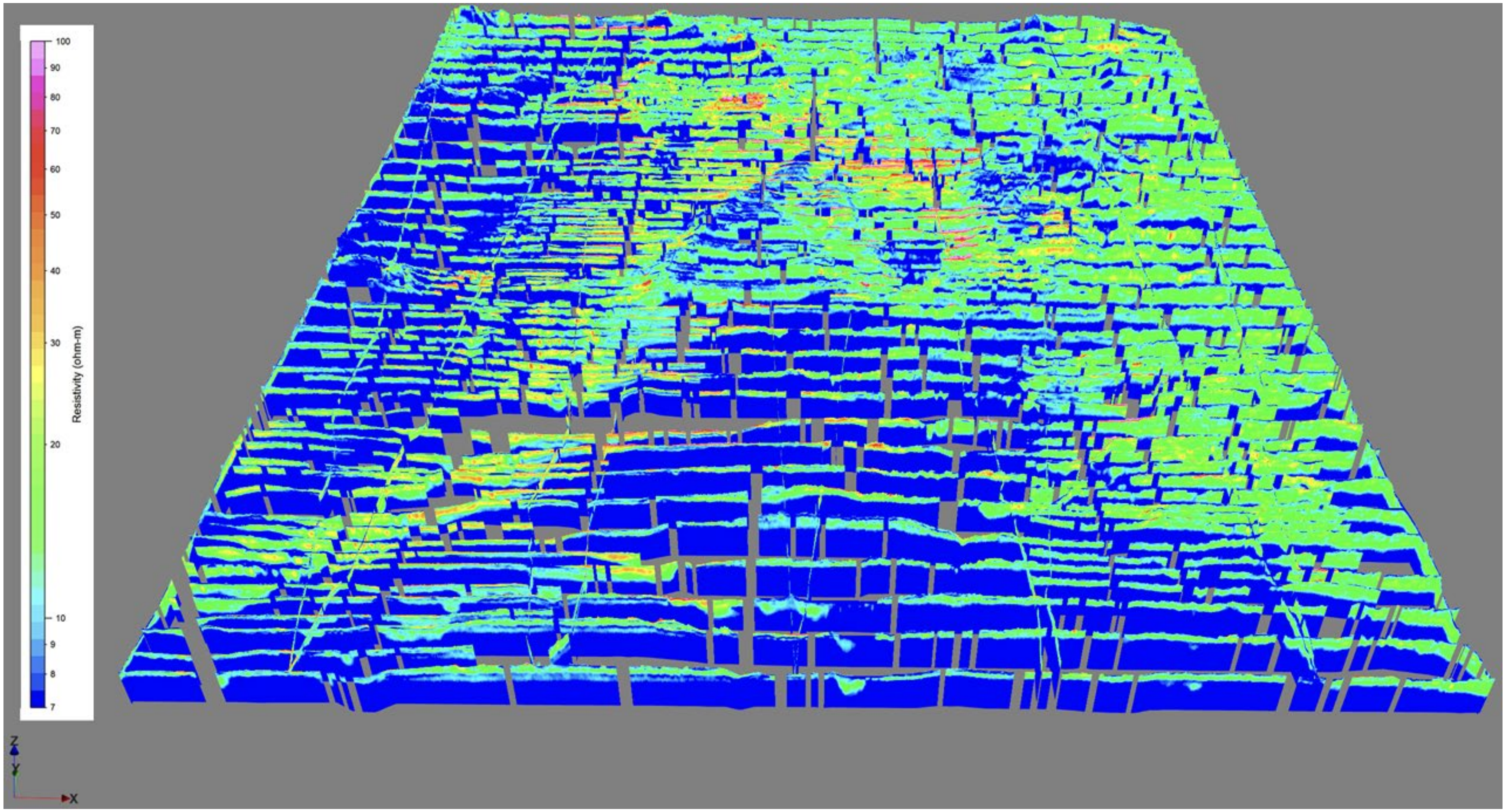

Figure 7-4. Example 3D fence diagram displaying the results of Area 1 AEM survey. The color scale is from 7-100 ohm-m, log-based. The view is to the north. Vertical Exaggeration 10x.

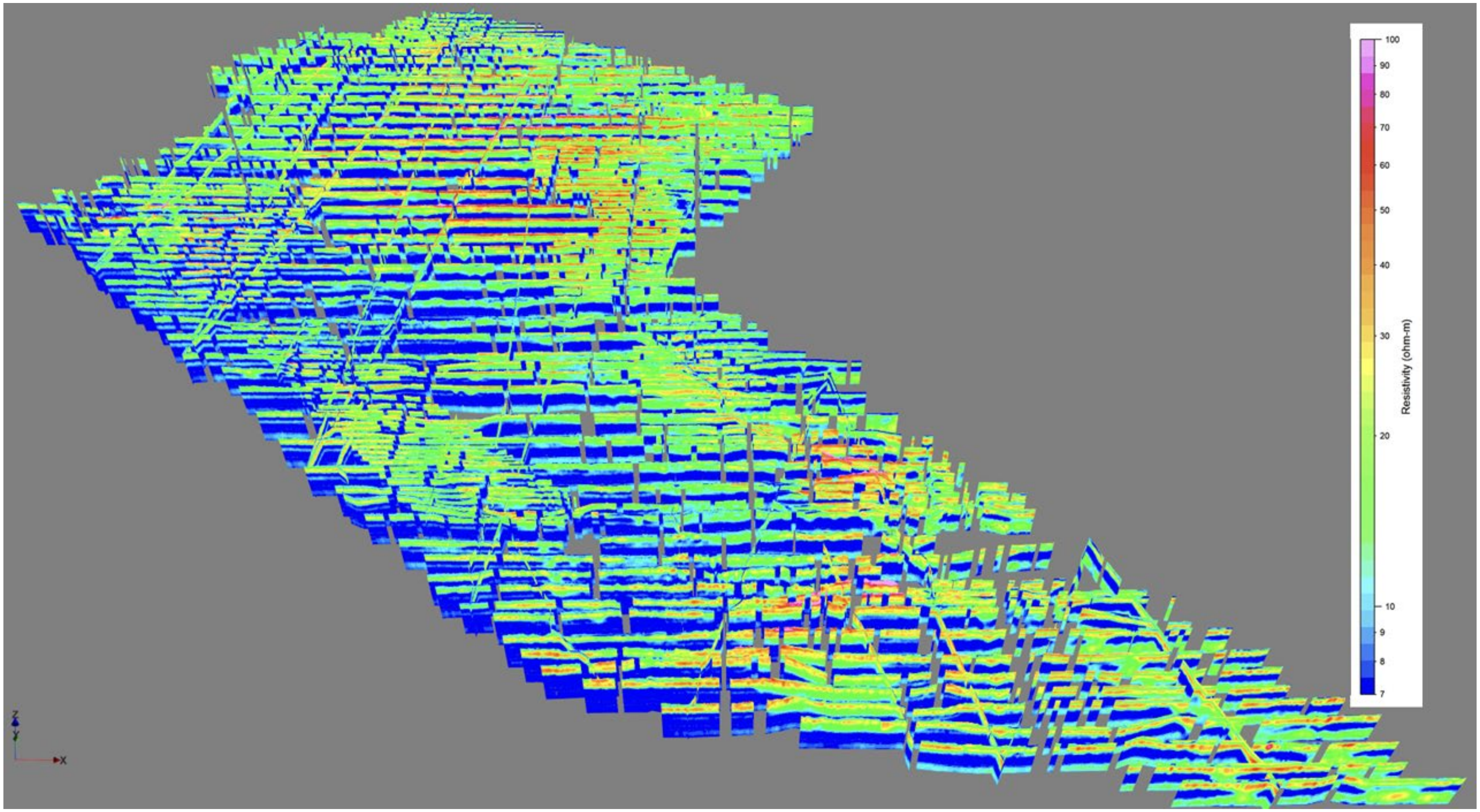

Figure 7-5. Example 3D fence diagram displaying the results of the Area 2 AEM survey. The color scale is from 7-100 ohm-m, log-based. The view is to the north. Vertical Exaggeration 10x.

7.3 Resistivity Depth Layers

Resistivity depth layers were created based on the SCI model cell spacing (Table 5-1) and were used to produce resistivity layer plots of the both the Area 1 and Area 2 AEM survey areas. To create these grids, the resistivities of the individual model layers were imported to a Geosoft Oasis montaj (OM) database. The individual model layers were then gridded independently using the OM Minimum Curvature Gridding (MCG) algorithm. The cell size was set to 50 feet, a blanking distance of 3,000 feet was applied, and the "cells to extend beyond" set to 0 cells. All other parameters were either left as the default or blank. These layers are useful for inspecting the vertical changes in the resistivity. The color scale that was used for these maps was selected to illuminate the sands and gravels within the Quaternary section.

Figure 7-6 is an example of model depth layer 17 covering the depth interval of -158 ft to -175 ft from the Area 1 AEM survey area. At this depth the basic fabric of the Quaternary sands and gravels are indicated by the high resistivities (hot colors). The color scale is the same as for all the profiles, from 7 to 100 ohm-m. Figure 7-7 is the same layer but using a color scale that is automatically stretched to cover the range in resistivities for the layer using a histogram distribution.

Figure 7-8 is an example of model depth layer 18, covering the depth interval of –193 to -212 ft from the Area 2 survey area. The color range is the same as used in the profiles and fence diagrams, a log distribution from 7 to 100 ohm-m. In this example the sands and gravels are also indicated by the high resistivities (reds). A set of images with the log distribution 7 to 100 ohm-m color scale and the auto-range per layer histogram distribution color scale was made for each model layer. The 7 to 100 ohm-m color scale will be consistent through the profiles and 3D fence diagrams while the histogram stretched color scale will allow inspection of subtle details in each layer.

It is important to note that the auto scaled histogram color scales cannot be directly compared to the profiles nor different layers. These layers have been combined into both PDF files and Google Earth KMZ's to allow the user to inspect the individual layers by selecting a specific layer under the Data tab in the layered pdf files which are located in *Appendix 3 – Deliverables\PDF*. The grids of these layers can be found in *Appendix 3 – Deliverables\Grids* as well as layered KMZ's in *Appendix 3 – Deliverables\KMZ*.

7.4 Voxel Grids

Voxel grids were developed for the Area 1 and Area 2 survey areas. The voxel grids were made using a 500 ft grid cell size and the model layer thicknesses (Table 5-1). A minimum curvature method was used within Datamine Discover PA (Datamine Discover, 2024). The grid was allowed to interpolate to the extents of the survey with some areas of no data coverage due to EM coupling clipped from the grids. All layers were referenced to their depth from the surface. After the grid was calculated, the DEM was added as an offset.

The voxels allow for another view with which inspection of the 3D distribution of the inverted model resistivities can be made. Specifically, for the inspection of the Area 1 survey, the paleochannel deposits can be highlighted using an 18 ohm-m threshold. Figure 7-9 is a 3D Fence Diagram plot of the AEM resistivities with a >18 ohm-m resistivity threshold on the materials below 50 feet in depth on the voxel for the Area 1 AEM survey area looking to the north. The paleochannel deposits (yellow-green) are visible amongst the low resistivity clays and shale (blue).

Figure 7-10 presents a 3D plot of a voxel with a >30 ohm-m threshold for the Area 2 AEM survey area with the 3D Fence Diagrams looking to the north. The paleochannel deposits (orange-red-pink) are visible amongst the low resistivity clays and shale (Blue). Specifically, the Sheyenne Delta deposits are prominent as resistive materials.

The complete collections of the 2D profiles are contained in *Appendix 1* and the images of the 3D Fence Diagrams, resistivity depth layers, and voxels, are contained in *Appendix 2*. Layered PDF's of resistivities of model layers can be found in *Appendix 3 – Deliverables\PDF* and as Binary Raster Grids (.flt). The voxel may be found in *Appendix 3 – Deliverables\Voxel* as an ASCII *.xyz.

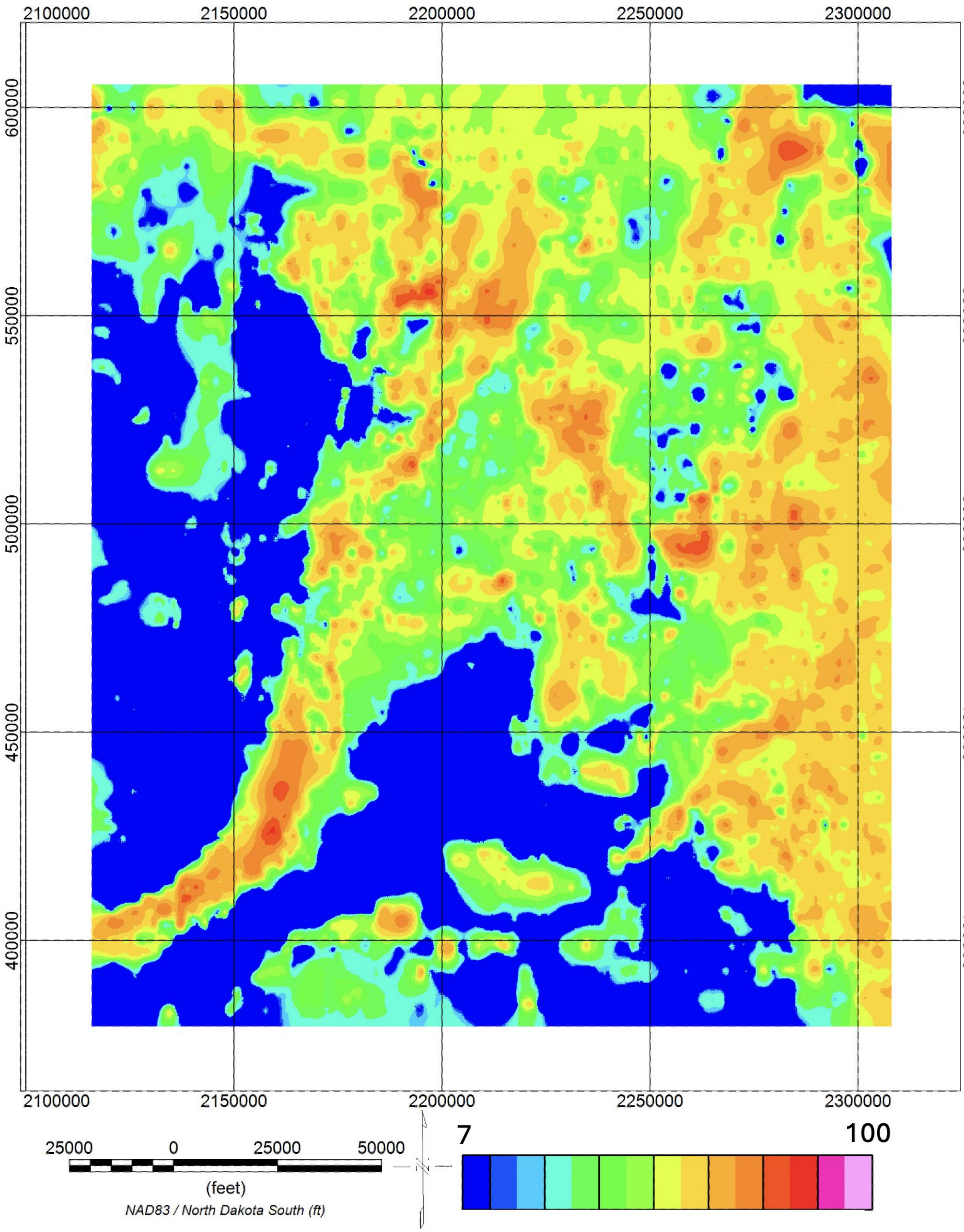

Figure 7-6. Map view of the inverted AEM resistivity for the 17th SCI model layer from –158 ft to –175 ft feet for the Area 1 survey area. The color scale is a log distribution from 7 to 100 ohm-m.

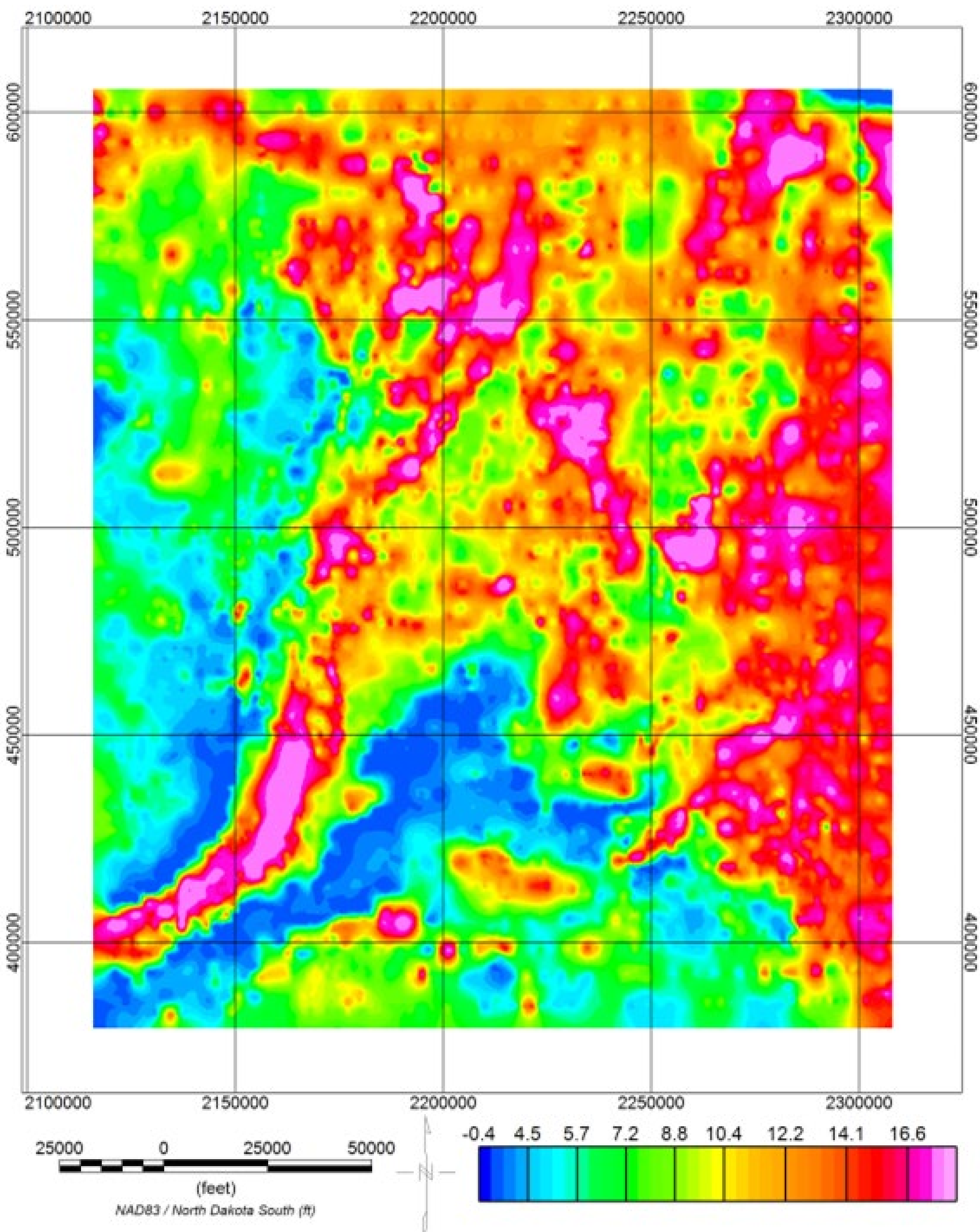

Figure 7-7. Map view of the inverted AEM resistivity for the 17th SCI model layer from –158 ft to –175 ft feet for the Area 1 survey area. The color scale is an automatically scaled histogram distribution.

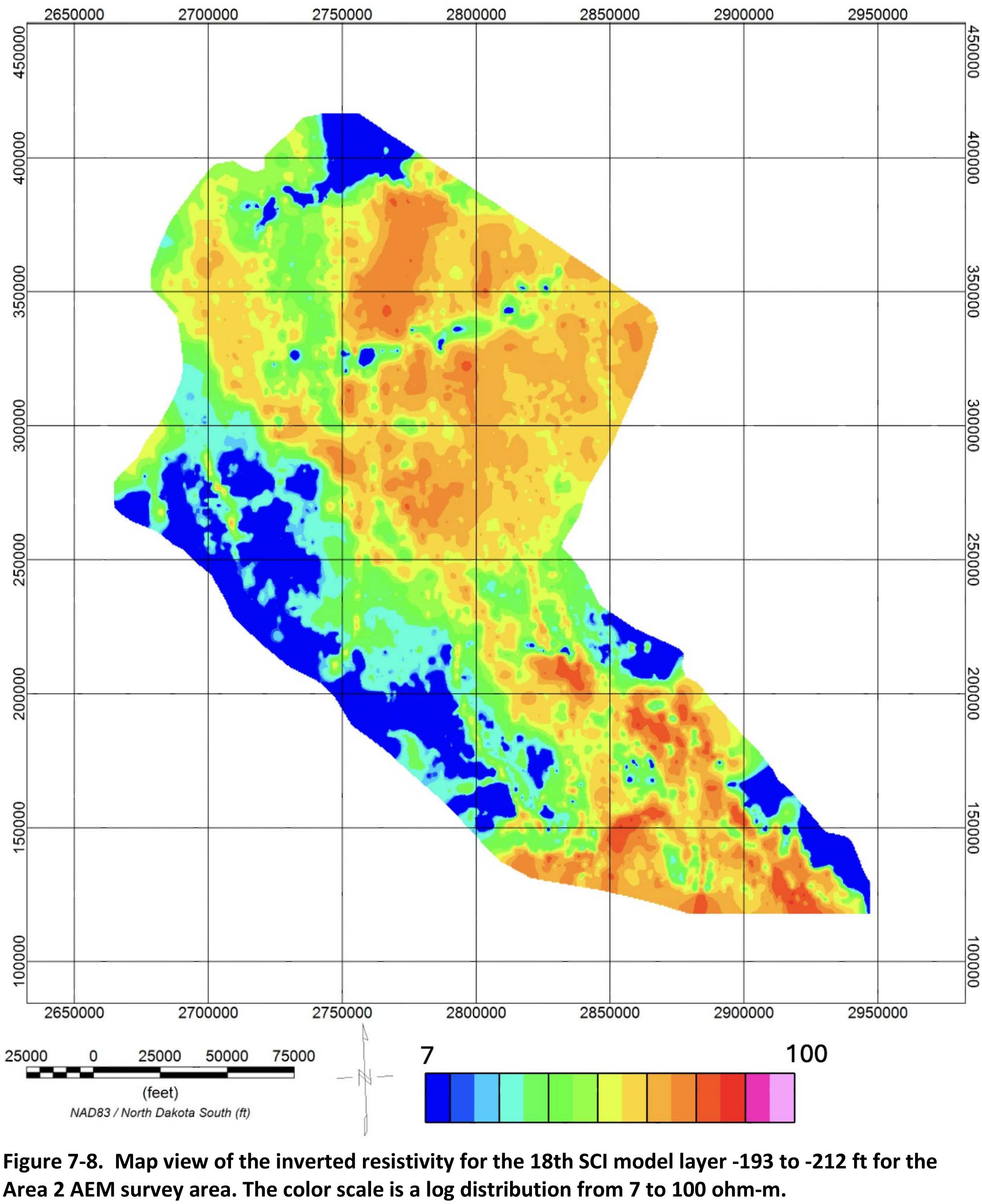

Figure 7-8. Map view of the inverted resistivity for the 18th SCI model layer -193 to -212 ft for the Area 2 AEM survey area. The color scale is a log distribution from 7 to 100 ohm-m.

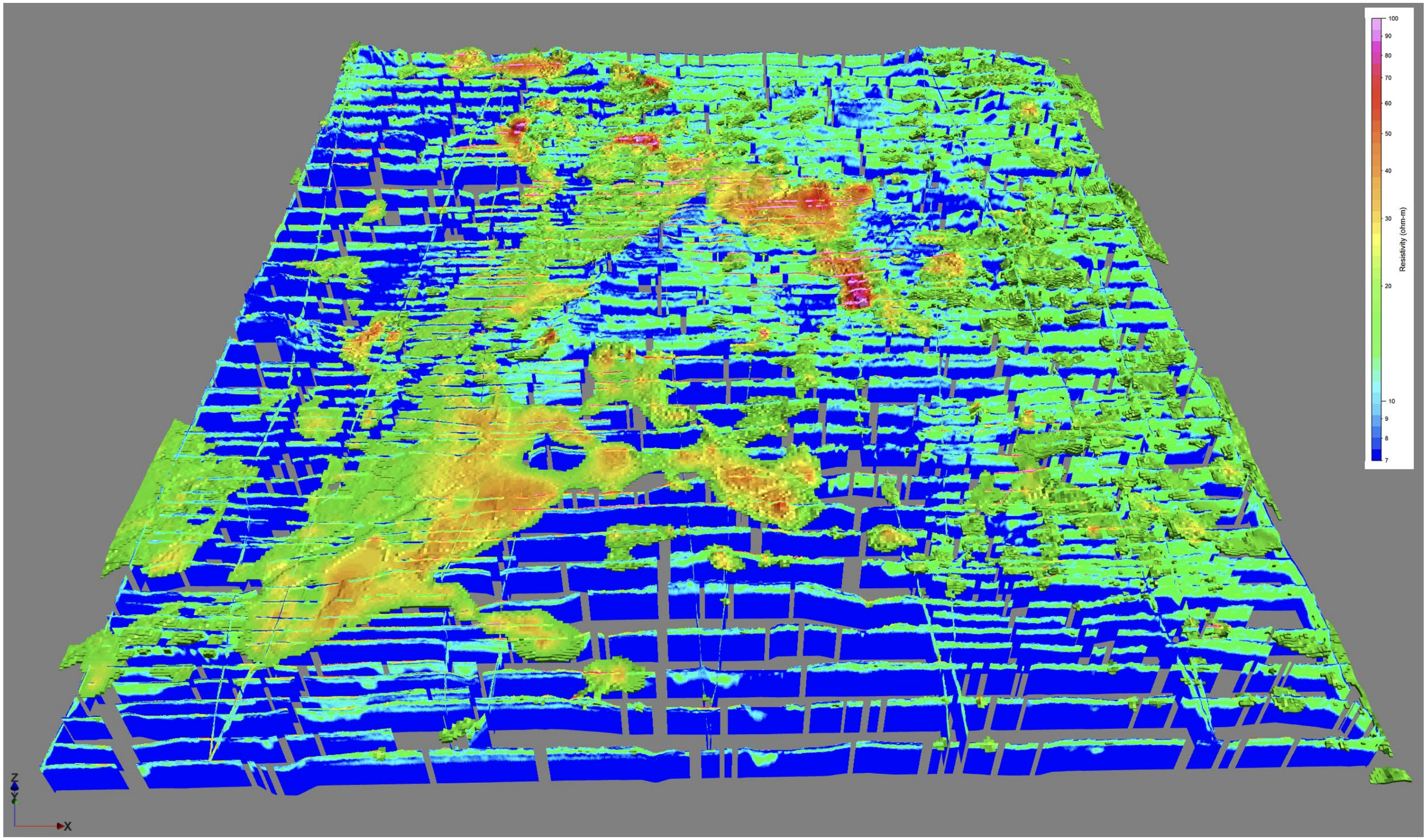

Figure 7-9. 3D image of a >18 ohm-m voxel below 50 feet and 3D fence diagrams of the Area 1 AEM survey area. The view is looking from the to the north. Vertical Exaggeration is 10x.

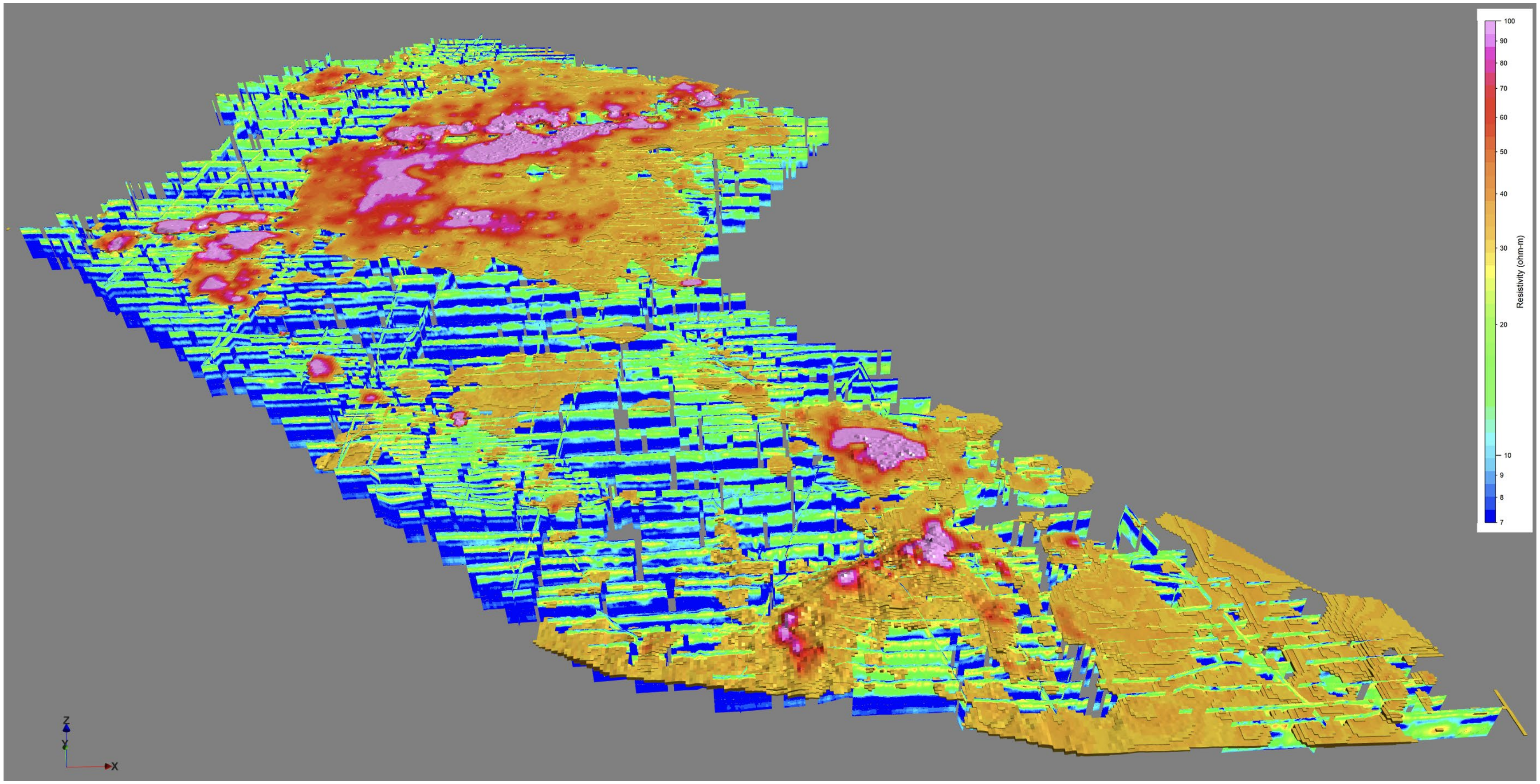

Figure 7-10. 3D image of a >30ohm-m voxel and 3D fence diagrams of the Area 2 AEM survey area. The view is looking to the north. Vertical Exaggeration is 10x.

7.5 Resistivity Elevation Layers

Resistivity elevation layers were created based on the SCI inversion results in order to assist in the visualization of the resistivity variations related to the elevations of the deposits. To create these grids, the SCI inversion results were sampled at discrete elevation ranges and the resulting resistivities were gridded at a 50 ft cell size. Figure 7-11 is an example of two elevation layers, 1450 ft and 1650 ft, from the Area 1 AEM survey area. For Figure 7-11 the color scales are automatically stretched to cover the range in resistivity in each layer using a histogram distribution per layer. Thus, the two color scales are not equal, but emphasize the details per layer.

Figure 7-12 presents four examples of resistivities at elevations 425 ft and 775 ft (Figure 7-12ab) and elevations 850 ft and 925 ft (Figure 7-12cd) of the Area 2 AEM survey area. These four layers show the changes in the deposits with elevation and are at the same color scale of 7 to 100 ohm-m with a log distribution.

All the elevation layers for both Area 1 and Area 2 were combined into two different PDF files and Google Earth KMZ's for the two different color scales and allow the user to inspect the individual layers. These files are located in *Appendix 3 – Deliverables\PDF*. The grids of these layers can be found in *Appendix 3 Deliverables\Grids*.

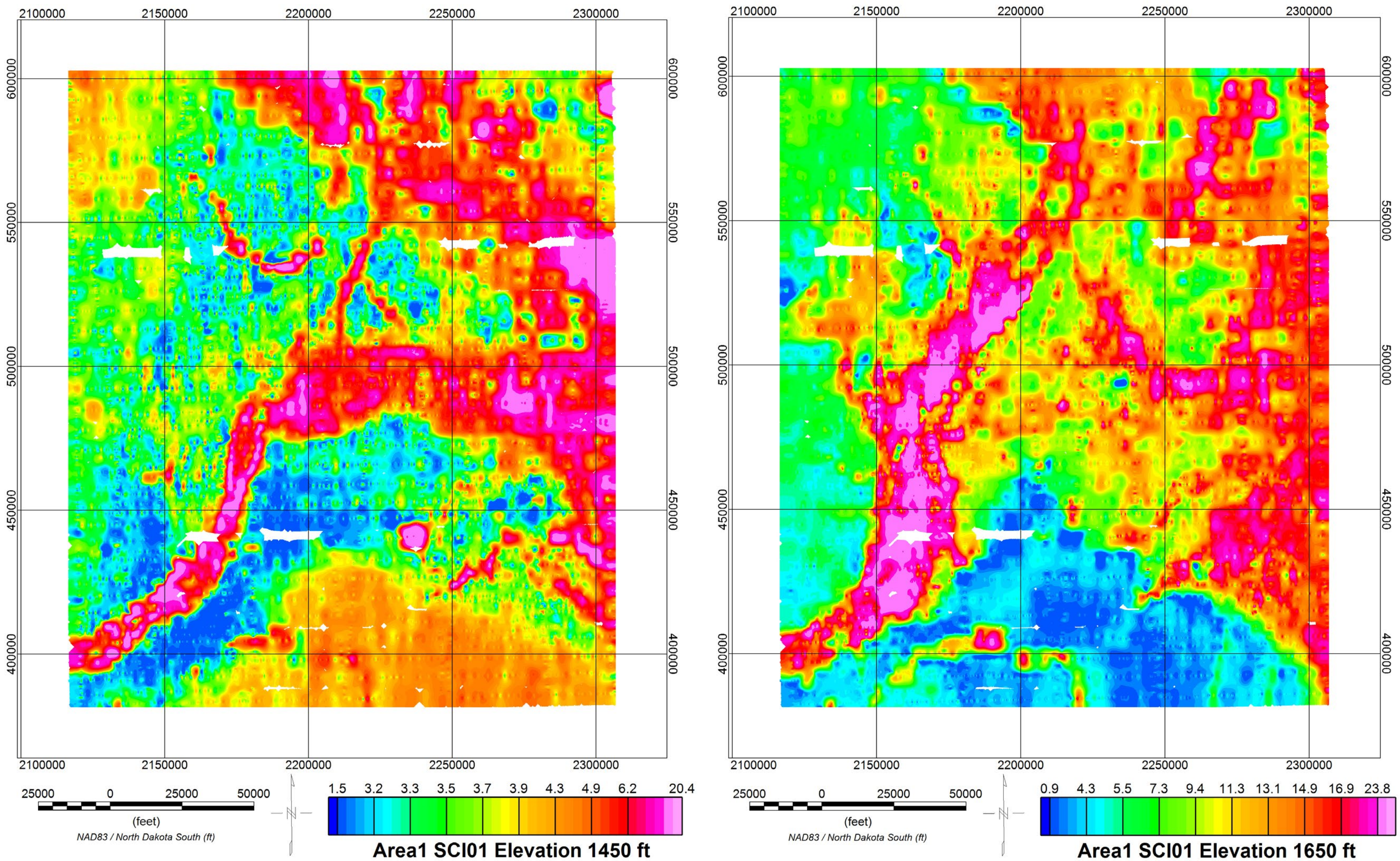

Figure 7-11. (a) Resistivity layer at an elevation of 1450 ft of the Area 1 AEM survey area (b) Resistivity layer at an elevation of 1650 ft of the Area 1 AEM survey area. The color scale is an automatic scaled histogram distribution for each layer.

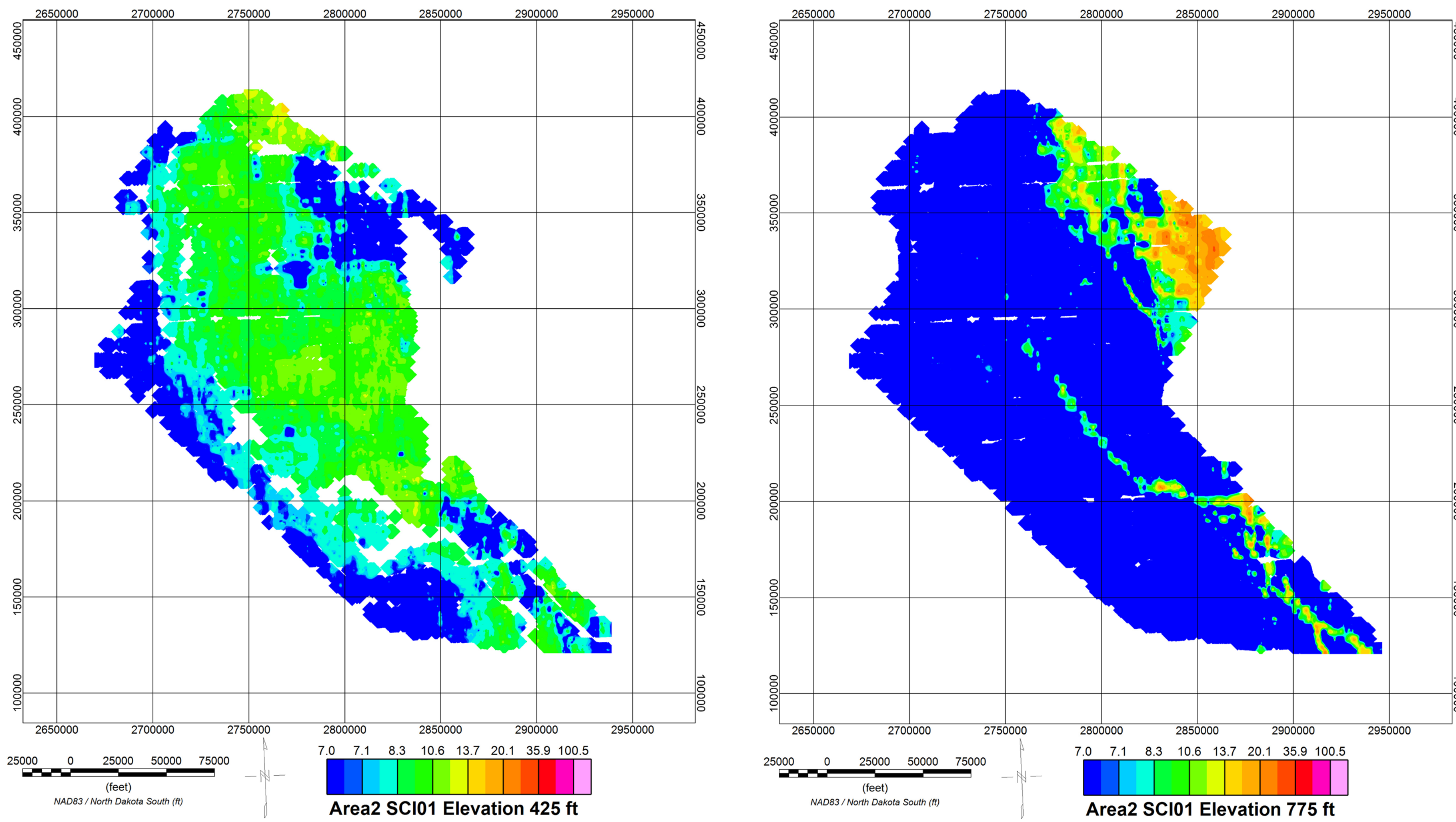

Figure 7-12ab. (a) Resistivity layer at an elevation of 425 ft of the Area 2 AEM survey area (b) Resistivity layer at an elevation of 775 ft of the Area 2 AEM survey area. The color scale is a log distribution from 7 to 100 ohm-m.

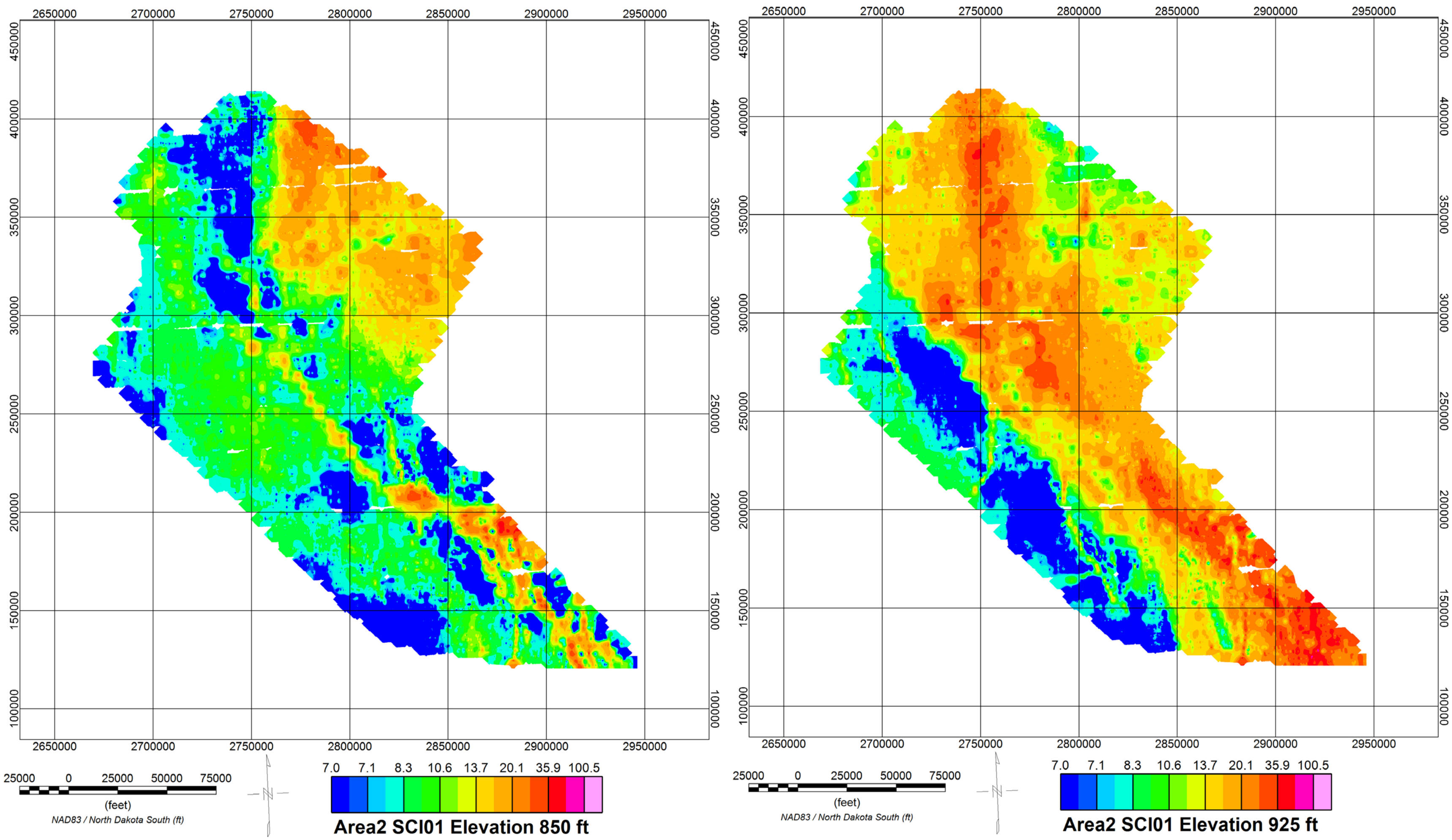

Figure 7-12cd. (c) Resistivity layer at an elevation of 850 ft of the Area 2 AEM survey area (d) Resistivity layer at an elevation of 925 ft of the Area 2 AEM survey area. The color scale is a log distribution from 7 to 100 ohm-m.

7.6 Examples of Borehole Electrical Resistivity and Lithology Compared to AEM Inversion

Two borehole databases were downloaded from the NDDWR website to assist in comparing existing borehole logs to the AEM. One was the Test Hole database, and the other was the Observation Well database (NDDWR, 2024). The databases contained information on the interpreted lithology from well drilling and were examined within the area. Only the NDDWR-owned boreholes were used in this project. Edits were conducted on the database to correct typos or inconsistencies in the lithology descriptions.

Two boreholes within Area 1 and five boreholes within Area 2 include electrical resistivity and lithology logs. These logs were correlated with depth to the AEM. Several observations have been noted below that will hopefully assist the NDDWR in the interpretation of the AEM inverted resistivities including pointing out some areas of good correlation with the borehole lithology as well as areas of poor correlation of the borehole lithology to the inverted AEM resistivity. It is of paramount importance that the interpreter understands the limitation of the lithology descriptions as compared to the resistivity as well as understand the limitations of the AEM.

An AEM system is responding to changes in the electrical resistivity of the subsurface while flying at approximately 50 mph at approximately 100 ft above ground level (AGL) with a finite EM bandwidth. This means that it is possible that the AEM could provide a fuzzy or unfocused view of the subsurface as compared to borehole lithology or borehole geophysics. As the EM signal diffuses down into the earth, the amplitude of the signals returned to the receiver on the AEM platform have detectable decreases. This has the impact of decreasing the resolution of the EM signals with increasing depth. The AEM inversion models also increase layer thickness with depth that also express the possible decreased resolution of the technique with depth (Table 5-1).

Lithology logs are also limited by the following: drilling method, drilling mud, drilling speed, and skill and experience of the geologist performing the descriptions. The lithology log is an interpretation by the geologist of the material that is brought to the surface. Lithology logs catalogued at different times by different geologists may have varying accuracies in specific picks of similar lithologies. Cores are an improvement in the interpretation of the lithology over other methods but are also plagued with difficult recovery in unconsolidated materials. With all the limitations of the lithology logging of well cuttings, the fact remains that they are still a window into the subsurface and provide important clues to the geology. Below are several examples of comparisons of boreholes with the AEM inverted resistivities. *Appendix 1 – 2D Profiles* includes these examples and others for comparison of selected flight lines with the borehole lithology logs.

7.6.1 E-Log Comparisons to AEM

The 16-inch Short Normal and the 64-inch Long Normal resistivity logs were used to validate the calibration of the SkyTEM 304M. The survey lines were flown as per the approved flight plan and the lines near the flight lines were examined for validate that the calibration. A summary of the flight lines that were close to the geophysical logs are presented in Table 7-1.

Table 7-1. Flight lines with E-log test holes in Area 1 and Area 2.

Flight Lines	Test hole	Area
L101201	14207225BCC	Area 1
L101201	14207220DDD	Area 1
L200301	8_14502118576	Area 2
L202201	5_16301130373	Area 2
L3000101	1_111248452	Area 2
L403201	2_10553010405	Area 2
L403801	4_13050220134	Area 2

Figure 7-13 is a comparison of the Area 1 SCI inversions of line L101201, flown over test holes **14207225BCC** and **14207220DDD**, of 16-inch Short Normal and 64-inch Long Normal resistivity logs. The 16-inch Short Normal and the 64-inch Long Normal resistivity logs present quite similar resistivities indicating that there is limited lateral variation on the order of the 64 inches around the borehole. There is a slight increase in the resistivity in the 64-inch as compared to the 16-inch within the resistive zone indicating a larger amount of resistive materials around the borehole. The AEM and the E-logs correlate well at the top of the low resistivity materials at an elevation of ~ 1,700. At the very top of the 64-inch there appears to be some interference from the equipment limitation on the shallow portion of the borehole, indicated by a resistive zone near the gray area on the plot, indicates no data was collected at the top of the borehole.

Figure 7-14 is a comparison of the Area 2 SCI inversions of line L200301 flown over test hole *8_14502118576* for both the 16-inch Short Normal and 64-inch Long Normal in the northern portion of the AEM survey area. The 16-inch Short Normal and the 64-inch Long Normal logs are similar indicating low spatial variation. However, both show increased resistivity as compared with the AEM, but at the same elevation as other zones in the AEM. The AEM line is south of the borehole and the area shows zones of increased resistivity of short distances (related to channel deposits likely) and with the line and hole not collocated, the difference may be attributed to the spatial variability between the hole and the AEM.

Figure 7-15 is a comparison of the Area 2 SCI inversions of line L202201 flown over test hole *5_163011130373* for both the 16-inch Short Normal and 64-inch Long Normal resistivity logs. The 16-inch Short Normal and the 64-inch Long Normal logs are similar indicating low spatial variation. Both the E-logs and the AEM show the increased resistivity materials at elevation ~ 1,150 feet. There is a low resistivity zone at ~1,000 feet that is indicated in the E-logs and the AEM inversion results, suggesting Cretaceous Pierre Shale bedrock.

Figure 7-16 is a comparison of the SCI inversions of line L300101 flown over test hole *1_1112848452* for both the 16-inch Short Normal and 64-inch Long Normal within the Area 2 AEM survey area. The 16-inch Short-Normal and the 64-inch Long-Normal logs are similar but not exactly the same in resistivity, indicating that there is some lateral variation on the order of the 64 inches around the borehole. However, both show the increased resistivity that correlates with the AEM.

Figure 7-17 is a comparison of the SCI inversions of line L403201 flown over test hole *2_10553010405* for both the 16-inch Short Normal and the 64-inch Long Normal within the Area 2 AEM survey area. The 16-inch Short-Normal and the 64-inch Long-Normal logs are similar but not exactly the same in resistivity, indicating that there is some lateral variation on the order of the 64 inches around the borehole. However, both show that the multiple layers of resistive materials are separated by lower resistivity zones. Both logs do show an increased resistivity at the bottom of the hole that is not indicated in the AEM.

Figure 7-18 is a comparison of the SCI inversions of line L403801 flown over test hole *4_13050220134* for both the 16-inch Short Normal and 64-inch Long Normal for the Area 2 AEM survey area. However, the 64-inch Long-Normal resistivity log shows that the equipment limitation on the shallow portion of the borehole, indicated by a resistive zone before gray area on the plot, indicates no data was collected at the top of the borehole. The AEM resistivity is very similar to the logs in this area.

The purpose of the above section is to verify that the AEM system was calibrated properly. The SCI inversion results indicate that the AEM system utilized for this survey (the SkyTEM 304M) was clearly calibrated. It is also important to understand the limitation of the AEM in resolving features at increasing depth. These comparisons indicate that the AEM is not able to resolve the absolute resistivity of the thin, deeper, more resistive, material. However, the AEM does indicate that there is a zone of increased resistivity. For this reason alone, a combined borehole and AEM interpretation is required to provide the best framework for the area. The resistivity tool will only provide good measurements in an uncased fluid filled hole and much of the upper sections of the logs are missing due to this limitation and are represented as gray areas on the figures at the top of the logs.

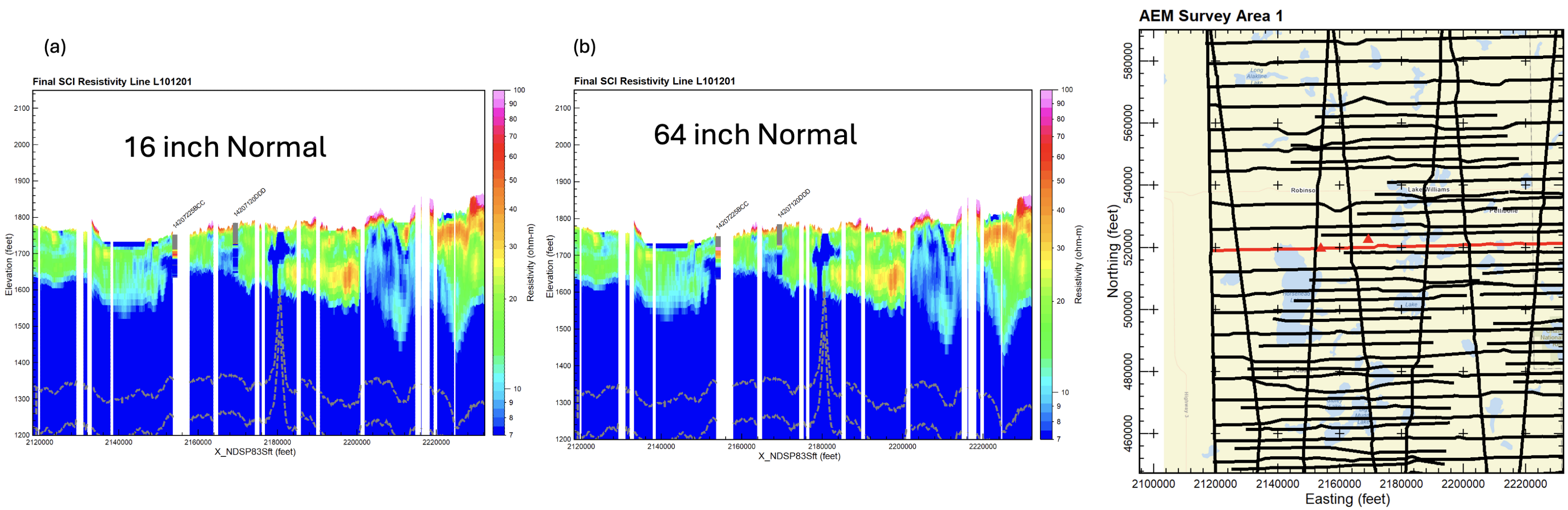

Figure 7-13. A comparison of the SCI inversions of line L101201 flown over test hole *14207225BCC* and *14207220DDD* for the (a) 16-inch Short Normal in the and (b) 64-inch Long Normal in the Area 1 AEM survey area.

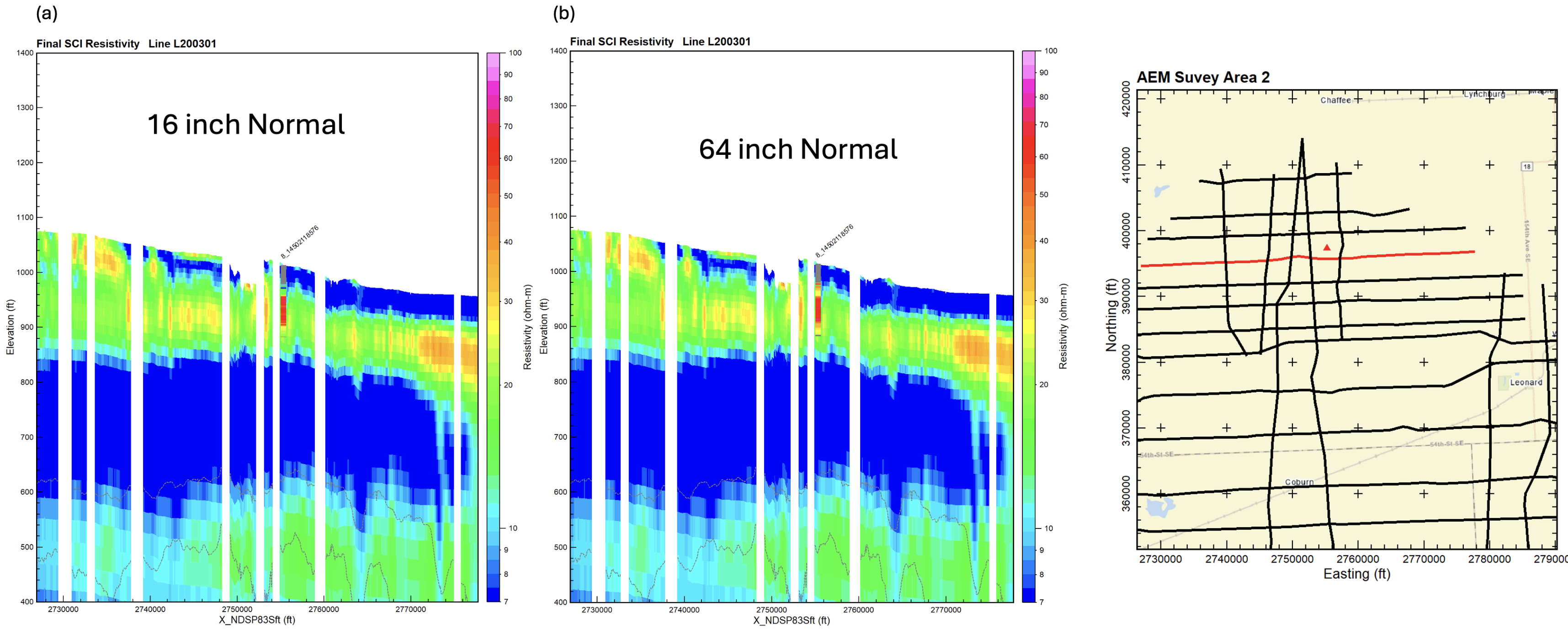

Figure 7-14. A comparison of the SCI inversions of line L200301 flown over test hole *8_14502118576* for both the (a) 16-inch Short Normal and (b) 64-inch Long Normal in the northern portion of Area 2 AEM survey area.

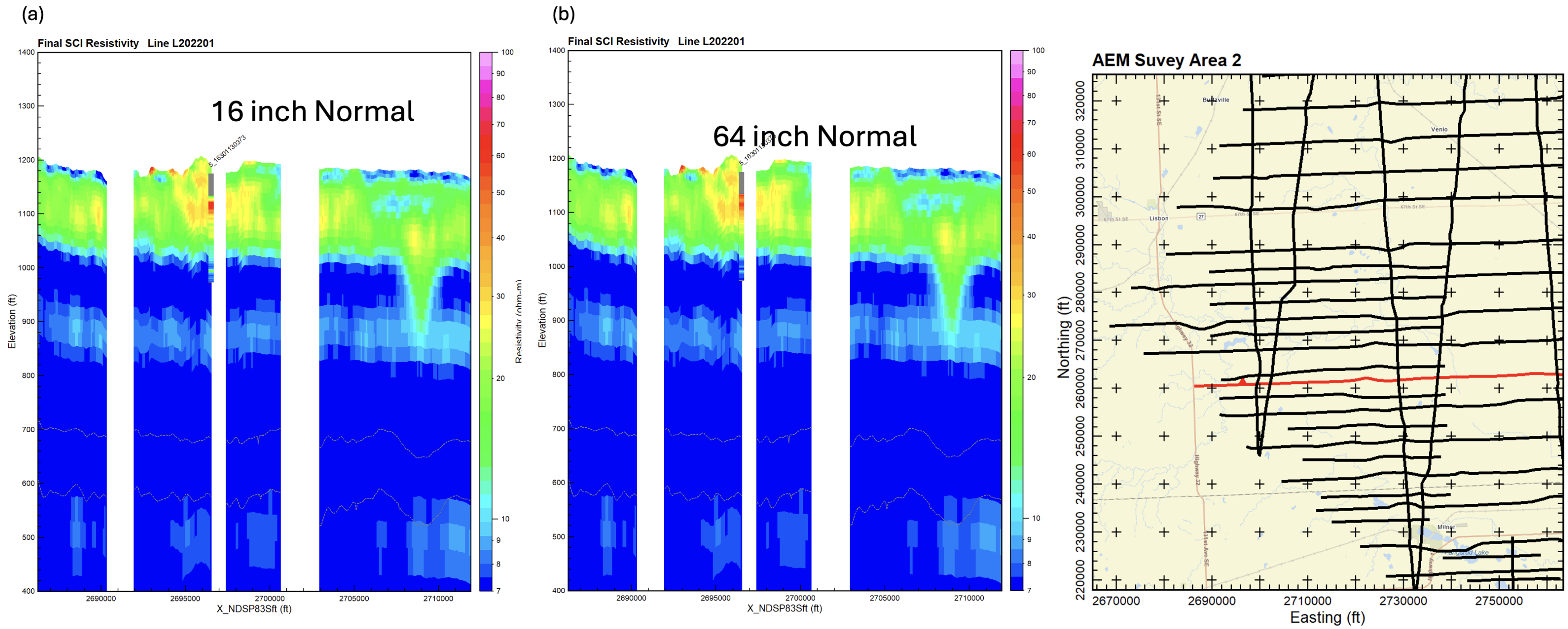

Figure 7-15. A comparison of the SCI inversions of line L202201 flown over test hole *5_163011130373* for both the (a) 16-inch Short Normal and (b) 64-inch Long Normal in the Area 2 AEM survey area.

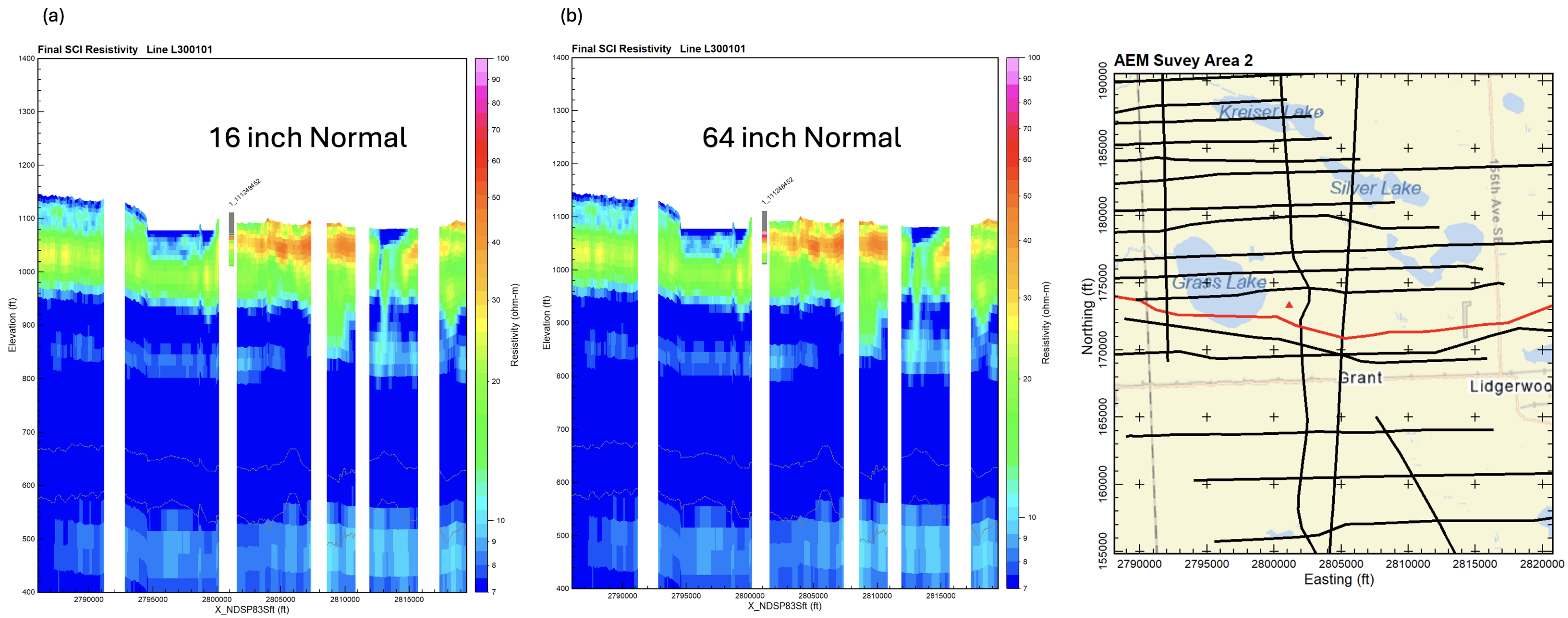

Figure 7-16. A comparison of the SCI inversions of line L300101 flown over test hole *1_1112848452* for both the (a) 16-inch Short Normal and (b) 64-inch Long Normal for the Area 2 AEM survey area.

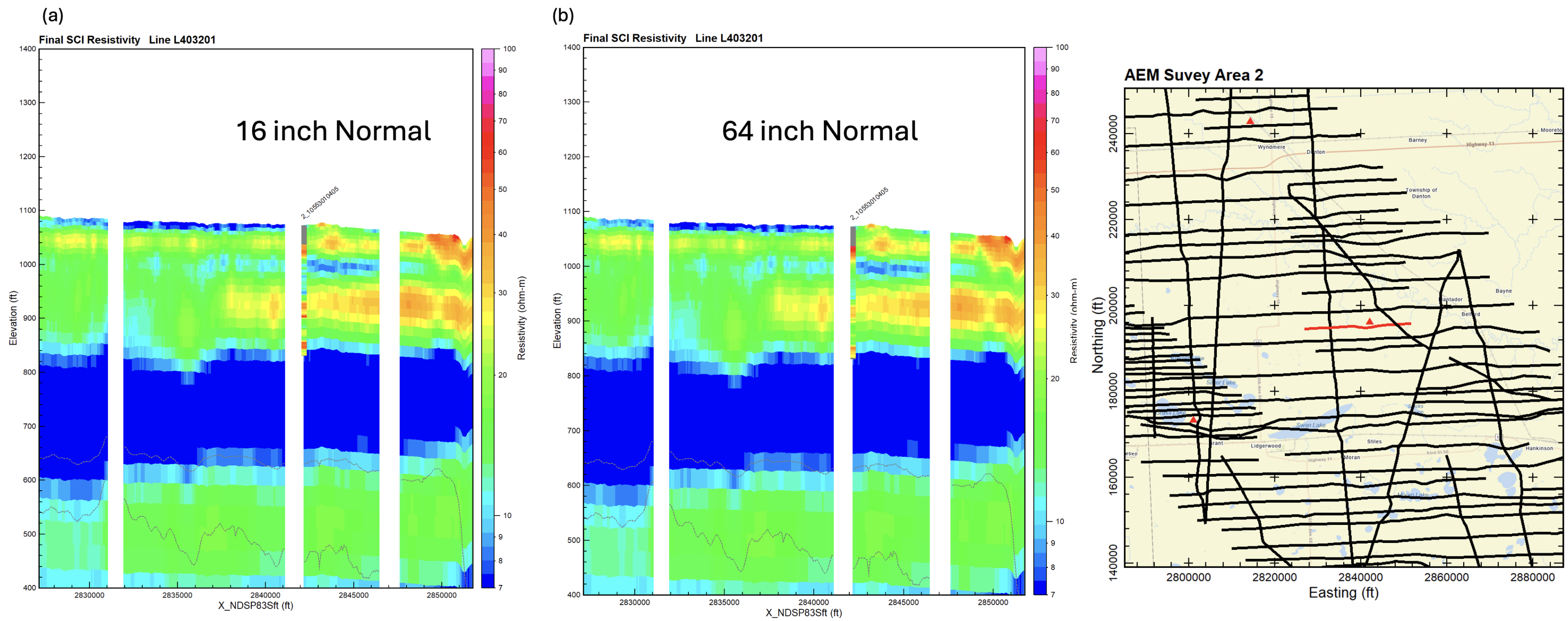

Figure 7-17. A comparison of the SCI inversions of line L403201 flown over test hole *2_10553010405* for both the 16-inch Short Normal and the 64-inch Long Normal for the Area 2 AEM survey area.

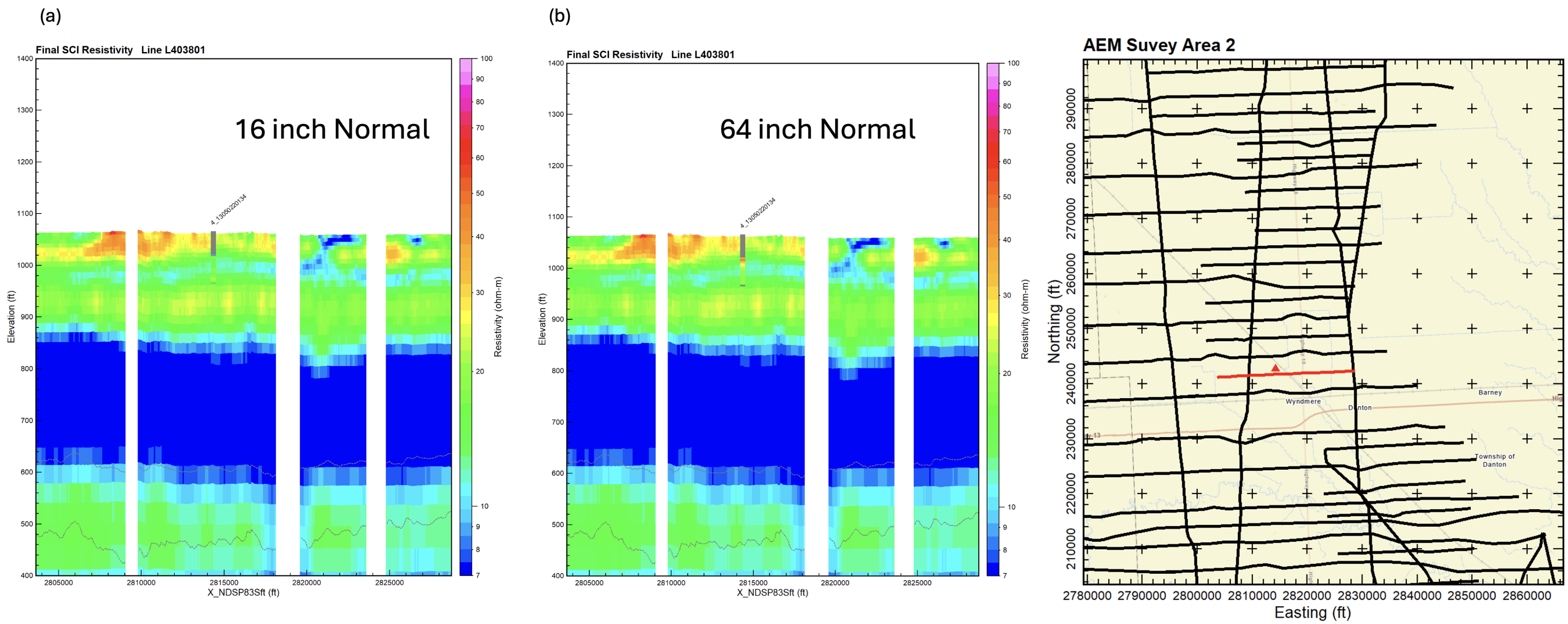

Figure 7-18. A comparison of the SCI inversions of line L403201 flown over test hole *4_13050220134* for both the (a) 16-inch Short Normal and the (b) 64-inch Long Normal for the Area 2 AEM survey area.

7.6.2 Area 1 AEM Survey Area

The structure of the subsurface Quaternary deposits of the Area 1 survey area is dominated by the presence of several systems of paleochannels. The resistive Quaternary sands and gravels in the paleochannels of Area 1 contrast with the clay and shale of the bedrock and the Quaternary fine-grained deposits. Selected AEM profiles will be examined with the borehole lithology as a comparison to verify the results of the AEM calibration and inversion. This also serves as a guideline that can be used in the interpretation of the AEM results.

Figure 7-19 is a profile view of east-west Line L102701 located in the southern portion of Area 1. Line L102701 has two discrete channelized deposits. There are several boreholes within 500 feet of the flight line, and they show good matches to the AEM.

Figure 7-20 is a profile view of north-south Line L190301, located in the southwestern portion of Area 1. There are two boreholes within 500 feet of the flight line that show good matches to the AEM bedrock as well as the lithology. All the wells are not in the deep section of the set of paleochannels that can be observed in the AEM.

Figure 7-21 is a profile view of the east-west line L101201, located in the central portion of Area 1. There are a few boreholes within 500 feet of the flight line that show good matches to the AEM bedrock as well as the lithology. There is a channel feature along the flight lines as well as two areas that exhibit low resistivity materials (shale/clay) above the bedrock surface. These low resistive material areas are curious features and may represent rip-up slabs of bedrock Cretaceous Pierre Shale.

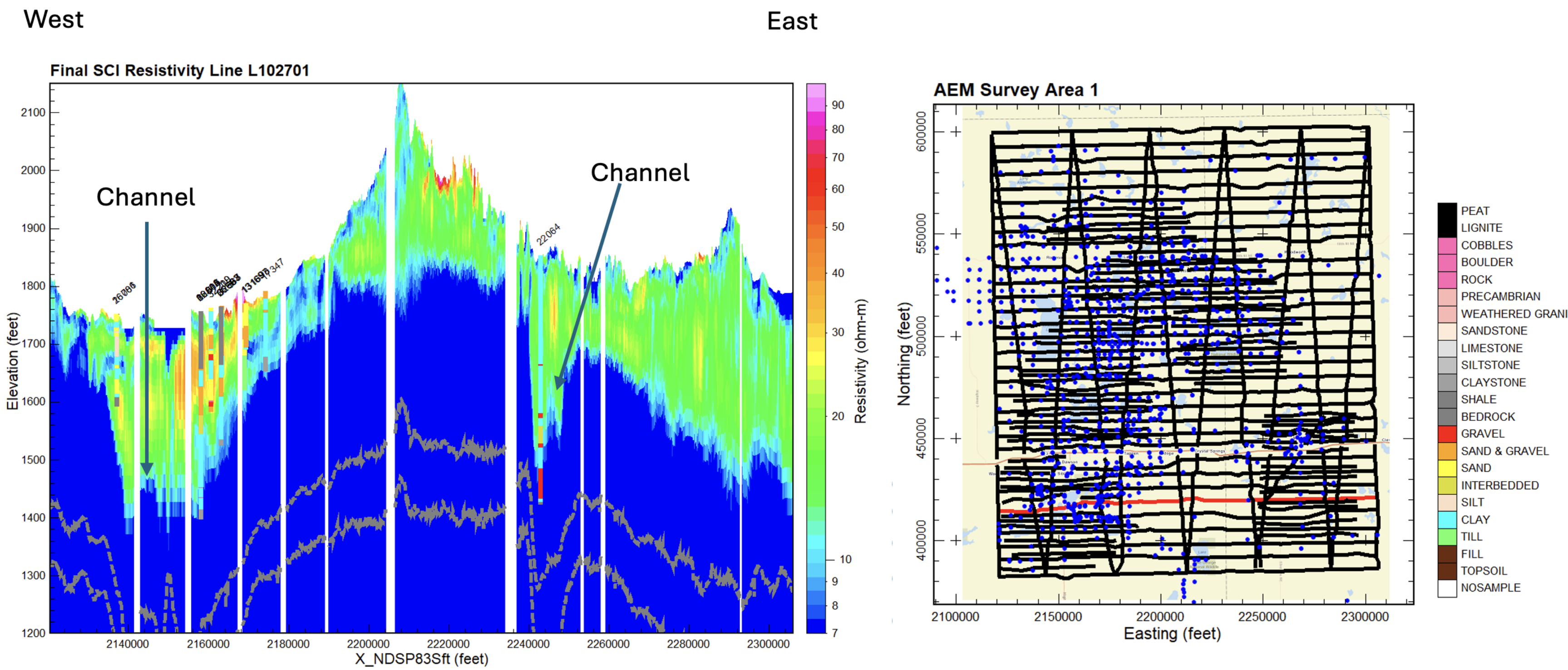

Figure 7-19. East-west flight line L102701 within the southern portion of the Area 1.

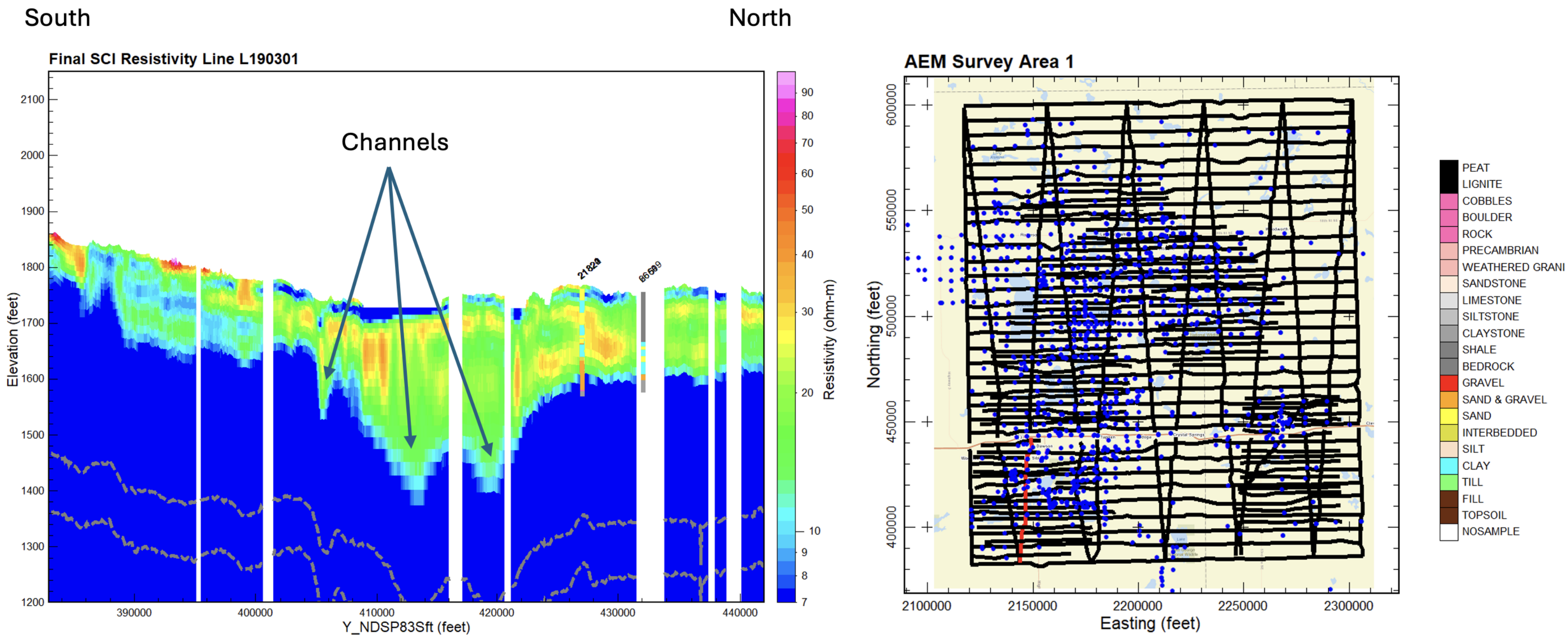

Figure 7-20. North-south flight line L190301 within the southwestern portion of Area 1.

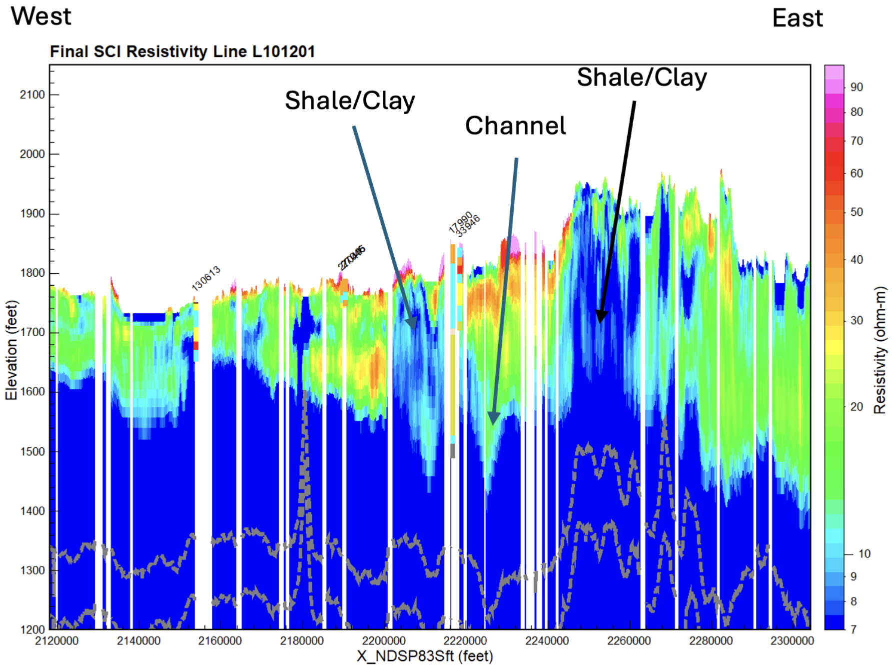

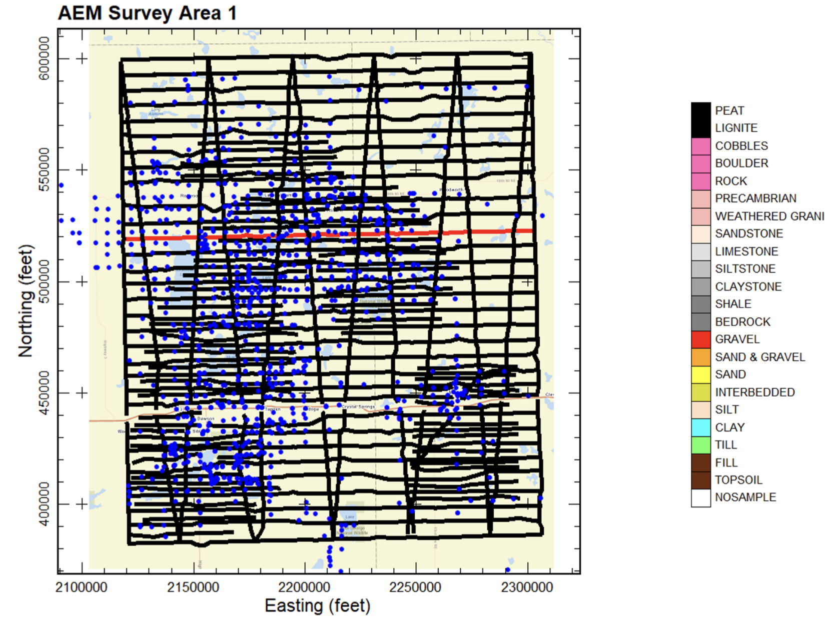

Figure 7-21. East-west flight line L101201 in the central portion of Area 1.

7.6.3 Area 2 AEM Survey Area

The dominant features in the Area 2 AEM survey area are the resistive coarse materials of the Sheyenne Delta which make up the large resistive paleochannel deposits. There are several paleochannels cross-cutting the area.

Figure 7-22 is a profile view of the AEM resistivity inversion along east-west Line L201401 in the northern part of the Area 2 that cuts across the Sheyenne Delta. There are several boreholes all in one location that show sands of the Sheyenne Delta. Also, the deeper geological units below the Cretaceous Pierre Shale is possibly the Cretaceous Niobrara Formation.

Figure 7-23 is a profile view of the AEM resistivity inversion along east-west Line L402701 in the western area of the Area 2 AEM survey area. A paleochannel feature can be observed along the line as well as the sand deposits. There is also some layering within the Cretaceous Pierre Shale related to some lithologic differences due to higher sand or limestone

Figure 7-24 is a profile view of north-south Line L290901, located along the eastern portion of Area 2. There are several boreholes within 500 feet of the flight line and they show good matches to the AEM bedrock as well as the lithology. There is a channel that is observed in the southern end of the line and many sand deposits that are confirmed by a borehole in the northern end of the line. The deeper geological units below the Cretaceous Pierre Shale can also be observed.

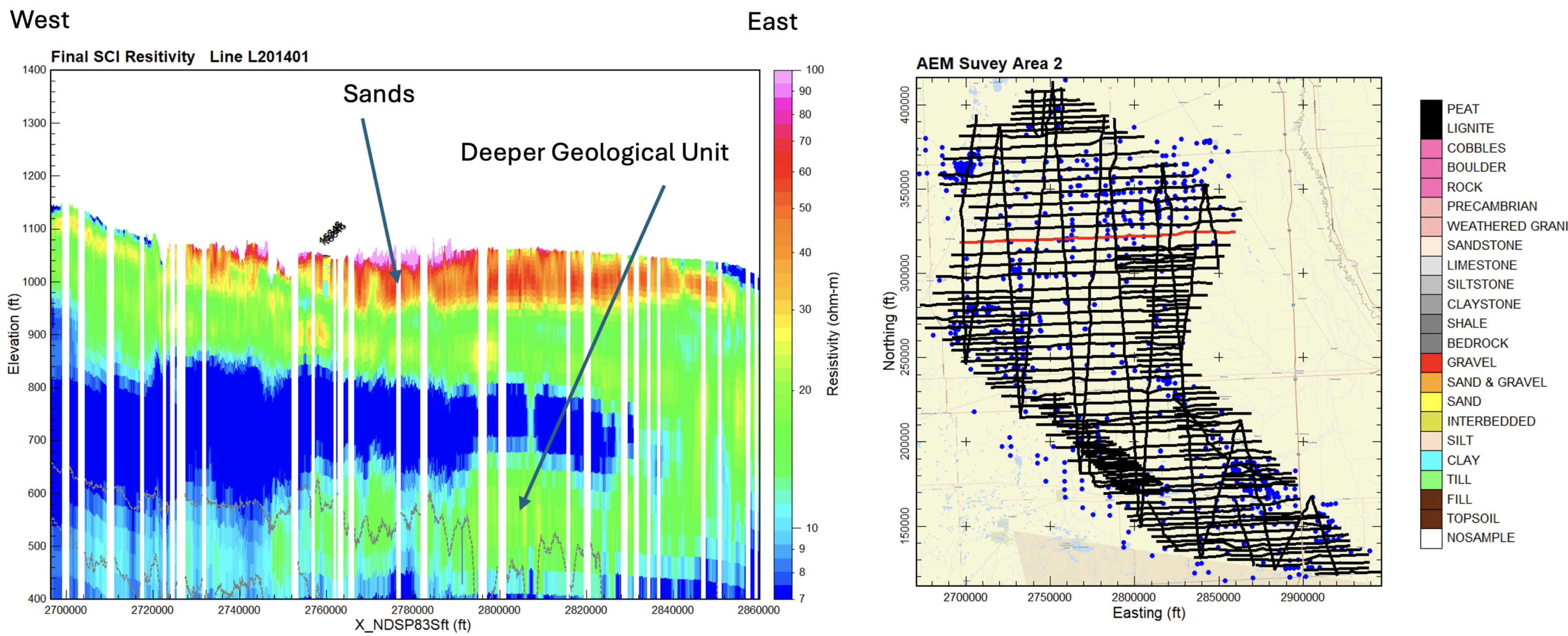

Figure 7-22. East-west flight line L201401 within the northern portion of the Area 2.

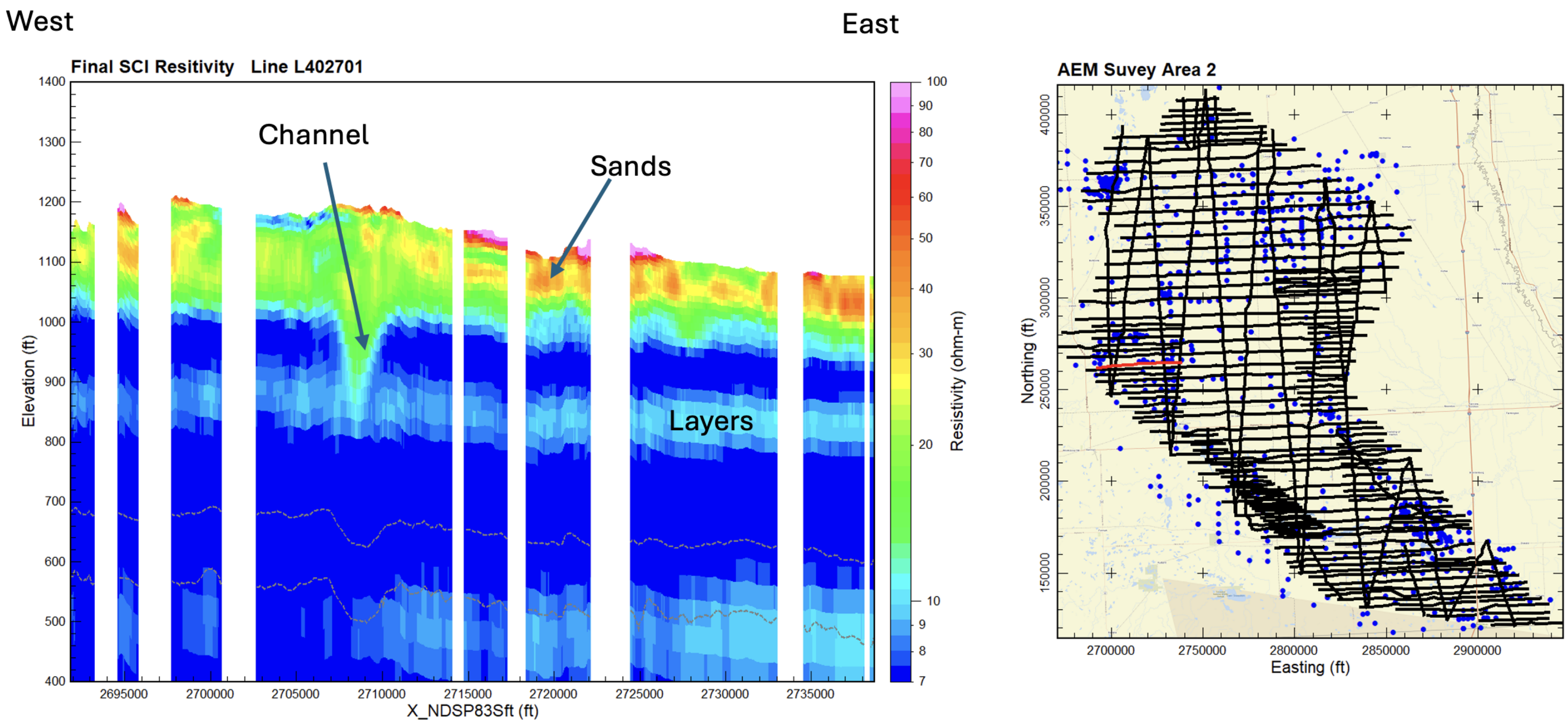

Figure 7-23. East-west flight line L402701 within the western portion of Area 2.

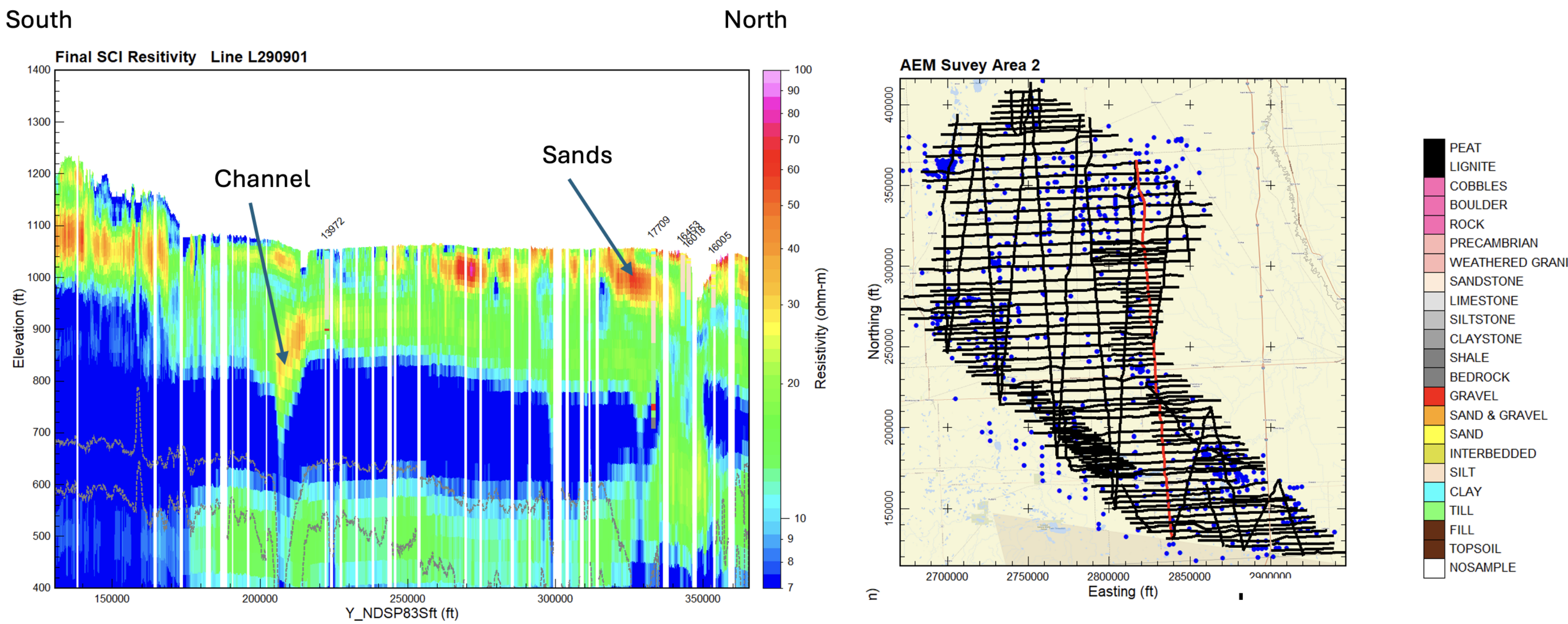

Figure 7-24. North-south flight line L290901 along the eastern side of Area 2.

7.8 Suggestions on Interpretation

The 2024 NDDWR Area 1 and Area 2 AEM survey areas provide rich details on the geology from the surface down to the Cretaceous basement. Even so, care needs to be exercised in the interpretation of the resistivity, keeping in mind the limitations of the AEM resolution and quality of the borehole lithologies. Care also needs to be used around the areas of EM-coupling as some of the areas may show impacts of pull ups in the conductive basement. This is a consequence of attempting to leave as much acquired data as possible in the inversion. The EM coupling has an impact at the later times, which image deeper, of adding to the conductive units. There will be no impact in the shallower depths. It is a tradeoff that needs to be understood in areas that may have pull-ups around EM-coupling cut outs.

The first suggestion in interpreting this dataset is to delineate the Cretaceous bedrock units. The next step would be to utilize resistivity thresholds on the Quaternary to identify the sand and gravel aquifers within the area. Another powerful technique is to adjust the resistivity color ramp to bring the details of the resistivity changes out of the Quaternary units without the need to display the Cretaceous low resistivity units.

Another suggestion related to interpretation of the multiple paleochannel deposits is to utilize the profiles and elevation layers to begin to pull out individual channel systems by digitizing their locations in X, Y, and Z and classifying the features as a specific system. Then begin to layer the systems from bottom to top by adjusting the classification of the channel system as needed.

8. Summary

This final report presents the Quality Assurance and Quality Control (QA/QC) procedures, and the results of that analysis, that were applied to the setup and data acquisition of the airborne electromagnetic survey of NDDWR Area 1 and Area 2 AEM survey areas. It also includes the preliminary LCI analysis, final SCI inversion results, and the SCI comparisons to E-logs and to lithology logs.

The QA/QC analysis included airborne testing of the system, the as-flown flight lines, and the flight altitude as the data was acquired. In addition, the power line noise monitor and magnetic field data were also examined and found to present no indications of any system or data acquisition issues. This first step included the generation of LCI inversions.

The final SCI results are presented as 2D resistivity profiles, 3D fence diagrams, 3D voxels, depth layers, and elevation layers. Google Earth KMZ files including the as-flown-retained flight lines, the residual errors in the inversion, and the resistivity depth and elevation slices. A link to the DropBox location of these files is presented below.

We believe that given the challenge of the infrastructure in the Area 1 and Area 2 AEM survey areas, these results provide a good, solid starting point for development of a hydrogeologic framework of the survey areas.

Dropbox Link:
https://www.dropbox.com/scl/fo/8downjhdd1tljr980wh4b/AB6gTrot4KDcBIQ0BZOOSgs?rlkey=qwwnhk0fcfmn6cku611o51f8h&dl=0

9. Deliverables

Table 9-1 describes the raw data files included in the zip file in *Appendix-3 - Deliverables\Raw Data\From SkyTEM.zip* that were delivered by SkyTEM within 24-36 hours after each flight plus the SkyTEM Final Report. As discussed above, forty-three (43) flights were required to acquire the 2024 Area 1 and Area 2 AEM data (Table 4-1). Grouped by flight date, there are four (4) native-format data files for each flight in the 01_RawData section. These files have extensions of ".sps" and ".skb". The ".sps" files include navigation and DGPS location data and the ".skb" files include the raw AEM data that have been PFC-corrected (discussed in Section 5.1). Two additional files are used for all the flights. These are the system description and specifications file (with the extension "*.gex") and the 'mask' file (with the extension "*.lin") which correlates the flight dates, flight numbers, and assigned line numbers in the 02_MASK_GEX subdirectory. The original gex and lin files were slightly modified prior to import of the raw skb data into WorkBench.

Also, in the From SkyTEM.zip file is the SkyTEM final report (Table 9-2) on the 2024 North Dakota work. The report includes five sections including RawData and MASK_GEX (discussed in the previous paragraph), Geosoft (a Geosoft Oasis montaj gdb of the processed SkyTEM data), Workbench_XYZ_Data - SkyTEM data in an XYZ format that can be imported into Workbench), finally a report on the acquisition and processing. The data report and deliverables provided by SkyTEM describes the Area 1 and Area 2 AEM surveys and system acquisition parameters.

Table 9-3 describes the data columns in the processed SkyTEM 304M data that is in the Geosoft gdb and in ASCII EM_MAG *.csv files for the Area 1 and Area 2 2024 AEM survey areas that are included in *Appendix 3 – Deliverables\Processed Data*. Given the size of the survey areas, the processed data have been broken up into smaller CSV files that can be opened in Microsoft EXCEL. The processed data contains the electromagnetic raw data plus the magnetic and navigational data as supplied from SkyTEM in an ASCII format (versus the Geosoft gdb format in the SkyTEM deliverable).

Table 9-4 lists the final SCI inversion results, ND2024_Area1_SCI01.csv and ND2024_Area2_SCI01.csv, delivered as ASCII files. The data columns of these databases are described in Table 9-4 (SCI) and are included in *Appendix-3 - Deliverables\SCI*. PDF's of elevation and depth layer maps are also included in the \SCI folder.

Table 9-5 lists the grid files included in the QGIS GeoPackage: ND_AEM_2024_Resistivity.gpkg and Table 9-6 lists the columns in the Voxel files in *Appendix 3 – Deliverables\Voxel*.

In addition, Table 9-7 lists Google Earth KMZ files of the As Flown flight lines, the data retained for inversion, Upper and Lower DOI's, the SCI residual data errors for Area 1 and Area 2, and SCI model Elevation and Depth layers can be found in *Appendix 3 – Deliverables\KMZ*.

In summary, the following are included as deliverables:

- Raw Data Files - SkyTEM files *.gex, *skb, *.lin, .xyz and SkyTEM final report
- Processed data used in the SCI inversion as an ASCII *.csv
- SCI results including Geosoft database, ASCII *.csv files, and model layer (Depth, Elevation) pdfs

- Google Earth KMZ files of AsFlown, Retained, Area 1 and Area 2 SCI01 ResData, DOI Upper, Lower, and model layer (Depth, Elevation) plots
- QGIS GeoPackage of the North Dakota 2024 Area 1 and Area 2 depth and elevation slice maps and DEM layers
-

Table 9-1. Raw SkyTEM data files

Folder	File Name	Description
Data	..NavSys.sps, …PaPc.sps, ...RawData_PFC.skb, …DPGS.sps, ….Workbench_Input.XYZ	Raw data files included for each flight used in importing to Aarhus Workbench
Geo	*.gex, SR2.gex & SR2.sr2.	SkyTEM304 System Description
Mask	*.lin	Production file listing dates, flights, and assigned line numbers

Table 9-2. SkyTEM data delivery report to AGF

Folder Name:	Description of files
01_RawData	SkyTEM provided raw data files as Workbench_SKB and SPS (Aarhus Workbench files), by Flight Date
02_MASK_GEX	SkyTEM production file (LIN) and system description files (GEX)
03_Geosoft	SkyTEM provided raw data in Geosoft format
04_Workbench_XYZ_Data	SkyTEM provided Workbench XYZ data in ASCII format
05_Report	SkyTEM report to AGF as a *.pdf

Table 9-3. Raw Data - Channel name, description, and units for 20083_NorthDakota_Area1_EM_MAG_FINAL_CSV.zip and 20083_NorthDakota_Area2_EM_MAG_FINAL_CSV.zip with EM, magnetic, DGPS, Inclinometer, altitude, and associated data.

Parameter	Description	Unit
Line	Line Number	
X_UTM14Nm	Easting, WGS84 UTM Zone 14N	Meters [m]
Y_UTM14Nm	Northing, WGS84 UTM Zone 14N	Meters [m]
DEM_M	Digital Elevation	Meters [m]
X_NDSP83Sft	Easting, North Dakota State Plane, NAD83, South	Feet [ft]
X_NDSP83Sft	Northing, North Dakota State Plane, NAD83, South	Feet [ft]
DEM_ft	Digital Elevation	Feet [ft]
Fid	Unique Fiducial Number	
Flight	Name of Flight	yyyymmdd.ff
DateTime	DateTime Format	Decimal days
Date	DateTime Format	yyyymmdd
Time	Time UTC	hhmmss.sss
AngleX	Angle (in flight direction)	Degrees
AngleY	Angle (perpendicular to flight direction)	Degrees
Height	Filtered Height Measurement	Feet [ft]
Lon	Longitude, WGS84	Decimal Degrees
Lat	Latitude, WGS84	Decimal Degrees
Alt	DGPS Altitude above sea level	Meters [m]
GDSpeed	Ground Speed	Kilometers/hour [km/h]
LMcurrent	Current, Low Moment	Amps [A]
HMcurrent	Current, High Moment	Amps [A]
LM_Z_dBdt [Gates 0-27]	Normalized (PFC-Corrected) Low Moment Z-RxCoil value	$pV/(m^4*A)$
HM_Z_dBdt [Gates 0-36]	Normalized (PFC-Corrected) High Moment Z-RxCoil value	$pV/(m^4*A)$
HM_X_dBdt [Gates 0-36]	Normalized (PFC-Corrected) High Moment X-RxCoil value	$pV/(m^4*A)$
_60Hz_Intensity	Power Line Noise Intensity monitor	
bmag_Raw	Raw Base Station Mag Data filtered	nanoTesla [nT]
Diurnal	Diurnal Drift corrections	nanoTesla [nT]
Mag_raw	Raw Total Magnetic Field Intensity	nanoTesla [nT]
TMI	Total Field Magnetic Field Intensity	nanoTesla [nT]
RMF	Residual Magnetic Field	nanoTesla [nT]
IGRF	International Geomagnetic Reference Field	nanotesla (nT)
INC	Magnetic Inclination	degrees
DEC	Magnetic declination	degrees
RelUnc_LM_Z_dBdt	dB/dt Relative Uncertainty, LM Z	$pV/(m^4*A)$
RelUnc_HM_Z_dBdt	dB/dt Relative Uncertainty, HM Z	$pV/(m^4*A)$
RelUnc_HM_X_dBdt	dB/dt Relative Uncertainty, HM X	$pV/(m^4*A)$

Table 9-4. Channel name, description, and units for ND2024_Area1_SCI01.xyz and ND2024_Area2_SCI01.xyz files with AEM inversion results.

Parameter	Description	Unit
LINE	Line Number	
X_NDSP83Sft	Easting NAD83, State Plane North Dakota, South	Feet [ft]
Y_NDSP83Sft	Northing NAD83, State Plane North Dakota, South	Feet [ft]
DEM_FT	Gound Surface Elevation	Feet [ft]
X_UTM14Nm	Easting WGS84, UTM Zone 14	Meters [m]
Y_UTM14Nm	Northing WGS84, UTM Zone 14	Meters [m]
DEM_M	Gound Surface Elevation	Meters [m]
DATE	Date: Year-Month-Day	YYYYMMDD
TIME	Date Time Format	Decimal days
ALT_M	Measured Altitude of system above ground	Meters [m]
INVALT_M	Inverted Altitude of system above ground	Meters [m]
INVALT_STD_M	Inverted Altitude Standard Deviation of system above ground	Meters [m]
RESDATA	Residual of individual sounding	
RESTOTAL	Total average residual for inverted section	
RHO_I_0 THROUGH RHO_I_38	Inverted resistivity of each later	Ohm-m
RHO_STD_0 THROUGH RHO_STD_38	Inverted resistivity standard deviation	
SIGMA_I_0 THROUGH SIGMA_I_38	Conductivity	S/m
DEP_TOP_FT_0 THROUGH DEP_TOP_FT_38	Depth to the top of individual layers	Feet [ft]
DEP_BOT_FT_0 THROUGH DEP_BOT_FT_38	Depth to the bottom of individual layers	Feet [ft]
THK_FT_0 THROUGH THK_FT_38	Thickness of individual layers	Feet [ft]
DEP_TOP_M_0 THROUGH DEP_TOP_M_38	Depth to the top of individual layers	Meters [m]
DEP_BOT_M_0 THROUGH DEP_BOT_M_38	Depth to the bottom of individual layers	Meters [m]
THK_M_0 THROUGH THK_M_38	Thickness of individual layers	Meters [m]
ELEV_TOP_FT_0_THROUGH_ELEV_TOP_FT_38	Elevation of Top of each model layer	Feet [ft]
ELEV_BOT_FT_0_THROUGH_ELEV_BOT_FT_38	Elevation of Bottom of each model layer	Feet [ft]
DOI_UPPER_FT	More conservative estimate of DOI	Feet [ft]
DOI_LOWER_FT	Less conservative estimate of DOI	Feet [ft]
DOI_UPPER_M	More conservative estimate of DOI	Meters [m]
DOI_LOWER_M	Less conservative estimate of DOI	Meters [m]

Table 9-5. Included Grids in QGIS Geopackage: ND_AEM_2024_Resistivity.gpkg

QGIS Geopackage Layer Name	Description	Grid Cell Size (feet)
Area1_SCI01_ElevationGrids_RhoXX	Area 1 Resistivity Slices in Elevation from 600 ft to 2300 ft in 25ft increments	50
Area2_SCI01_ ElevationGrids_RhoXX	Area 2 Resistivity Slices in Elevation from -25 ft to 1275 ft in 25ft increments	50
Voxel_Area1_SCI01_DepXX_YYft	Area 1 Resistivity Slices in Model Layer Depth from Layer 1 to 39 (XX) and 0 to 995 ft (YY)	50
Voxel_Area2_SCI01_DepXX_YYft	Area 2 Resistivity Slices in Model Layer Depth from Layer 1 to 39 (XX) and 0 to 995 ft (YY)	50
ND2024_Area1_AsFlown_FlightLines	As Flown flight lines for ND 2024 Area 1	
ND2024_Area2_AsFlown_FlightLines	As Flown flight lines for ND 2024 Area 2	
Area 1, Area 2 DEM TIFs	Area 1, Area 2 Digital Elevation Models in TIF format	500

Table 9-6. Channel name, description, and units for Voxel_Area1_SCI01_Dep_Ft.csv and Voxel_Area2_SCI01_Dep_Ft.csv.

Parameter	Description	Unit
E_NDSP83Sft	Easting NAD83, State Plane North Dakota South	Int. Foot [ft]
N_NDSP83Sft	Northing NAD83, State Plane North Dakota South	Int. Foot [ft]
Depth_ft	Elevation of Voxel Node	NAVD88 [ft]
Area1_voxel_500ft_winI	Area 1 (and 2) Voxel cell inverted resistivity model value	Ohm-m

Table 9-7. List and Descriptions of included KMZ for both Area 1 and Area 2 (XX)

KMZ	Description
XX_AsFlown	Area1, Area 2 As-Flown AEM flight lines
XX_Retained	Data retained for inversions
XX_DOI_Upper	Depth of Investigation – Conservative level
XX_DOI_Lower	Depth of Investigation – Standard level
XX_ModelDepthLayers	SCI Model Depth Layers, Color Scale 7-100 ohm-m
XX_SCI01_Elevation_Rho_7-100ohm-m	SCI Model Elevation Layers, 25 ft intervals, Color Scale: 7-100 ohm-m
XX_SCI01_Elevation_Rho_AutoScaled	SCI Model Elevation Layers, 25 ft intervals, Color Scale: Autoscale ohm-m
XX_SCI01_ResData	SCI Residual Data/Model Error

10. References

Aarhus Geosoftware, 2024, Aarhus Workbench, available on the world-wide web at: https://www.aarhusgeosoftware.dk/aarhus-workbench (accessed December 3, 2024)

Asch, T.H., Abraham, J.D., and Irons, T., 2015, "A discussion on depth of investigation in geophysics and AEM inversion results", Presented at the Society of Exploration Geophysicists Annual Meeting, New Orleans.

Auken, E., Christiansen, A.V., Kirkegaard, C., Fiandaca, G., Schamper, C., Behroozmand, A.A., Binley, A., Nielsen, E., Efferø, F., Christensen, N.B., Sørensen, K., Foged, N., and Vignoli, G., 2015, An overview of a highly versatile forward and stable inverse algorithm for airborne, ground-based and borehole electromagnetic and electric data: Exploration Geophysics, Vol. 46, No. 3, 2015, p. 223-235, http://dx.doi.org/10.1071/EG13097

Christensen, N. B., Reid, J. E., and Halkjaer, M., 2009, "Fast, laterally smooth inversion of airborne time-domain elecromagnetic data." *Near Surface Geophysics* 599-612.

Christiansen, A. V., and E. Auken, 2012, "A global measure for depth of investigation." *Geophysics,Vol. 77, No. 4* WB171-177.

Christiansen, A.V., Auken, E., Kirkegaard, C., Schamper, C., Noel, C., Vignoli, G., 2016, An efficient hybrid scheme for fast and accurate inversion of airborne transient electromagnetic data: Exploration Geophysics, Vol. 47, No. 4, 2016, p. 331-340, http://dx.doi.org/10.1071/EG14121

DatamineDiscover, 2024, Datamine Discover Profile Analyst, available on the world-wide web at: https://www.dataminesoftware.com/mineral-exploration-software/#discover (accessed on December 3, 2024).

Foged, N., Auken, E., Christiansen, A.V., and Sorensen, K.I., 2013, Test-site calibration and validation of airborne and ground based TEM systems: Geophysics, v.78, No.2: E95-E106. https://library.seg.org/doi/10.1190/geo2012-0244.1

Geosoft, 2024, Oasis montaj software, https://www.seequent.com/products-solutions/geosoft-oasis-montaj/

HydroGeophysics Group, Aarhus University, 2010, "Validation of the SkyTEM system at the extended TEM test site." Aarhus, Denmark.

HydroGeophysics Group, Aarhus University, 2011, "Guide for processing and inversion of SkyTEM data in Aarhus Workbench, Version 2.0.".

North Dakota Department of Water Resources (NDDWR), 2024, Map Services, available on the world-wide web at: http://mapservice.swc.nd.gov (accessed December 3, 2024).

Sapia, V, Oldenborger, G.A., Jorgenson, F., Pugin, A.J-M., Marchetti, M, and Viezzoli, A., 2015, 3D modeling of buried valley geology using airborne electromagnetic data: Interpretation, Vol 3, No.4, p. SAC9-SAC22. http://dx.doi.org/10.1190/INT-2015-0083.1

Schamper, C., Auken, E., and Sorensen, K., 2014, Coil response inversion for very early time modelling of helicopter-borne time-domain electromagnetic data and mapping of near-surface Geologic

Layers: European Association of Geoscientistis & Engineers, Geophysical Prospecting, v. 62, Issue 3, p. 658–674. https://www.earthdoc.org/content/journals/10.1111/1365-2478.12104

U.S. Geological Survey (USGS), 2024, The National 3D Elevation Program, 3DEP products and services: The National Map, 3D Elevation Program Web page, https://www.usgs.gov/3d-elevation-program (accessed December 3, 2024).

Viezzoli, A., Christiansen, A.V., Auken, E., and Sorensen, K., 2008, "Quasi-3D modeling of airborne TEM data by spatially constrainted inversion." Geophysics Vol. 73 No. 3 F105-F11. https://www.em-ergo.it/resource-types/publications/page/4/.